Linear optimisation of the portfolio of generators in a district heating network

Reducing energy costs, emissions of particulate matter and greenhouse gasses

This image was generated with the assistance of AI

Yavor Yavorov Razboinikov; №6363180; yavor.razboinikov@outlook.com
First supervisor: Javanshir Fouladvand
Second supervisor: Wen Liu
25.XI.2024

Utrecht University

Abstract

This work explores to what extent renewable energy technologies in a district heating network could reduce air pollution and greenhouse gas emissions while maintaining minimal costs. The neighbourhood of Orlandovtsi in Sofia, Bulgaria, is used as a case study for this research. A linear programming optimisation was developed, to determine the optimal installed capacities and hourly outputs across five scenarios – two using traditional technologies, two with renewable technologies, and one combining all considered technologies. These scenarios were optimised for the energy prices in 2017 and 2022 to explore how the changing energy markets call for different installed capacities and their dispatch. Moreover, the optimal capacities of each scenario obtained under the 2017 prices, were dispatched under the energy prices observed between 2018 and 2022. In this way, the ability of each scenario to deliver heat at a consistent price was tested. Lastly, the two renewables scenarios were optimised for different supply temperatures to map the effects of supply temperature reductions on the levelized costs of heat.

The integration of renewable technologies significantly enhanced all performance metrics. The best-performing scenario "All technologies" under the 2017 price optimisation reduced PM2.5-equivalent emissions by more than 90% and GHG emissions by 45% compared to the current status quo in the neighbourhood while consistently maintaining significantly lower prices than the current district heating network.

Overall, the optimal portfolio of generators consists of an air source heat pump (ASHP) unit for baseload work, an electric boiler for making use of low electricity prices, a pit thermal energy storage (TES) to augment the flexibility of the ASHP and electric boiler and a natural gas technology to tap into an alternative energy source at times of high electricity prices. This natural gas technology could be either a combined heat and power plant (CHP) or a simple boiler. If coupled with TES, a CHP unit was found to be of great benefit when the system is confronted with high electricity prices, as it can produce surplus heat and electricity in moments of peak electricity demand. When the system was optimised for lower electricity prices, however, the CHP was replaced by a cheaper natural gas boiler. The supply temperature was found to have minor effect on the cost of the produced heat, although it does reduce the role of ASHP units, which makes the respective scenarios less resilient when faced with escalating electricity prices.

The results of this study show unequivocally that the transition away from fossil fuels is needed beyond addressing climate change. On top of reduced greenhouse gas emissions, the integration of renewable energies holds promise to reduce the cost of energy for the final consumer while mitigating air pollution.

Keywords: Sofia, district heating network, linear optimisation, air pollution, renewable energy technology

Резюме

Това проучване разглежда до каква степен замърсяването на въздуха и емисиите на парникови газове могат да бъдат намалени чрез въвеждането на възобновяеми източници на енергия в топлофикационна мрежа, като едновременно с това цената на произведената енергия е сведена до минимум. Разработката е направена с данни от столичния квартал Орландовци. Беше разработена оптимизация чрез линейно програмиране, за да се определят оптималните инсталирани капацитети и часови товари в пет сценария – два използващи традиционни технологии, два с възобновяеми технологии и един, комбиниращ всички разглеждани технологии. Тези сценарии бяха оптимизирани за цените на енергията през 2017 и 2022 година, за да се изследва как промените на енергийните пазари изискват различни инсталирани капацитети и тяхната употреба. Освен това, оптималните капацитети от всеки сценарий, получени при цените от 2017 г., бяха разпределени при

наблюдаваните енергийни цени между 2018 и 2022 г. По този начин беше тествана способността на всеки сценарий да доставя топлина на предвидима цена. Последната стъпка от разработката включва оптимизацията на двата сценария с възобновяеми източници при различни температури на подаващата вода, за да се направи обзор на ефектите от намаляването на този параметър върху нивелираните разходи за топлина.

Въвеждането на възобновяеми технологии води до значително подобряване по всички показатели. При оптимизацията с цените от 2017 г. най-добре представящият се сценарий „Всички технологии“ намалява емисиите от PM2.5-екв. с повече от 90% и емисиите на парникови газове с 45% в сравнение с текущото състояние в квартала. Това беше постигнато успоредно със значително намаляване на цените на топлинна енергия спрямо цените на Топлофикация София.

Оптималният микс от генератори включва термопомпа въздух-въздух (ASHP) за базова работа, електрически котел, който се включва в моменти, в които цената на тока е ниска, яма за съхранение на термална енергия (TES), която за да увеличава гъвкавостта на производство, и топлогенератор, който използва природен газ. Последният предоставя алтернативен източник на топлина при високи електрически цени и може да бъде или комбинирана топлоелектрическа централа (КТЕЦ), или прост котел. Когато системата е изправена пред високи цени на тока, комбинацията от TES и КТЕЦ е от голяма полза, тъй като КТЕЦ може да произвежда електричество в моменти на пиково търсене на електричество. От друга страна, когато системата беше оптимизирана за по-ниски електрически цени, КТЕЦ беше заменен с по-евтин природен газов котел. Температурата на подаващата вода няма сериозен ефект върху цената на произведената топлина, но в сценариите с висока температура ролята на ASHP е по-малка, което намалява сподобността им да произеждат евтино, дори в периоди на високи цени на електроенергията.

Резултатите от това проучване категорично показват, че въвеждането на възобновяеми източници на енергия не само намалява емисиите на парникови газове, но и води до намаляване на замърсяването на въздуха и по-ниски цени за енергия за крайния потребител.

Acknowledgments

This work wouldn’t have been possible without the dedication and efforts of my supervisor Javanshir Fouladvand. I am deeply indebted to him for always having the patience to listen to my ideas and take the time to review my work. I was incredibly lucky and fortunate to meet him and to have him take me under his wing. I can’t help but thank Bas Bolomey too for opening the door to Novar for me and being so eager to always give me the best guidance and access to the most valuable resources.

Succulents, the next one is for you – you people defined my life in Utrecht and thanks to you I loved every moment in this city, even during the gloomiest days of the winter. Some of you spent so many hours with me on campus; Noemie, Adam, Gen, Alexis, Zach, you don’t know how much you helped me by being around. On that note, I would like to thank the kind and friendly staff of the UU campus that puts so much work in giving students a pleasant environment where they can focus on their studies. Last but not least, none of this would have been the same without my parents, sister and girlfriend who have supported me in every choice I make, good or bad. Thank you all!

Table of contents

List of tables

List of figures

List of abbreviations

ASHP	Air Source Heat Pump	**NH3**	Ammonia
BAU	Business as Usual	**NMVOC**	Non-Methane Volatile Organic Compounds
BAU-opt	Scenario of installed capacities of BAU technologies, optimised to balance costs and particulate matter emissions	**NOx**	Nitrous Oxides
BAU-econ	Scenario of installed capacities, optimised for lowest costs	**PM**	Particulate Matter
CHP	Combined Heat and Power	**SO2**	Sulphur Dioxide
EEA	European Environmental Agency	**SO3**	Sulphur Trioxide
H2SO4	Sulfuric Acid	**RE**	The scenario of installed capacities of renewable energy technologies, optimised for lowest costs
LCIA	Lifecycle Impact Assessment	**RE-ST**	The scenario of installed capacities of renewable energy technologies with a minimum of solar thermal capacity, optimised for lowest costs
LCOH	Levelized Cost of Heat	**SOx**	Sulphur Oxides
M€	Million Euros	**WHO**	World Health Organisation

1. Introduction

Heat accounts for the vast majority of the energy consumed by households in the European Union (EU) (Eurostat, 2023). As of 2021, 64% of household energy consumption in the EU was destined for space heating, and a further 15% was used for water heating (Eurostat, 2023). This energy need can be satisfied either through individual or communal heating technologies (Yoon et al., 2015). Communal heating is provided using district heating networks (DHNs). In a DHN, heat is generated in a few centralised locations and transported to the consumers through pipes with hot water (Werner, 2017, 2022). A major advantage of DHNs is that they can capture and distribute waste heat produced as a by-product of electricity generation, leading to higher primary energy efficiency (Lund et al., 2014; Yoon et al., 2015). Plants designed to deliver the waste heat while producing electricity are called combined heat and power plants (CHPs) and supplied the majority of the heat distributed by DHNs in the EU in 2014 (Werner, 2017). The vast majority of DHNs around the world are powered by fossil fuels, mainly coal and natural gas, with renewables providing a mere 8% of the heat distributed by DHNs worldwide in 2020 (Jodeiri et al., 2022).

The implementation of DHNs, and provision of residential heat more broadly, are intertwined with major societal and environmental issues, including climate change and air pollution; the paragraphs below elaborate on how these issues are connected.

1.1. The energy transition

The combustion of fossil fuels releases greenhouse gasses (GHG) like carbon dioxide (CO_2) or methane (CH_4), and other pollutants, intensifying the greenhouse effect and leading to climate change (United

Nations, n.d.). Particularly, in the European Union, as one of the main consumers of fossil fuels, the residential sector is a major contributor of greenhouse gas (GHG) emissions, representing 35% of energy-related EU emissions in 2021 (EEA, 2023b). The ongoing energy transition is the process of moving away from fossil fuels and substituting them with renewable energy sources and other low-carbon technologies whenever possible (IEA, 2024).

Approximately 70% of total energy consumption of European households is for heating purposes and approximately a quarter of it is delivered via DHNs (Eurostat, 2023; Werner, 2017). Thus, decarbonising the DHN sector is a prerequisite for the successful energy transition in the EU. Fossil fuels can be replaced with geothermal and solar thermal installations or by tapping into waste heat produced as a by-product of industrial processes (Jodeiri et al., 2022). Other solutions include the substitution of fossil fuels with biomass, biogas and municipal waste or the usage of heat pumps to extract heat from the ambient air, the subsurface or the sea (Danish Energy Agency, 2024).

There are various studies which are focused on the climate impact of heating systems. As forgoing fossil fuels is unconventional, and, therefore, more expensive (Geels, 2012), finding the balance between higher prices and lower GHG emissions is frequently the domain of optimisation studies. These techno-economic studies explore what technology portfolios could feasibly satisfy heat demand and at what cost. Dorotić (2022) develops a multi-objective optimisation tool that finds the generation portfolio with the lowest CO_2 emissions, lowest exergy destruction and lowest cost for the DHN of the town of Velika Gorica in Croatia. Delangle et al. (2017) investigate how the optimal energy mix of a small DHN of an unnamed district changes under different expansion scenarios. The system is first optimised with respect to the lowest costs and then with respect to the lowest GHG emissions.

1.2. Air pollution

Air pollution is the contamination of the atmosphere by an agent that alters the natural characteristics of the atmosphere (WHO, n.d.). Major pollutants include particulate matter (PM), carbon monoxide (CO), ozone (O_3), nitrogen dioxide (NO_2) and sulphur dioxide (SO_2) (WHO, n.d.). Both indoor and outdoor air pollution can come from similar processes, such as the incomplete combustion of fuels. Major sources of contamination include heating with polluting technologies and high-temperature combustion in vehicles or power-generating facilities (WHO, n.d.). Air pollution restrictions stipulate maximum average concentrations for their respective pollutants over a particular time period (e.g. 20 $\mu g/m^3$ of $PM_{2.5}$ over a year) (European Commission, n.d.).

Similarly to the climate change impact, the residential heating sector is an important contributor to air pollution when polluting energy sources are used (Paardekooper et al., 2020; Shesho et al., 2018; Weng et al., 2022; Wojdyga et al., 2014). In general, solid combustible fuels like coal, municipal waste or biomass have higher air pollution impact than liquid and gaseous fuels or renewables, especially when considering particulate matter emissions (EEA, 2023a; Mahmoud et al., 2021). Geothermal energy, a renewable energy source free of GHG emissions, is associated with hydrogen sulphide emissions (Kristmannsdóttir & Ármannsson, 2003). This means that the air pollution impact of heating systems is closely related to its climate impact, but the two are not identical. A climate-neutral solution based on geothermal energy or biomass could still have a negative impact on air quality. In that context, European DHNs used coal products for 24% of the delivered heat and biomass for other 34% (Euroheat & Power, 2024), revealing a significant dependence on polluting energy carriers. Still, thanks to its efficiency and centralised nature, which enables better flue gas treatment, relative to individual heating options, DHN is frequently considered to be mitigating air pollution (Danish Energy Agency, 2024; Lotrecchiano & Sofia, 2022; Paardekooper et al., 2020).

Although there are several studies which used multi-objective optimisations for studying balancing costs and GHG emissions of DHNs, such as (Dal Cin et al., 2023; Dorotić et al., 2019a), no optimisation that attempts to balance air pollution and costs was found.

1.3. Literature gap & research question

To recap, the provision of residential heating significantly contributes to multiple issues like climate change, air pollution. District heating networks (DHNs) could mitigate or exacerbate each of these issues, depending on how they are applied and the literature can be divided into two main branches.

On the one hand, techno-economic approaches like the optimisation studies of (Dal Cin et al., 2023; Delangle et al., 2017; Dorotić et al., 2019a; Weinand et al., 2019) do not consider the air pollution of the proposed system. On the other hand, studies that investigate the effects of residential heating on air pollution in a neighbourhood focus on the reduction of air pollution by the conversion of residential biomass and coal boilers to district heating, rather than considering the air pollution impact of the DHN itself (Lotrecchiano & Sofia, 2022; Paardekooper et al., 2020). Only one paper was found where the DHN's emissions are taken into account (Moradpoor et al., 2022). Still, it prescribes the installed capacities of the different generatiors across the different scenarios, a limited approach to the design of the DHN which cannot guarantee that the selected capacities are optimal. Therefore, there is a gap in understanding the influence of DHNs on air pollution while it is techno-economically feasible.

Therefore, this study aims to investigate the potential of renewable energy sources in DHNs to reduce GHG, and air pollution emissions. In order to achieve its aim, the study employs an optimisation to find the portfolio of generators with the lowest air pollution emissions and lowest costs. The cost aspect is included, as a system needs to be at least competitive in terms of prices if it is to gain traction with important stakeholders and the general public. The detailed reasoning and information on this approach is presented in Chapter 4.

In order to address the knowledge gap systematically and structurally, the thesis will specifically focus on the neighbourhood of Orlandovtsi in Sofia, the capital of Bulgaria. The DHN within this neighbourhood currently serves only two large apartment buildings, but the network operator plans its expansion (Toplofikatsiya Sofia, 2022b). In the context of a large city with a legacy DHN from the 1950s, the case study of Orlandovtsi offers the opportunity to study how new concepts could be developed from the ground up. Further details and reasons for choosing this specific case study are presented in Chapter 2.

For the purpose of these research aims, the following research question (RQ) and sub-questions (SQ) are crafted, in which, all of them assume that a hypothetical DHN would cover Orlandovtsi's full heat demand.

> RQ: To what extent could renewable energy technologies in a district heating network contribute to reducing air pollution and greenhouse gas emissions while maintaining the lowest possible system cost?
>
> > SQ1: What are the technical, environmental and economic characteristics of the energy sources of the potential DHN?
> > SQ2: Considering these technical, environmental and economic characteristics, what is the optimal portfolio of heating generation in a DHN?
> > SQ3: How can different techno-economic conditions, such as energy prices and different supply temperatures, influence the optimisation results?

2. The case study: Orlandovtsi, Sofia, Bulgaria

The city of Sofia presents an interesting case for studying the way an old second-generation DHN adapts to the dynamic challenges of decarbonisation, air pollution reduction and supply security. Besides that, as the following paragraphs will show, the DHN operator places a focus on the expansion of the natural infrastructure, which leaves a gap in the understanding of the impact that renewable energy technology could have. The only academic work that attempts to address this is the paper of Garbev (2023), which estimates the feasibility and economic viability of implementing electric boilers. He, however, does not include thermal energy storage in his analysis, which significantly reduces the potential impact of this technology.

The capital of Bulgaria is officially home to 1.3 million residents (Dimitrova & Velizarova, 2021). The DHN of the city meets a maximum thermal load of 5.9 GW_{th} and serves more than 410,000 connections (Georgiev et al., 2020). The network uses pressurised water at 130°C as an energy carrier and is divided into four main districts and has five other separate mini-systems with Orlandovtsi being one of these (KEVR, 2020; Stanimirov, 2008). Further information on the main districts and the plans of the DHN operator is available in Appendix E: Sofia's DHN.

2.1. Orlandovtsi

Energy demand

The neighbourhood of Orlandovtsi and its separate DHN network have been selected as the case study for this research. The neighbourhood with a population of 13 700 people (GIS Sofiaplan, n.d.) is a significant emitter of particulate matter pollution from domestic heating (Toplofikatsiya Sofia, 2022b) and is experiencing high concentrations of that pollution too (Dimitrova & Velizarova, 2021). The municipality and the district heating provider want to address this by expanding the district heating network and replacing polluting domestic boilers with cleaner natural gas CHP. Moreover, the district heating provider considers the thermal plant that serves this district heating island obsolete and plans on making large capital investments in its replacement and connection to the natural gas grid. This means there is a window of opportunity to develop an alternative plan, in which the DHN will be designed with renewable energy generation in mind, rather than investing in fossil fuels. Lastly, the smaller network of Orlandovtsi can be regarded as a pilot case where new concepts are experimented with, before they are applied to the overarching DHN in the city.

Table 1: Data on residential heating energy consumption for Orlandovtsi in 2017. Own elaboration based on (GIS Sofiaplan, n.d.) and (Georgiev et al., 2020)[1]

Energy carrier	Consumed energy (MWh/y)	Percentage
Electricity	29 100	67.7%
Biomass	7 500	17.4%

[1] The data for the neighbourhood is taken from (GIS Sofiaplan, n.d.) and the category "Solid fuels, heating oil and LPG" is disaggregated based on the ratio between these fuels in the 2015 fuel balance for the city presented by (Georgiev et al., 2020)

Coal	2 844	6.6%
Heating oil	24	0.1%
LPG	2 475	5.8%
District heating	1 047	2.4%
Total	**42 990**	**100%**

Further data on household heat consumption of Orlandovtsi is provided above in Table 1 for the year 2017. The total emissions of particulate matter and greenhouse gasses and the contributions of the different energy carriers are shown in Figure 1 below. It is important to note the different scopes of the two emission types – GHGs have a global impact and thus, the emissions of electricity production are taken into account. The impact of particulate matter is highly localised (Dimitrova & Velizarova, 2021), and so the particulate matter impact on electricity production is disregarded, as it occurs away from Orlandovtsi. PM emissions are dominated by the use of biomass and coal, while GHG emissions are almost solely comprised of electricity use. This is somewhat hopeful, as the electricity sector is experiencing a significant decarbonisation, with emission intensity falling from its 2011 peak of 577 $kgCO_2$-eq/MWh to 335 $kgCO_2$-eq/MWh in 2023 (Statista, 2024).

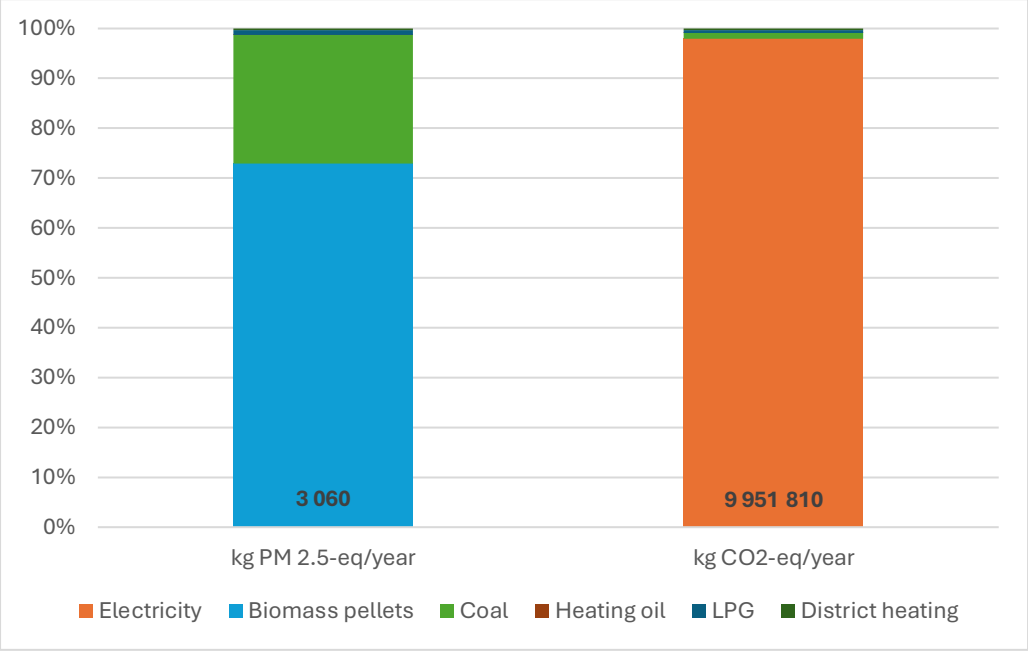

Figure 1: Yearly total emissions of particulate matter and GHGs and the contributions of every energy carrier. Figure calculated assuming 70% efficiency of residential stoves and 100% efficiency of electric heating appliances (EEA, 2023a)

Land availability

Land availability is an important aspect in the context of a renewables-based society. Although deciding on the land policy of the city of Sofia is clearly outside of the scope of this study, it is assumed that roughly 11 hectares of land could be made available for either solar thermal or photovoltaics and a further 3 ha

could be dedicated to thermal energy storage and new heat generating facilities. The reasoning behind these numbers is explained below.

Orlandovtsi is a neighbourhood at the northern edge of the city; a screenshot from the spatial plan with the neighbourhood's borders is highlighted as shown below (Figure 2). It is surrounded by industrial areas to the east and west and the main cemetery to the south. In the future, the municipality plans to densify the western edge of the neighbourhood and to develop two areas for sport and recreation (Figure 2) ('Общ устройствен план на СО', n.d.). Currently, this part of the neighbourhood is either uninhabited and covered by informal landfills, or populated with ad-hoc living quarters. In the north, a new denser mixed zone of dwellings and shops will be developed along the railway line. The agricultural lands north of it will be turned into a park. Little is planned to change to the west of the neighbourhood, except for the slight enlargement of the industrial area and the greening of the node of the railway line.

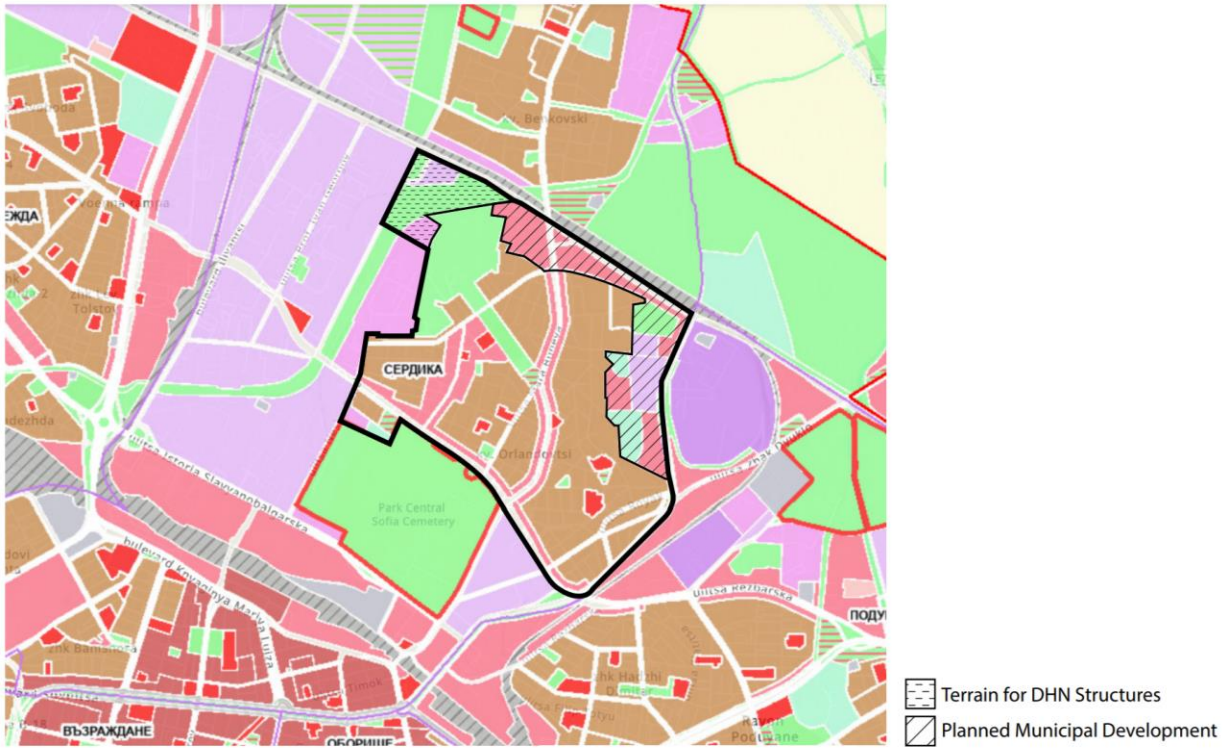

Figure 2: Screenshot of Sofia's masterplan with Orlandovtsi highlighted in a black box. Brown-red hues represent residential areas. Green shows parks and other green spaces. Cyan shows sport and recreational facilities. Shades of purple show industrial terrains. Source: ('Общ устройствен план на СО', n.d.).

It is precisely the railway node that is considered available for renewables. The node has an area of approximately 11 ha and was used when the power plant of Sofia was running on coal to bring fuel in and take the generated ashes away. Since the conversion of the TPP to natural gas and its connection to the natural gas grid, the branch line has fallen into disrepair. The area of the railway node is currently abandoned, covered with shrubs and other vegetation. The municipality plans to maintain it better in the future, but to still leave it in mostly natural condition as part of a "green corridor" stretching to the city centre. Only one small industrial plot will be developed within it with a size of 3 ha. Clearly, the impact of placing solar thermal or photovoltaic panels on the local biodiversity and the functioning of the "green corridor" is of high importance, but is beyond the scope of this study. From the point of view of societal acceptance, it is assumed that such development would cause little resistance. The land is not used by

humans and will barely be in the future, which should limit competing interests. Besides that, the solar farm would be enclosed by industrial terrains on three of four possible sides. The fourth side faces the "Bratska mogila" park, but it is separated from it by a riverbed. Presumably, if a sufficiently high visual barrier is constructed on the side of the park, the solar farm would be practically invisible from the public view.

Lastly, the roughly 3 ha of land that will be added to the western industrial terrains could be used to house the thermal energy storage of the modelled DHN, together with any other new facilities like heat pump houses, new boiler units, etc. It is assumed that the space currently dedicated to the heavy fuel boiler house would be insufficient to fit the new portfolio of generators, given its small size (390 m^2).

3. Research context

The introduction of this work sketched how district heating is intertwined with the topics of air pollution and the energy transition. Further details are provided in this chapter, together with further explanation on assumptions made in the model.

3.1. Air pollution

When discussing air pollution caused by the residential heating sector, researchers frequently focus on the following pollutants – NO_x, SO_x and particulate matter of varying diameter (Kaczmarczyk et al., 2020; Li et al., 2022; Paardekooper et al., 2020; Ravina et al., 2021; Salva et al., 2023; Weng et al., 2022). One way to combine the emissions of these different pollutants into a single index is to use the characterisation factors developed by lifecycle impact assessment methodologies (LCIA). These frameworks group air pollution in the following overarching impact categories – particulate matter formation, terrestrial acidification and photochemical oxidant formation (Bare, 2011; GreenDelta, 2017; Huijbregts et al., 2017). Emissions of particulate matter (PM), nitrous oxides (NO_x) and sulphur oxides (SO_x) are the main contributors to each of these categories.

In the case of Bulgaria, the emissions of particulate matter are consistently above the thresholds established by the World Health Organization (WHO) (EEA, n.d.-a). The characterisation factors developed by the ReCiPe2016 LCIA framework are used to calculate the impact score of the selected technologies (Huijbregts et al., 2017; RIVM, 2017). This is one of the most widely used LCIA methodologies, that accounts for a variety of pollutants, with calibration factors developed such that they provide an adequate representation of impacts worldwide. This makes it a fitting choice for this study. The emissions are quantified using Tier 1 emission factors on small combustion developed by the European Environment Agency to assess national emission inventories (EEA, 2023a). A table with the characterisation factors of the ReCiPe2016 and further elaboration on why this research focuses on the chosen pollutants can be found in Appendix A: Air pollution details.

3.2. Energy technologies

Multiple technologies could be used to power the district heating network. This work engages with the technologies listed below. The details regarding the input data of each of these energy technologies is presented in Appendix B: Energy technologies input data.

- Natural gas boiler
- Piston engine CHP that uses natural gas as fuel
- Electric boiler (e-boiler)

- Air source heat pump (ASHP)
- Solar thermal collectors
- Photovoltaic panels –not used to produce heat directly, but as a way to produce electricity for the ASHP and the e-boiler.
- Steel tank thermal energy storage (TES)
- Pit TES

Clearly, the list above does not include all possible technologies. The natural gas boiler and CHP are included as a way to represent the currently predominant approach to district heating, as illustrated in this review (Danish Energy Agency, 2024). The renewable energy technologies are taken from the list provided by Jodeiri et al. (2022). Tank and pit storages offer high heat capacity, with high charging and discharging rates (Danish Energy Agency, 2018).

Ground source heat pumps and geothermal installations were not included because of a lack of data on the subsurface water and its temperature, which makes it impossible to establish their potential; similar consideration precluded the integration of borehold and aquifer TES.

The following paragprahs dive deeper into important aspects of some of the technologies and how these were incorporated in the model.

CHP

In the proposal for the development of the DHN in Orlandovtsi the operator proposes the installation of 2 natural gas piston engines with 3.5 MW thermal capacity each. Consequently, the same CHP technology is investigated in this research, with the maximum possible capacity increased to 35 MW of thermal output. As the ramp-up and ramp-down times of this technology are in the range of a few minutes, and the model uses an hourly timestep, it is assumed that the CHP could be on and on full capacity at any timestep, regardless of its state in the previous or following timesteps. The model does not account for plant downtime, maximum full load hours per year nor minimum load, as introducing such constraints would have required introducing binary variables with the corresponding increase in computational time.

A gas engine CHP provides heat along two vectors - its exhaust fumes and the engine heat that is captured by the cooling oil (Vašek Novotný, 2020). If the CHP is supplying a DHN, both the fumes and the oil are ran through heat exchangers and the heat is transferred to the DHN supply (Vašek Novotný, 2020). A gas engine is a back pressure device in which heat and electricity are produced at a fixed ratio of about 0.95-0.99 units of heat per unit of electricity (Danish Energy Agency, 2024). If the CHP works in power-only mode, the fumes are vented directly in the atmosphere. The cooling oil is passed through another heat exchanger that dissipates in a similar way. It is thus assumed that:

- The ratio between heat and electricity output is 1:1
- The operator could simultaneously use the atmospheric exchanger and the DHN exchanger. Then, the power output can be ramped up to the maximum during moments of high electricity prices to produce the maximum amount of electricity. The heat demand of the DHN is covered fully and any leftover heat is released to the atmosphere.

The possibility of working in electricity-only mode is achieved by creating a dummy plant in the model, called CHPe. It has the same installed capacity as the CHP unit, and it has no capital or fixed O&M costs. The produced electricity is accounted for when calculating the variable O&M costs, costs of fuel and CO_2 permits and the emissions of particulate matter. The variable O&M costs of the electricity-only mode are 90% of the regular variable O&M (Danish Energy Agency, 2024). The production of both heat and electricity has a thermal efficiency of 96%, compared to the 44% of the electricity-only mode. An advantage of having

two “separate” power plants is that the energy conversion efficiencies of the two processes can be handled separately (Equation 1, Equation 2).

$$Input\ fuel_{CHP,t} = \frac{E_{CHP,t} + Q_{CHP,t}}{\eta_{CHP}} \quad \text{Equation 1}$$

$$Input\ fuel_{CHPe,t} = \frac{E_{CHPe,t}}{\eta_{CHPe}} \quad \text{Equation 2}$$

Another simplification is that it is assumed that the CHP’s CO_2 emissions are covered by the EU’s emission trading system regardless of its size. This is not completely accurate, as the directive applies only to units larger than 20 MW of thermal input (European Commission, 2023). The boiler (the only other fossil-fuelled system) is limited to below 20 MW of thermal input, thus being permanently excluded from the emission trading system.

Thermal energy storage

Modelling the storage unites posed several distinct challenges that required particular assumptions to deal with. The two technologies overlap in the capacity range they offer – 500:10 000 m^3 for tanks and 5 000:40 000 m^3 for storage pits (Danish Energy Agency, 2018). Besides that, the model has the propensity to construct both when given a choice and to trade energy in-between them; a highly unlikely behaviour in a real-world system. Besides that, capital costs of tanks are non-linear and vary between 130-300 €/m^3 (Danish Energy Agency, 2018) which poses an issue for a linear model.

The simplest way to approach these was to limit the maximum tank size to 6 000 m^3 and select an average capital cost that is appropriate for that range (238 €/m^3). The pit storage is then available from 6 001 m3, thus providing the model with the option to choose any storage size up until 40 000 m3.

Lastly, the charge/discharge limits of the two storage types were fixed to 5 MW and 12.5 MW for tank and pit respectively. The first number is based on the graphs presented by (Dorotić et al., 2019a), and the latter is taken from the description of the Dronninglund pit TES (Sifnaios et al., 2023).

Solar thermal energy

Solar thermal energy can be harvested by a variety of collector designs. The most popular collector types are the flat plate collector (FPC) and the evacuated tube collector (ETC) (Fadzlin et al., 2022). These designs are mounted without tracking mechanisms and do not make use of any reflectors to concentrate the incident solar radiation (Kalogirou, 2004). In general, FPCs are cheaper and offer worse efficiency at similar supply temperatures (Fadzlin et al., 2022; Kalogirou, 2004).

The third modelled collector type are parabolic throughs (PTCs) – more expensive than ETCs but with better performance characteristics. They can achieve that by being mounted with tracking systems that increase the received irradiance and by concentrating the solar rays on a smaller surface. PTCs are not used in district heating networks because of their high costs, but to supply heat to industrial processes or for electricity generation (Tian et al., 2018). A major exception is the DHN in the Danish city of Taars where FPCs and PTCs are arranged in series – the FPCs preheat the heating fluid, and the PTCs deliver the final temperature lift (Tian et al., 2018). By adopting this approach, the capital expenditure on PTCs is minimised, while the inefficiencies of the FPCs are mitigated. This array operation is modelled with a cutoff temperature of 50°C.

The irradiation datasets are downloaded from PVGIS (*PVGIS*, 2024). PTCs are modelled with a separate irradiation dataset compared to FPCs and ETCs to reflect that they do not receive any beam irradiation (Kalogirou, 2004), and that they are mounted on a tracking system. Ideally, the irradiance data of a horizontal N-S axis with E-W tracking would have been used (Figure 3 right) (Tian et al., 2018). Although such tracking offers less cumulative irradiance than a horizontal E-W axis with N-S tracking, it offers more consistent output throughout the year, rather than a peak output in the summer and a relative lack of output during the winter (Kalogirou, 2014a). This is especially beneficial for a DHN where the peak demand occurs during the winter season. No reliable data for E-W tracking was found, however as PVGIS does not support such simulation and thus the data for an N-S system had to be used.

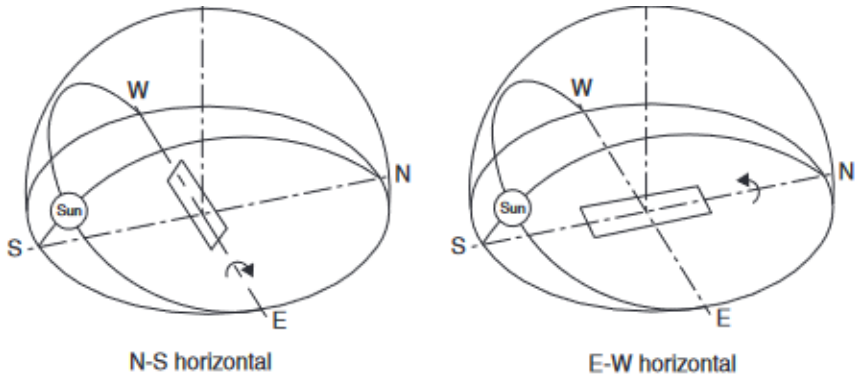

Figure 3: Tracking collector configurations. N-S axis with E-W tracking is shown on the right. Adapted from (Kalogirou, 2014a)

4. Research method

The chapter that follows explains how the characteristics of the different technologies described above are woven into a research method that can accomplish the research objectives of the study.

4.1. Optimisation framework

Optimization models set the objectives for a system under analysis and can be applied to explore trade-offs between different goals, identify extreme conditions or best-case scenarios (Bynum et al., 2021). An optimization algorithm systematically searches for the best solution to a problem within a defined set of objectives and constraints (Nocedal & Wright, 2006). The process begins by defining an objective function, which represents the goal, and needs to be minimised (e.g. emissions) or maximised (e.g., revenue). Constraints are then added to reflect limitations, such as resource availability or physical boundaries (Nocedal & Wright, 2006). A solver is the algorithm responsible for finding the best solution to a given problem (Nocedal & Wright, 2006). Such tool is GLPK (GNU Linear Programming Kit), an open-source software package designed to solve large-scale optimization problems. It provides tools to efficiently model, solve, and analyse optimization problems (Meindl & Templ, 2012).

A way to assess the trade-offs between two goals is the so-called ε boundary condition. One of the goals is set as the objective function of the study. The second is presented as a constraint (ε). The model can then be solved for different values of ε, which provides a range of solutions. The result can then be visualised as a Pareto front of optimal solutions, where the optima considering both functions' objectives is the solution with the shortest distance to the point of intersection, like in Figure 4 (Sporleder et al., 2022). The constraints in a model (ε or any other), can be linear and continuous (referred to as linear programming–LP), and linear and non-continuous (referred to as mixed-integer linear programming–

MILP). Nonlinear problems are divided in the same subcategories (nonlinear programming–NLP and mixed-integer nonlinear programming–MINLP). As a general rule, non-linear and non-continuous problems are more realistic, but are more complex and take longer to compute.

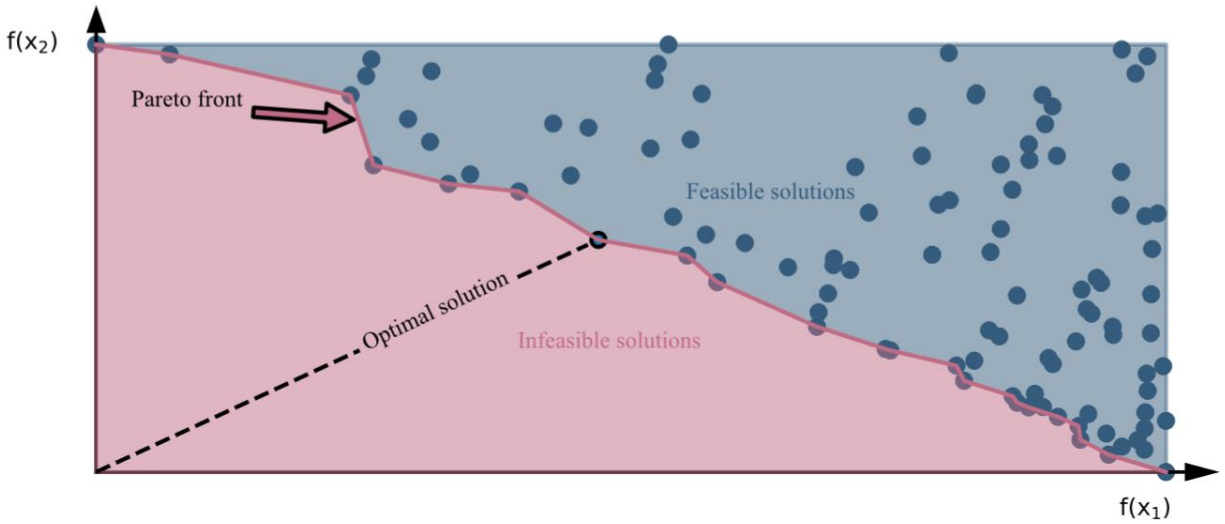

Figure 4: Qualitative graph of a Pareto front for two objective functions, f (x1) and f (x2). Source: (Sporleder et al., 2022).

This research developed a linear programming, single objective model that uses and ε constraint to limit PM2.5 emissions. The latest version of the GLPK solver is used. The study follows closely the steps of (Dorotić et al., 2019a), who find the lowest costs of a portfolio of generators in a DHN for different maximum thresholds of GHG emissions and exergy destruction (a proxy for energy efficiency). In a similar vein, the portfolio of generators that can offer the lowest energy costs per threshold of PM2.5 emissions is searched for.

4.2. Model structure

With the background theory of what constitutes an optimisation model sketched, the following section delves into how the model of this research is constructed.

District heating model

A schematic overview of the model is presented in Figure 5. The model is capable of selecting the installed capacities of the available technologies (marked in white), and of determining their heat and electricity outputs (marked with black and yellow flow arrows). The outputs are impacted by the relevant external conditions: ASHP's coefficient of performance and the efficiency of solar thermal panels are temperature dependent and all solar technologies are impacted by the irradiance. The Bulgarian hourly electricity prices of 2017 are sourced from (EMBER, 2024) and the Bulgarian gas prices for consumers who purchase between 100 PJ and 999 PJ are obtained from (Eurostat, 2022). The price of the EU CO_2 credits is fixed at €50/tonne. It reflects an assumption that in the long run the prices of carbon emissions will stabilise around somewhat lower levels than those at the time of writing (€53/tonne - €84/tonne in the last twelve months (*EU Carbon Permits*, n.d.)). The hourly demand profile is derived from the heat consumption in Orlandovtsi in 2017, the only year for which this data is available. The precise steps related to the derivation are explained in the Hourly load heat profile section.

It is important to stress that the electricity prices are not affected by the sales of any of the generators in the model. It is assumed that the combined generation of the modelled system (below 50 MW) is not large

enough to influence the Bulgarian network with its loads between 2.5 GW and 7 GW (ECO, 2024). Other simplifying assumptions are that the electricity production of the CHP and PV units do not cause grid congestion and can always sell all electricity they produce.

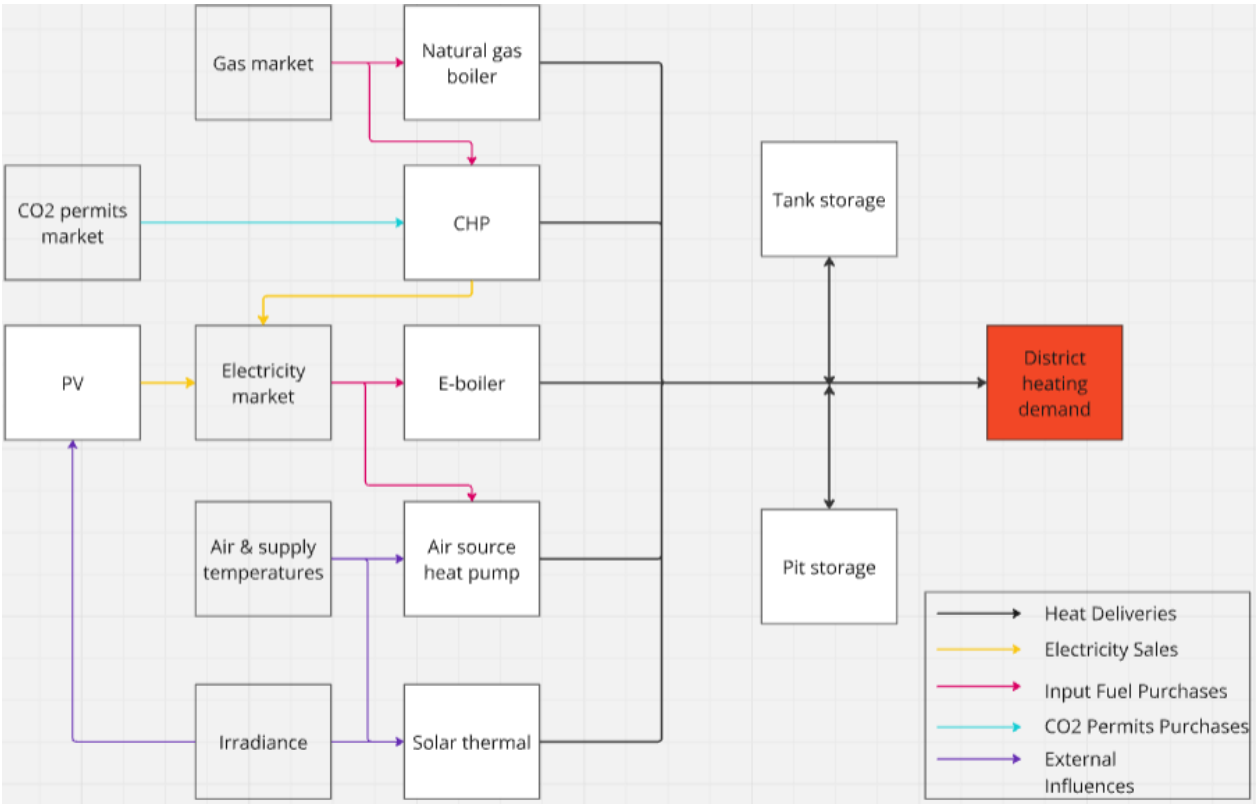

Figure 5: Overview of the district heating model

Objective function

The objective function of the study is the minimisation of the total present costs of the system. An epsilon-constraint method is applied to reflect the effect of different particulate matter emission caps on the cost of the system. The model is ran for one year with an hourly resolution (8760 timesteps) and all generators are installed in that first year of operations. In order to simplify the calculation of the present value of the total system costs, it is assumed that the rest of the years of the system's lifetime will be identical to the first. This allows to apply an annuity factor *alpha*, calculated with a system lifetime of 25 years for all technologies (Dorotić et al., 2019a) and a discount rate of 3% (Tian et al., 2018).

The objective function has two summation signs – one for temporal scale (t), and for technology type (i). The cost function has the following expression (Equation 3), where f_{obj} represents the total discounted costs. C_{DHN} are the capital costs of building the district heating network, $C_{investment,i,n}$ is the discounted investment cost of technology *i*, $C_{fuel,i,t}$ is the fuel cost for technology *i* in a time step *t*, $C_{O\&M,i,t}$ is the operation and maintenance (O&M) cost of technology *i* in a time step *t* (accounting for both fixed and variable operational costs), while $Income_{i,t}$ is the additional income of technology *i* in a time step *t*. The last term has a negative sign because it lowers the total cost of the system and it represents the electricity sales.

$$f_{obj} = C_{DHN} + \sum_{i} C_{investment,i} + \frac{\sum_{t=1}^{8760} \sum_{i} (C_{fuel,i,t} + C_{O\&M,i,t} + C_{CO2} - Income_{i,t})}{alpha}$$ Equation 3

For simplicity and ease of understanding, the total discounted costs are converted in a levelized cost of heat (LCOH) using Equation 4, where $Q_{tot,y}$ is the total heat delivered by the DHN over a year.

$$LCOH = \frac{f_{obj} * alpha}{Q_{tot,y}}$$ Equation 4

The impact of the system on air pollution is expressed with the following equation (Equation 5). As explained in section 3.1, the particulate matter impact category of ReCiPe2016 is used as an air pollution index. f_{PM} is the total system's particulate matter emissions summed across all pollutants *p*. $Q_{i,t}$ and $E_{i,t}$ are the heat and electricity outputs of technology *i* for a time step *t* and η_i the efficiency of technology *i*. The emission factor for technology *i*, of pollutant *p* ($e_{p,i}$) is taken from (EEA, 2023a), and the pollutants are weighted using the ReCiPe characterisation factors (w_p) taken from (RIVM, 2017). Natural gas is the only considered input energy that emits particulate matter; thus the values of $e_{p,i}$ for the technologies that convert electricity or solar energy into useful outputs are by default zero. The units of the function are kilograms of $PM_{2.5}$-equivalents.

$$f_{PM} = \sum_{t=1}^{8760} \sum_{i} \sum_{p} (e_{p,i} * w_p * \frac{Q_{i,t} + E_{i,t}}{\eta_i})$$ Equation 5

Equations 3 and 5 are combined together using the ε constraint method. For each scenario, the system is initially ran without any constraints on the particulate matter emissions. The total emissions during these runs are recorded and then passed to the model as the maximum possible emissions for their respective scenario. Ten iterations of the model are ran per scenario, in which the maximum allowed emissions are decreased by 10% of the initial maximum value. In this way, all scenarios converge on having one run with 0 allowed emissions. The results are then structured in a Pareto front.

The most suitable solutions in the different scenarios are found using the knee-point method (Dorotić et al., 2019a; Sporleder et al., 2022). The most suitable solution per scenario is the point on the Pareto front that has the lowest Euclidean distance to the Utopia point. The Utopia point is an ideal, but unfeasible solution where both functions achieve their optimal values – the minimum possible cost found in the scenario and exactly 0 emissions of particulate matter.

Decision variables

The optimization is carried out for the following set of decision variables: the size of supply technologies (P_i), including thermal storages' size (TES_size_i), solar thermal aperture area A_{ST}, and the hourly operation of each technology (heat output $Q_{i,t}$, $TES\_var_{i,t}$ and electricity output $E_{i,t}$) for a whole year. For computational purposes the state of charge of the two TES units is defined as a decision variable, which the model continuously calculates ($SOC_{i,t}$).

Hourly load heat profile

This research considers an expansion scenario, in which the DHN serves the entire neighbourhood of Orlandovtsi. As of 2017 this amounts to 43 GWh/yr; this value was increased by 50%. In the 2000-2022 period, electricity consumption per capita in Bulgaria increased by 51% (IEA, n.d.). It is assumed that over the coming decades a similar increase will take place again, especially in Sofia, given the population growth the city is experiencing (Dimitrova & Velizarova, 2021) and the suppressed energy consumption in energy poor households (Peneva, 2022). The cost of the system is calculated based on the data of the Pan-European Thermal Atlas, Peta version 5.2 (Möller, 2021). According to that research, the construction costs of a DHN in Orlandovtsi are circa 15 €/GJ.

Converting this total consumption value into an hourly heat profile requires splitting it in demand for domestic hot water (DHW) and space heating (SH) (Conolly et al., 2015). DHW demand is roughly 33% of the total yearly heat demand in Sofia (GIS Sofiaplan, n.d.). Following the methodology of (Dorotić et al., 2019b), it is assumed that DHW demand follows the exact same pattern every day. Clearly, this is a simplified presentation of reality, yet as it affects just a third of the overall consumption, it is assumed that it has a minor influence on the overall result. The total yearly DHW consumption is divided by 365 days and an the respective hourly weight is assigned to each hour of every day ($Q_{DHW,h}$).

Estimating the space heating demand is based on the heating degree hours for the city of Sofia (Conolly et al., 2015) while taking into account that district space heating in Sofia is available only between 01.10 and 30.04 (Toplofikatsiya Sofia, n.d.). A heating degree hour (HDH) is the difference between a set-point temperature (16°C for the Balkans, according to Conolly et al.) and the outside temperature. Data on the outside hourly temperature in 2017 is available in the ERA5 database (C3S, 2018). Once the total number of HDH for 2017 is known (HDH_y), an average factor that relates HDH and the total yearly SH ($Q_{SH,y}$) can be calculated. The total heat demand in an hour ($Q_{tot,h}$) is thus presented in Equation 6, and the yearly heat demand is visualised below (Figure 6).

$$Q_{tot,h} = Q_{DHW,h} + Q_{DHW,y} * \frac{HDH_h}{HDH_y} \qquad \text{Equation 6}$$

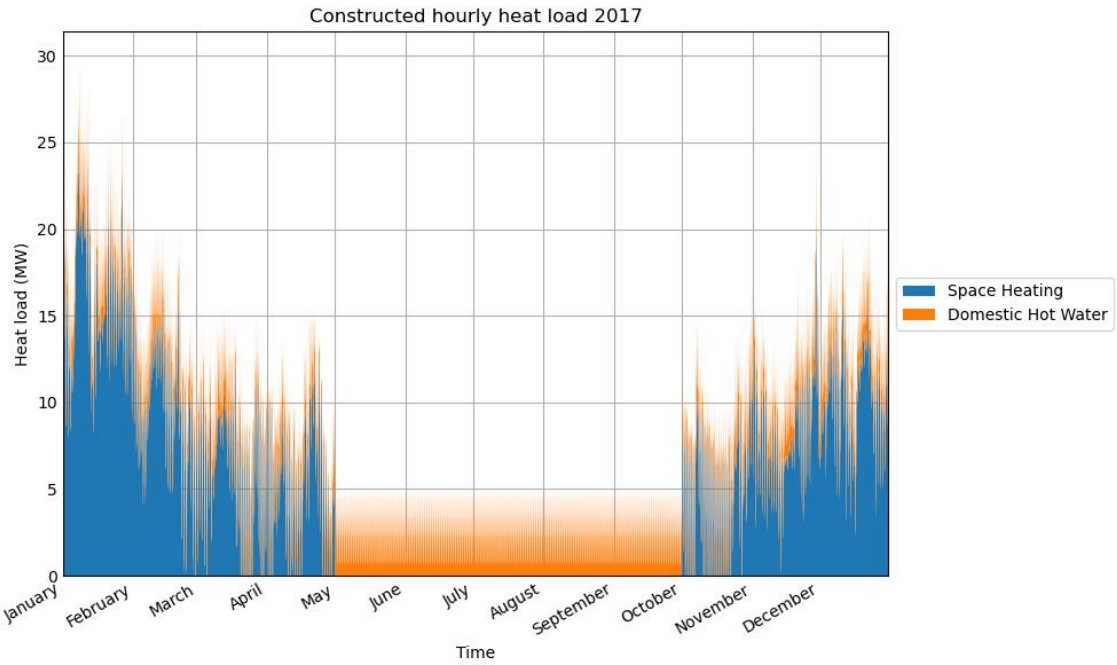

Figure 6: The constructed hourly heat load with a 50% demand increase compared to 2017

It is important to stress that 2017 is the only year for which heat consumption data is available. As per the method described above, that requires accessing temperature data about 2017 too. For consistency purposes, in all other datasets – solar irradiance, gas and electricity prices – 2017 values are taken in the core group of scenarios that forms the backbone of this study. Further information can be found in section 4.3 Scenarios.

Key constraints

The following section introduces the crucial model constraints that make the model function. They underpin the main assumptions presented in the Energy technologies section.

CHP

As already explained, the CHP unit can produce either electricity and heat in a 1:1 ratio, or only electricity. The first aspect is achieved by enforcing a constraint that the two outputs should be equal (Equation 7). Both are decision variables that the model can choose freely, subject to the constraint that they cannot be bigger than the installed capacity P_{CHP} of the CHP unit. Conversely, the heat output of the dummy plant CHPe is fixed to zero, while its electricity output is limited by Equation 8. This way, the model cannot produce more electricity in a given timestep than the CHP unit has the capacity to, even if it is engaging both the CHP and the CHPe dummy plant.

$$E_{CHP,t} = Q_{CHP,t} \qquad \text{Equation 7}$$

$$E_{CHPe,t} \leq P_{CHP} - Q_{CHP,t} \qquad \text{Equation 8}$$

TES

The TES losses are modelled with Equation 9, as per (Dorotić et al., 2019a). This equation applies to both storage types individually with their respective loss factors. SOC_t is the state of charge of a TES unit at a particular step in time. TES_var_t is the amount of energy the TES absorbs or releases per timestep. The used sign convention is that if TES_var_t is negative, the state of charge increases and energy is withdrawn from the system.

$$SOC_t = \frac{SOC_{t-1} - TES\_var_t}{1 + loss} \quad \text{Equation 9}$$

$$SOC_{t=1} = SOC_{t=8760} = SOC_{start-end} * TES_{size} \quad \text{Equation 10}$$

The constraint expressed by Equation 10 ensures that the TES units end the year with the same state of charge as they started with. $SOC_{start-end}$ for the buffer thermal storage is equal to 50%, as it is assumed it charges and discharges on a daily basis, while for the pit storage it is put to 0% since it is charged during the summer season and is completely discharged during the winter season (Dorotić et al., 2019a).

Solar technologies

The efficiency of solar thermal panels is dependent on the temperature at which they operate and the temperature they deliver heat at (Kalogirou, 2014b). This relationship is expressed in the following formula (Equation 11Equation 4) (Kalogirou, 2014b). η_0 is zero-loss efficiency, a_1 is first order heat loss coefficient, a_2 is second order heat loss coefficient and T_{amb} is the temperature of the surrounding air. T_m is the mean solar thermal collector temperature, calculated as the average between the temperature of the input and output flows (Dorotić et al., 2019a; Tian et al., 2018). For the ETC collectors, these are the return and supply temperatures of the DHN, respectively. As already explained, the FPCs and PTCs work in an array; thus the output temperature of the FPC is 50°C, which is the input temperature of the PTC. Finally G_t is the global solar irradiance for ideal azimuth and elevation angles obtained from (*PVGIS*, 2024) for the different collector types. For more information, see section Solar thermal energy.

$$\eta_t = \eta_0 - a_1 * \frac{T_{m,t} - T_{amb,t}}{G_t} - a_2 * \frac{\left(T_{m,t} - T_{amb,t}\right)^2}{G_t} \quad \text{Equation 11}$$

The output of the solar thermal types (subscript *c*) is calculated with Equation 12, where A_c is a decision variable.

$$Q_c = \eta_{c,t} * A_c * G_{c,t} \quad \text{Equation 12}$$

A summary of the coefficients of the solar thermal panels is presented below (Table 2). The EPC data are taken from the Solar Keymark database (*Solar Keymark*, n.d.) and the PTC and FPC from (Tian et al., 2018).

Table 2: Solar thermal coefficients

	EPC	PTC	FPC
ni0	0.737	0.75	0.839
a1	0.504	0.04	2.596
a2	0.006	0	0.016

Model	TVP Solar MT - Power v4	Arcon-Sunmark A/S	HEAT boost 35/10

The FPC-PTC array is modelled based on the mass flow $\dot{m}$ between the two panel types (subscript *c* in Equation 13). $Q_{c,t}$ is the output of the solar thermal panel in question per timestep (in MWh/h which simplifies to MW), c_v is the specific heat capacity of water, the assumed heat exchange fluid. The mass flows through the two parts of the array need to be equal at each timestep up to a tolerance value of 10kg/h (Equation 14). This was introduced to reduce the calculating time of the model. As the PTC-FPC array was never selected by the model, this tolerance value has no impact on the accuracy of the model.

$$\dot{m} = \frac{Q_{c,t}}{c_v * (T\_outlet_{c,t} - T\_inlet_{c,t})} \quad \text{Equation 13}$$

$$\dot{m}_{PTC,t} = \dot{m}_{FPC,t} \pm \varepsilon \quad \text{Equation 14}$$

The output of the photovoltaics was far easier to calculate, given the vast amount of freely available resources on that topic. The hourly capacity factor of 1 kW of PV panels located at optimum tilt and azimuth in Sofia was taken from PV GIS (*PVGIS*, 2024). The hourly electrical output is then calculated as follows (Equation 15) with P_{PV} as the decision variable. As it is assumed that the electricity market can always absorb the full output of the PV farm, no provisions are made in the model to simulate production curtailment.

$$E_{PV,t} = CF_t * P_{PV} \quad \text{Equation 15}$$

ASHP

The coefficient of performance (COP) of a heat pump is dependent on the temperatures of the cold and hot sinks it is operating between (Danish Energy Agency, 2024). The hourly COP is calculated using the Lorentz method. This method is preferable for "stepped" Carnot cycles, where heating and/or cooling are done in several steps. With such high-temperature increases, a heat pump system typically includes several condensers in series meaning that the system consists of several Rankine cycles (Danish Energy Agency, 2024). The equation for the real COP is given below (Equation 16Equation 4), where $\eta_{Lorentz}$ shows how well the heat pump in question approximates an ideal device.

$$COP_h = \eta_{Lorentz} * \frac{T_{lm,sink,h}}{T_{lm,sink,h} - T_{lm,source,h}} \quad \text{Equation 16}$$

$$T_{lm} = \frac{T_{in} - T_{out}}{\ln\left(\frac{T_{in}}{T_{out}}\right)} \quad \text{Equation 17}$$

T_{lm} is the log mean temperature of the source and sink heat exchangers (Equation 17). A table with the respective temperatures is provided below (Table 3).

Table 3: Relevant temperatures at the ASHP's heat exchangers

	T_{in}	T_{out}

Source	The ambient air temperature.	The ambient air temperature cooled by 5 Kelvin.
Sink	The return temperature of the DHN.	The supply temperature of the DHN.

Energy balance

Lastly, the heat supply and demand in the system should be equal on every timestep. This is expressed in Equation 18, where $Q_{i,t}$ is the hourly heat output of technology *i*, and $TES\_var_{s,t}$ is the hourly dynamic behaviour of storage unit *s*. A small tolerance of up to 0.1 Wh/h is given to the model to speed up the calculation process. The maximum possible cumulative deviation is 0.88 kWh per year, compared to total heat deliveries of 64 GWh/y. Given the vast discrepancy between these two values, it is assumed that the model is sufficiently accurate.

$$Demand_t = \sum_i Q_{i,t} + \sum_s TES\_var_{s,t} \pm tolerance \quad \text{Equation 18}$$

4.3. Scenarios

The scenarios explored in this work are marked by bundles of technology that are available to the model to optimise. These bundles are then subjected to varying external conditions, namely input energy prices and district heating supply temperatures. The rest of the chapter is dedicated to explaining the structure of this matter.

Technology bundles

Business as usual

The business-as-usual (BAU) bundle includes the standard technologies used in DHNs for the last century – fossil fuel boilers and CHPs and steel tank storage (Danish Energy Agency, 2018; Werner, 2017). The fossil fuel of choice is natural gas, reflecting the pronounced role this energy carrier in the European heating sector (Werner, 2017). Electric boilers are included in too, (a) to give the BAU scenario a possibility to reduce its particulate matter emissions to zero and (b) to reflect the trend that some fossil fuel DHNs incorporate power-to-heat technologies[2].

Two scenarios are extracted from the technology bundle, dubbed econ and opt. BAU econ shows the result of the cost minimisation optimisation in which there is no limit to the particulate emissions. BAU opt is the best solution of the Pareto front for the BAU technology bundle.

All technologies

As the name suggests, the "All technologies" scenario includes all technologies introduced in 3.2 Energy technologies – natural gas boiler and CHP, solar thermal energy, air source heat pump and PV. Both tank

[2] An example in this regard is the Rostock DHN, which currently runs on coal and natural gas and its ambition to integrate a 20 MW e-boiler (KNG, n.d.; SW Rostock, n.d.).

and pit TES are available for daily and seasonal storage, respectively. It is represented by the best solution of the Pareto front for the bundle.

RE ad RE-ST

Lastly, there are two scenarios where only renewable energy sources are included. This reflects the understanding that in the future electricity (generated by low-carbon sources) will form the backbone of the energy system (IEA, 2024). Both storage types are included too.

The only difference between the base renewable energy (RE) scenario and the renewable energy with minimum solar thermal (RE-ST) is that in the RE-ST half of the available land needs to be dedicated to solar thermal energy. Solar thermal is the only heat generator in the studied set of technologies that does not require any paid inputs (electricity or natural gas, respectively). On the other hand, it has a highly seasonal pattern of production, which means that other generators are needed to cover the rest of the demand. The goal of this scenario was to explore the interaction between these dynamics.

No Pareto front was calculated for these technology bundles, as the emissions are by default equal to zero.

External conditions

Among the factors that dictate the price performance of a DHN network are the portfolio of generators (Dorotić et al., 2019a), the supply temperatures that are required (Werner, 2022) and the prices of input energy (Garbev, 2023). These aspects are mutually connected – the supply and return temperatures constrain the integration of heat generators. This is especially the case for renewable energy sources (Lund et al., 2014) – all things other things being equal, lower supply temperatures increase the efficiencies of solar thermal energy and heat pumps (see Equation 11, Equation 16). The portfolio of generators on the other hand dictates what energy conversions take place and thus to what price fluctuations the DHN is exposed. For example, a DHN that is powered entirely by natural gas will be hit harder by a sudden gas price hike, compared to a DHN that uses solar thermal with seasonal storage and natural gas is used only in moments of peak demand.

The developed scenarios attempt to shed light on the interplay of these factors in the context of Orlandovtsi. Table 4 gives an overview of the performed model runs. The most crucial difference between them is whether they are full optimisation runs (marked with a cross) or simpler dispatch runs (marked with a dot). In a full optimisation run the model can determine both the installed capacities of the available technologies and their energy production at every timestep. In a dispatch run, in contrast, the model is given pre-determined installed capacities and is asked to find the optimal way of meeting the demand. Importantly, the model still calculates the LCOH in the same way as in the full optimisation, assuming that the pre-defined conditions will remain the same every year during the system's lifetime. The dispatch runs are performed using the optimal capacities found in the 70°C static, 2017 energy prices scenario.

The rest of the section delves into explaining the different prices and supply temperatures.

Table 4: Overview of the investigated scenarios[3].

Supply Temperatures	Energy Prices	BAU Econ	BAU Opt	All Technologies	Renewable Sources	Renewables with minimum ST
70°C static	**2017 energy prices**	x	x	x	x	x
	2018-2022 energy prices	.	.	.	.	.
	2022 energy prices	x	x	x	x	x
60°C static	**2017 energy prices**				x	x
100°C dynamic	**2017 energy prices**				x	x

Supply temperatures

As already explained, the supply and return temperature in a DHN have a significant impact on the operation of the network and the generators used. Cost reduction gradients have been estimated to be slightly above 0.1 euro/MWh per °C reduced in networks based on fossil fuels, and 0.5 euro/MWh per °C reduced in networks based on renewables (Werner, 2022). Experimenting with different supply temperatures in this work has two aims, explained below.

70°C and 60°C

Firstly, no quantification of the supply temperature dynamics of a DHN with a peak supply temperature of 70°C was found in the literature. Therefore, a constant supply temperature of 70°C and 60°C were tested, to bracket the best and worst possible performance of such system. These model runs were important for ensuring that the modelled network *in Orlandovtsi* is accurately represented.

The selected supply and return temperatures of the DHN are 70°C and 35°C respectively, based on the work of (Werner, 2022). These are the best practice temperatures of a well-maintained DHN that does not rely on any additional heating of the supplied hot water by the consumers (Werner, 2022)[4]. It is therefore assumed that if a new network is built in Orlandovtsi from the ground up, the best-practice technology will be used.

It is important to mention that these temperatures depend on the external conditions. In moments of peak demand such a network will increase its supply temperature to the maximum of 70°C. Assuming constant supply temperature of 70°C is the most conservative approach possible in such a system and it would place the highest strain on renewable generators. Put simply, a real-world system would likely supply water at lower temperatures during the summer months of high outside temperatures and low demand. 60°C is the lowest possible supply temperature, linked to the need to safeguard installed hot water tanks and hot water circulation against Legionella growth (Werner, 2022). Therefore, a diametrically opposed scenario was developed in which the system functions at a constant supply temperature of 60°C. This is a technically impossible scenario aimed at showing the performance of the system at the lower temperature bound.

[3] Crosses indicate model runs where a full optimisation was performed. Dots indicate model runs when fixed installed capacities were put, and the model was used to dispatch them in the best possible way. All dispatch runs used the optimal capacities found in the 2017 conditions, 70° scenarios of their particular technology bundle.

[4] Also known as 4th generation network.

100°C

Secondly, supply temperature reductions require an intervention from the DHN operator to physically change aspects of the system to change the way it functions, compared to the initial design – install new pipes, consumer sub-stations, pumps, etc. (Gadd & Werner, 2014). The DHN in Sofia operates at 130°C peak supply temperature, and it is assumed that it would make investments in its reduction in the future. Such investments and their associate costs are bigger, the bigger the targeted supply reduction (Gadd & Werner, 2014). Exploring different supply temperatures in this work is used to give an estimate of how large the expected benefits of such efforts are for reductions of the peak supply temperature down to 100°C, 70°C and 60°C respectively.

Data on the dynamic behaviour of the supply temperature in a DHN with higher temperature was found (Dorotić et al., 2019a) and it is shown below (Figure 7). In this scenario, return temperature of 50°C was used (Gadd & Werner, 2014). This scenario was developed to shine a light on two aspects: (i) the dynamic behaviour of the model with regard to the supply temperature and (ii) to provide a worst-case scenario of sorts for renewable energy technologies. Given their synergy with lower supply temperatures and the fact that high supply temperatures would occur precisely during peak winter loads, it was decided that such a scenario has merit. In this scenario the cutoff temperature for PTC-FPC is 60°C.

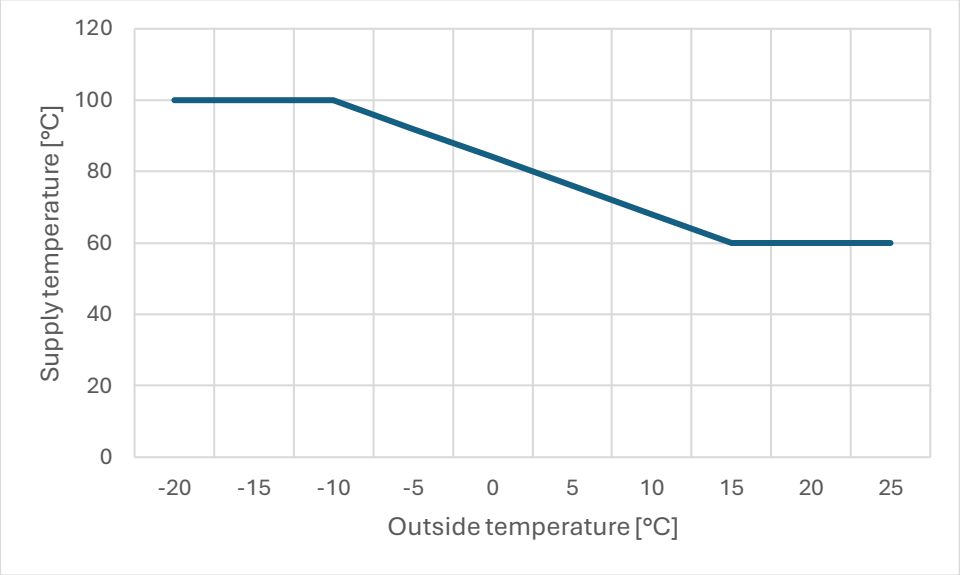

Figure 7: DHN supply temperature as a function of outside temperature. The linear dependence can be described as y = -1.6x+84. Source: (Dorotić et al., 2019a)

Energy prices

In order to explore the effect of varying energy prices on the DHN's performance, the electricity and gas prices of the 2017-2022 period were used. This timeframe covers both the COVID pandemic and the Russian invasion of Ukraine with the shocks both of these events caused to the energy system. An in-depth illustration on the way these prices have shifted is available in Appendix C: Energy prices.

The vastly different trends in the energy markets in the last few years raise the question of which conditions should be implemented as the baseline in the model. Two diverging assumptions can be made – either that the high prices are just a temporary spike and that the market will return back to the pre-invasion, pre-pandemic normal, or that the 2021-2023 conditions are the new normal and that future energy systems should be built with them in mind. A fundamental issue the model faces in that context is

that to calculate the LCOH, it needs to assume that the entire lifetime of the system will consist of 25 identical years. This compounds the importance of selecting an adequate baseline year.

The study approaches this conundrum by choosing 2017 as the baseline year for the full optimisation, and then conducts dispatch models for the 2018-2022 conditions. The LCOHs of all these runs are recorded and compared to one another. This way, each optimal technology scenario developed with the 2017 conditions in mind is exposed to the possibility that the coming 25 years will be different to what was envisioned. By conducting such analysis for each scenario separately this work highlights how dependent different technology mixes are to correct initial assumptions. Lastly, a full optimisation run was performed based on the 2022 conditions. 2022 is the most extreme year in the used timeframe; by comparing the selected mixes in the 2017-2022 conditions the range of potential outcomes can be estimated. 2017 in particular was selected as the baseline year, for consistency purposes, because the available heat data is from that year.

5. Modelling results

The following section delves into the modelling results. First, an overview of the modelling results under 2017 prices optimisation is presented, followed by in-depth analysis of each scenario. Then, the effects of the change in supply temperature is discussed in detail. Lastly, the outputs of the dispatch models and the 2022 prices optimisations are presented and discussed. Note that additional graphs and tables that illustrate the outputs of the model are displayed in Appendix D: Additional figures.

It is important to stress that the results of the model are measured against two different benchmarks. The emissions of the different scenarios are compared to the emissions of particulate matter and GHG of Orlandovtsi in 2017 (Figure 1 on page 13). The cost of the scenarios, on the other hand, are compared to price of heat in Sofia's DHN asked in the respective year, even though the DHN serves just a small part of Orlandovtsi. The reason behind this is twofold – firstly, estimating the cost of heat for the different energy carriers used by the residents of the neighbourhood and taking a weighted average would have been prohibitative. Second, the costs charged by the DHN in Sofia are uniform in every neighbourhood; thus, if a proposed portfolio of generators can perform better than the price charged across the city, it constitutes an attractive proposition from the point of view for the DHN operator.

5.1. 2017 prices, 70°C

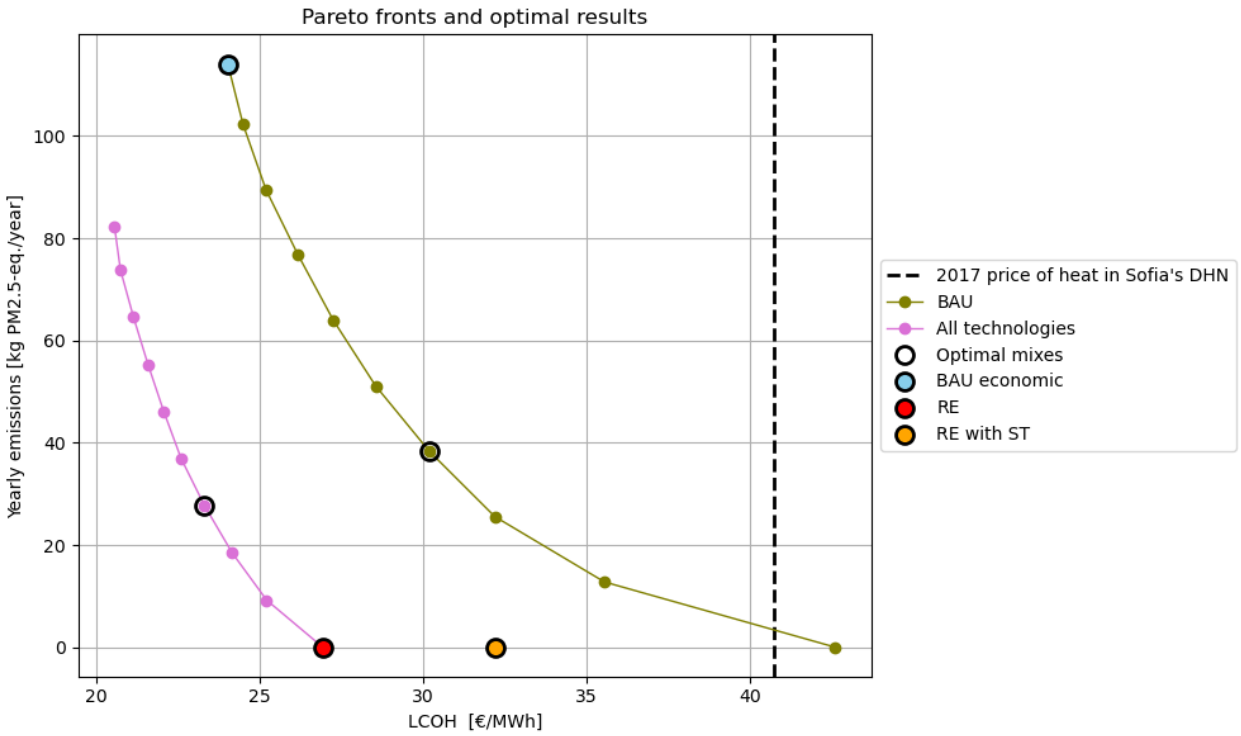

Figure 8: Pareto fronts and optimal results for the combination of 2017 prices and 70°C supply temperature[5]

Figure 8 gives a headline comparison of the different scenarios in terms of levelized cost of heat (LCOH) and particulate matter emissions. Several observations become immediately obvious. First, all proposed scenarios essentially resolve the issue of particulate matter pollution in Orlandovtsi. Even the most polluting technology scenario emits less than 120 kg of PM2.5-equivalent per year, or mere 4% of the 3060 kg emitted in 2017, the reference year. Second, the discussed scenarios are all competitive with Sofia's DHN, even the ones based entirely on renewable energy. The cost-spread across the different scenarios is in fact rather narrow, with less than €10/MWh of difference between the cheapest scenario ("All technologies") and the most expensive one (RE-ST). Third, when comparing the cost-efficiency of the bundle where all technologies were available versus just traditional DHN technologies, it is clear that adding renewable energy technologies consistently lowers system costs – the orchid Pareto front is on the left of the olive one.

[5] Tables with full details on each solution of the Pareto fronts are available in Appendix D1: 2017 prices, 70°C

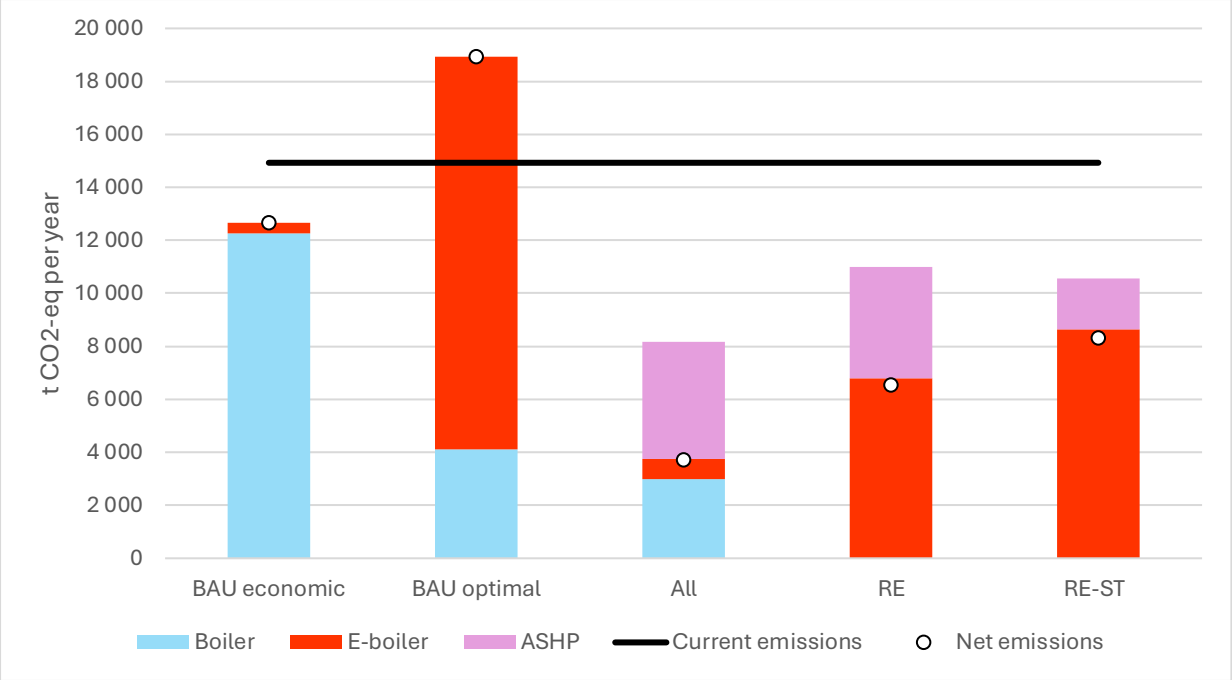

Figure 9: GHG emissions of the different scenarios

Figure 9 gives a comparison of the GHG emissions of the scenarios. The net emissions assume that all electricity generated by the installed PV systems is consumed behind the meter by the power-to-heat units. Alternatively, the total emissions presented by the stacked bars assume that all electrical input energy is taken from the Bulgarian national grid. The value of the current emissions is adjusted to reflect that in the modelled scenarios the quantity of heat delivered has increased by 50% compared to the baseline 2017 value.

Most scenarios have lower GHG emissions than the status quo, in a similar vein to the particulate matter and cost impacts. Considering the more conservative metric, the total emissions, shows that the emissions are reduced by 45% in the case of “All technologies”, between 25% and 30% for RE and RE-ST and 15% in the case of BAU econ, compared to the status quo. BAU optimal increases the emissions by 27% compared to the present conditions.

The scenarios that rely heavily on e-boilers – BAU opt, RE and RE-ST fare worse than the “All technologies” optimal scenario, which uses natural gas. The reason behind this is the relatively high GHG emissions factor of the grid (Statista, 2024). Heat-pumps, on the other hand, offer a more efficient electricity conversion, thus saving on GHG emissions in the RE and RE-ST scenarios in comparison to BAU opt. Lastly, with the current electricity mix in Bulgaria, converting natural gas to heat in a boiler creates less emissions than converting electricity to heat. Full elaboration on the quantities of delivered heat per technology are presented in the coming pages.

Business as usual scenarios

The following section delves deeper into the outputs of the BAU opt and BAU econ scenarios.

Table 5: Installed capacities for the two BAU scenarios

	Installed capacity boiler [MW]	Installed capacity e-boiler [MW]	Installed capacity tank [MWh]	Boiler output [GWh/yr]	E-boiler output [GWh/yr]	LCOH [€/MWh]
BAU optimal	17	16	132	21.1	43.46	30.19
BAU economic	20	5	17	63.38	1.15	24.01

The optimal BAU scenario revolves around the usage of the e-boiler, which delivers roughly two-thirds of the yearly energy demand (Table 5). The BAU econ, on the other hand, supplies the needed heat almost entirely with a natural gas boiler. The boiler installed capacity is almost identical in the two scenarios, with the main difference being how sparingly it is used in the BAU opt due to the emissions threshold. These two scenarios have the second and fourth cheapest levelized heat costs out of the five scenarios.

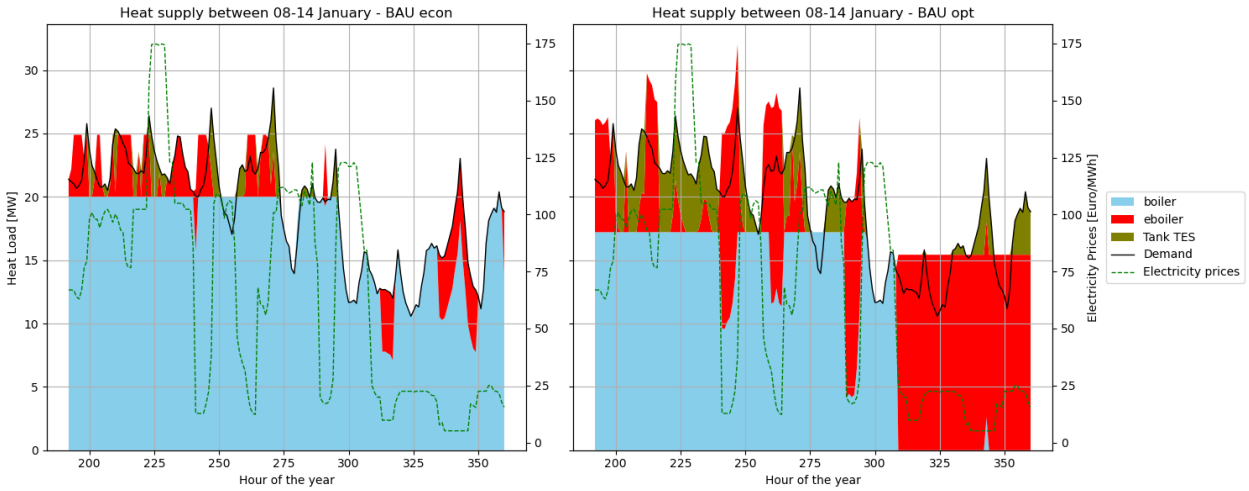

Figure 10: Heat supply by BAU economic (left) and BAU optimal (right) during the week of peak system load

The different behaviour of the two systems is clearly visible when comparing their heat output in the week of highest demand (Figure 10). Both systems operate their respective boilers at full capacity, using the e-boiler and the tank storage to clip the demand. Additionally, the e-boiler is used opportunistically in moments of low electricity prices to save on gas expenditure. In BAU opt, however, this dynamic behaviour is considerably more prevalent, especially during the summer (Figure 11), when both the heat demand and the electricity prices are low (note the different axis scales compared to the previous figure).

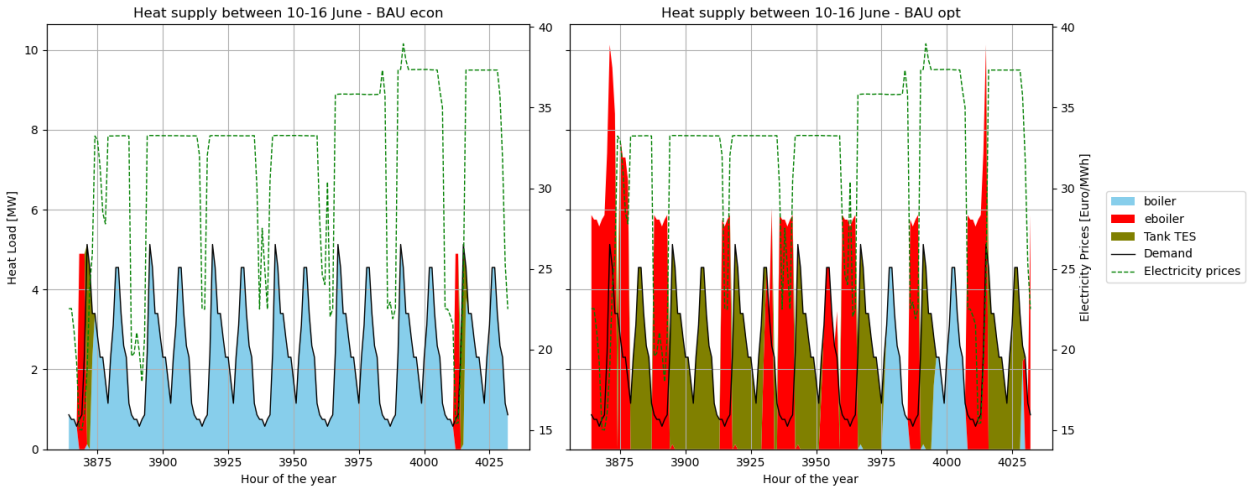

Figure 11: Heat supply by BAU economic (left) and BAU optimal (right) during a week of low load

Renewables scenarios

The two renewables-only scenarios are the third and fifth most expensive scenarios out of the five. They are centred around their respective e-boiler, ASHP and pit TES units (Table 6).

Table 6: Key metrics RE and RE-ST scenarios. Installed capacity (P) per technology and total yearly heat deliveries (Q)

	P e-boiler [MW]	P ASHP [MW]	P ETC [MW]	P pit [MWh]	P PV [MW]	Q e-boiler [GWh]	Q ASHP [GWh]	Q ETC [GWh]	LCOH [€/MWh]
RE	18	8	0	906	10	20.60	44.06	0.00	26.93
RE-ST	23	4	13	2558	5	26.17	18.47	20.23	32.22

In the RE scenario roughly two-thirds of the heat are delivered by the ASHP, while the e-boiler covers the rest. In the RE-ST scenario the three energy sources deliver approximately a third of the heat each, with the e-boiler having the largest role. In the RE scenario the model chooses to cover the entire available land with PV panels. In the RE-ST the pre-defined constraint forces it to dedicate half of the land to solar thermal energy; the rest is used for PV again. Regardless of the scenario, no significant correlation was found between the output of the ASHP or e-boiler and the output of the PV units.

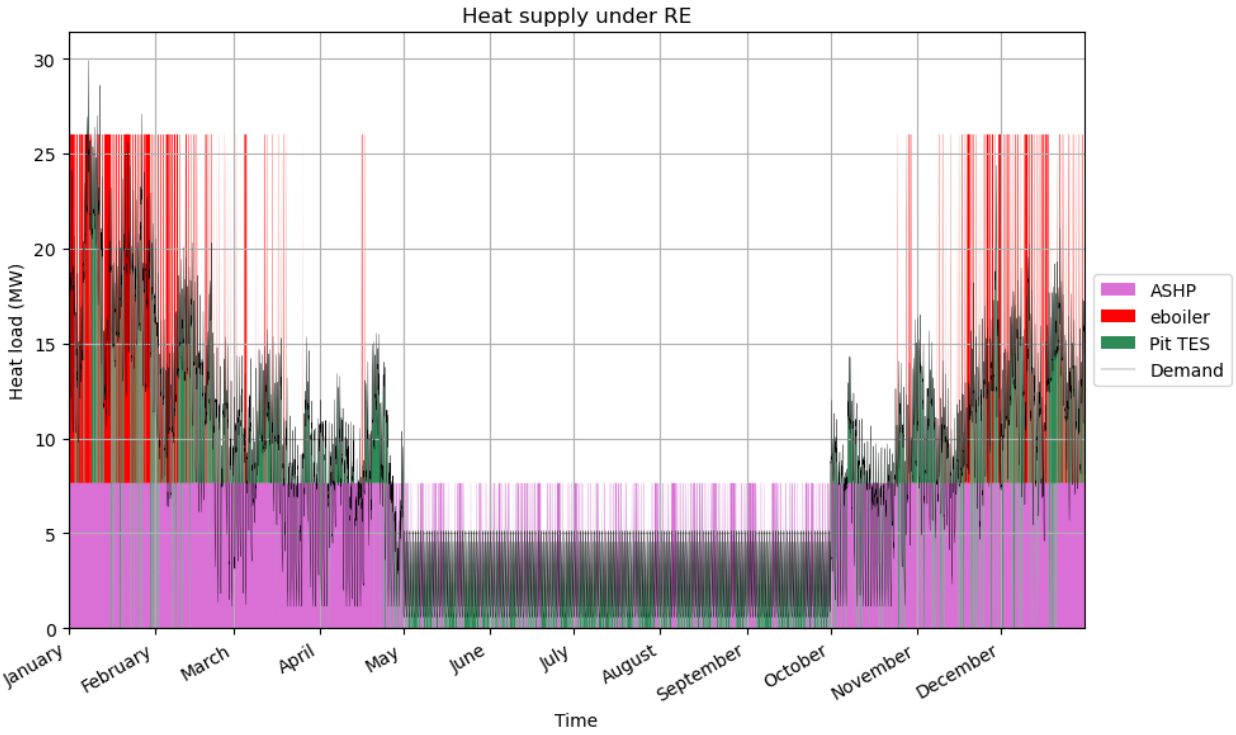

Figure 12: Heat supply RE scenario

The RE scenario revolves around the usage of ASHP to act as a baseload supplier with a capacity factor (CF) of 67% (Figure 12). The e-boiler is used sparingly (CF:12%) when the electricity process are sufficiently low. Its lower investment costs compared to the ASHP (M€0.16/MW_{th} versus M€1.01/MW_{th}) justify this behaviour. In the case of the RE-ST, the pivot of the system is the ETC installation (Figure 13). During the summer it is the sole source of heat in the system, and its role naturally fades away in the winter months. Outside the summer, a smaller ASHP (compared to the RE scenario) again acts as a baseload source of heat with a total CF of 53%. It appears that using the ASHP during the summer in order to fill the energy storage even further is uneconomical. The e-boiler ends up playing a larger role in this scenario wit 39% of the delivered heat, compared to 31% in RE.

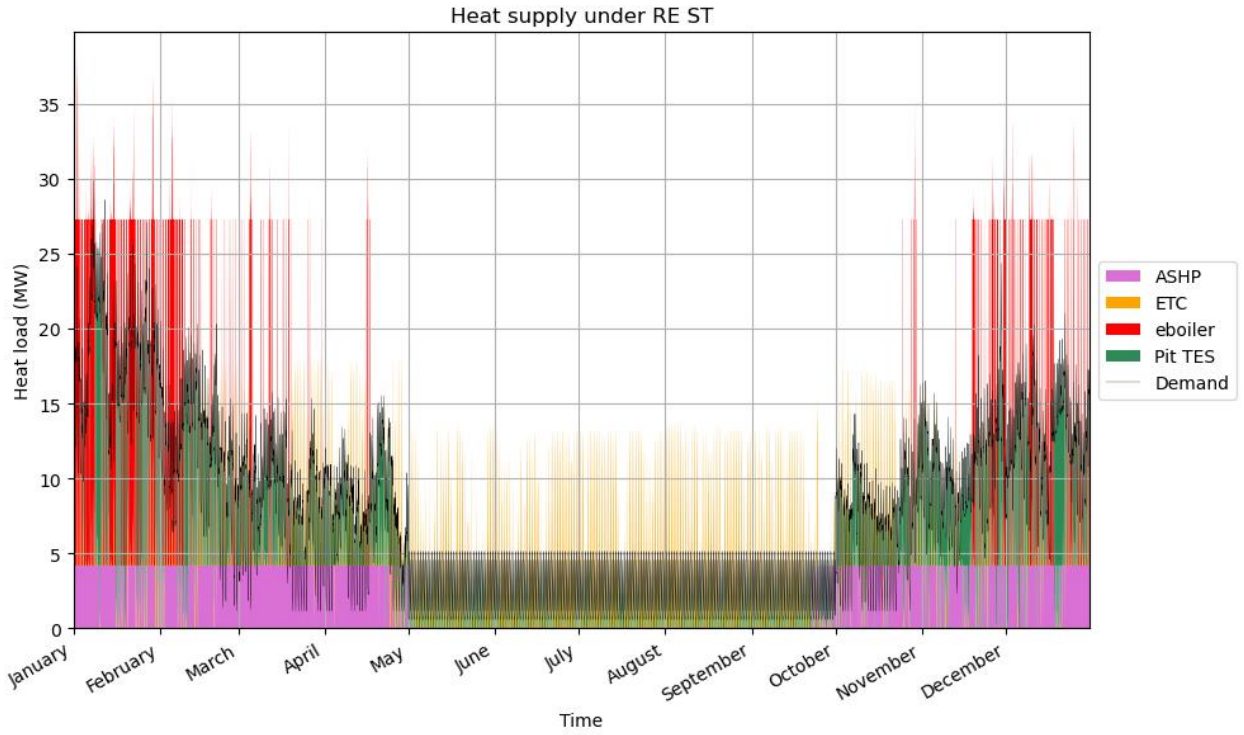

Figure 13: Heat supply RE-ST scenario

The pattern of integration between the heat and electricity markets is evident at every timestep of these scenarios. An example is an autumn week, when both the electricity prices and the heat demand are average to high (Figure 14). For both scenarios the e-boiler operates at its full potential at times of low electricity prices and fills the pit storage. This stored energy is then used at times of high electricity prices, when turning on any power to heat devices is uneconomical. In the case of RE-ST, there is still significant solar output that the ETC can have a meaningful contribution.

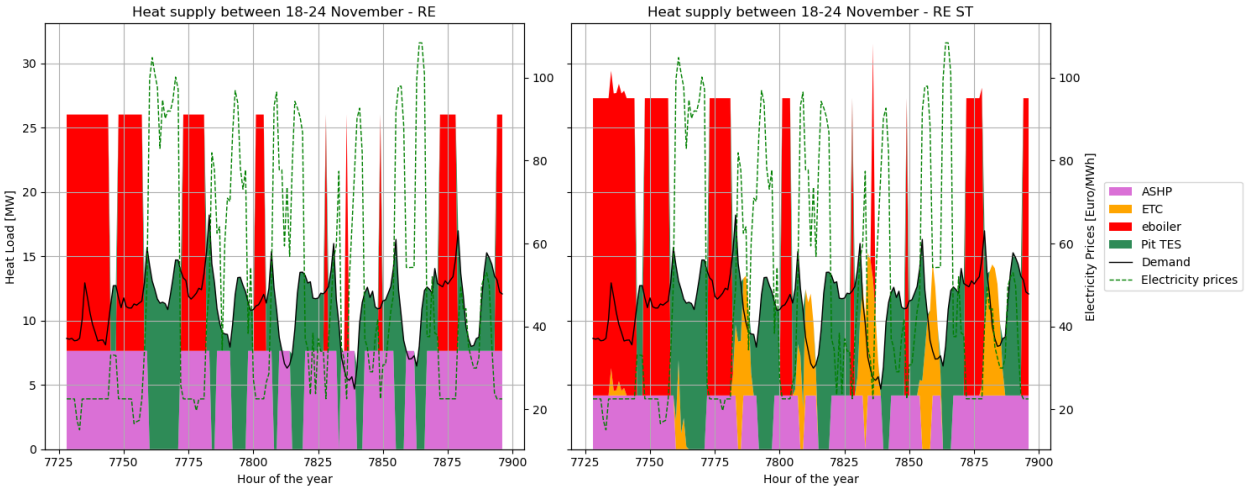

Figure 14: Heat supply during an autumn week by the RE (left) and the (RE-ST)

Overall, these two scenarios involve the two largest TES units among all optimisations made under the 2017 prices and 70°C supply temperature. The two TES follow largely the same pattern of behaviour in the

first five months of the year, when the TES contributions are dictated by the electricity prices (Figure 15). Both TES units reach a sustained peak in their SOC during the autumn; for the RE this is enabled by the overproduction of ASHP heat during the summer months, for the RE-ST is the summer "harvest" of solar thermal energy (Figure 16).

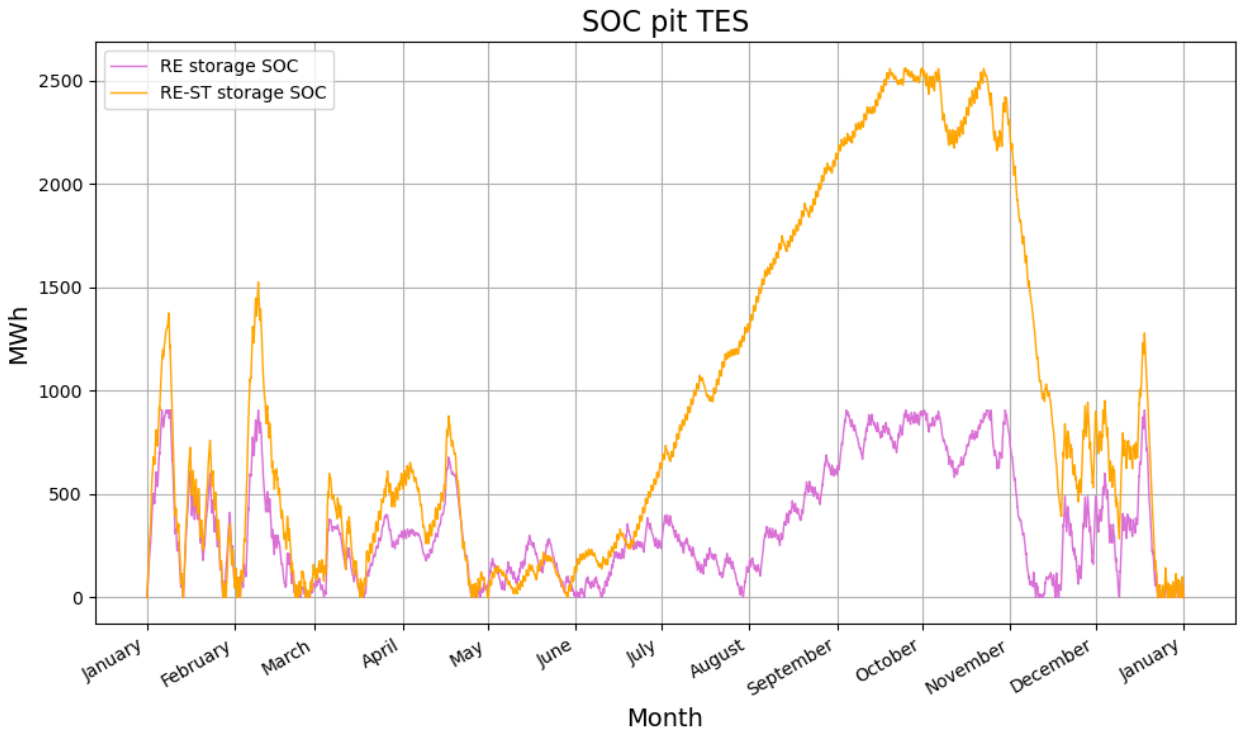

Figure 15: State of charge of the TES units in RE and RE-ST

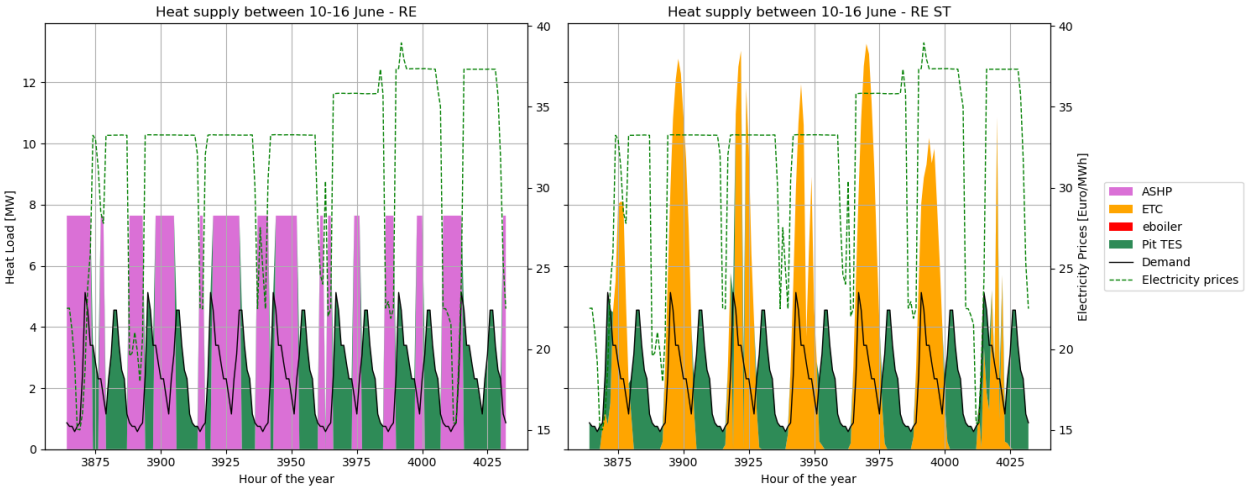

Figure 16: Heat deliveries during a summer week. RE (left) and RE-ST (right)

All technologies

The headline figures of the “All technologies” scenario are presented below (Table 7). At 23.31 €/MWh, this is the cheapest scenario of the five that were developed for the combination of 2017 prices and 70°C supply temperature.

Table 7: Installed capacities (P) and delivered heat (Q) in the "All technologies" scenario with the values of the RE scenario repeated for comparison

	P boiler [MW]	P e-boiler [MW]	P ASHP [MW]	P pit [MWh]	P PV [MW]	Q boiler [GWh]	Q e-boiler [GWh]	Q ASHP [GWh]	LCOH [€/MWh]
All	11	1	8	563	10	15.36	2.23	47.00	23.31
RE	0	18	8	906	10	0	20.60	44.06	26.93

Compared to the RE scenario, this one has the same installed PV capacity (the entire available field) and similar heat deliveries from the ASHP (47 GWh versus 44 GWh). The main differences are the significant presence of a natural gas boiler, the considerably smaller e-boiler and the significantly smaller pit TES. These changes naturally occur together – the model is allowed to emit up to 28 kg of particulate matter, which means that some gas combustion is possible. This results in a smaller e-boiler and enables a more compact storage unit, since there is no need to constantly make use of low electricity prices. All in all, the ASHP and the e-boiler function in an on-off mode where they are either functioning on full power or they are off. The boiler has a more subtle pattern, given it needs to balance the system (Figure 17). A visualisation of the heat supply during the week of highest demand is shown in Figure 18.

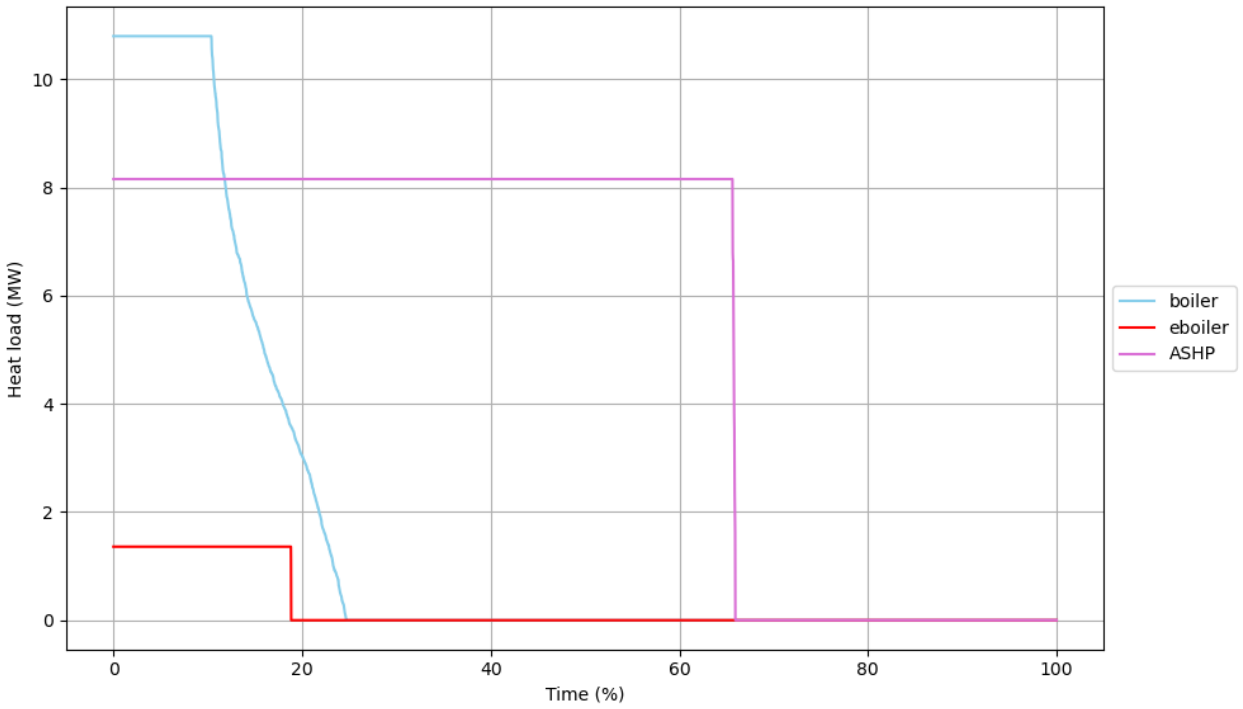

Figure 17: Load duration of generators in the "All technologies" scenario

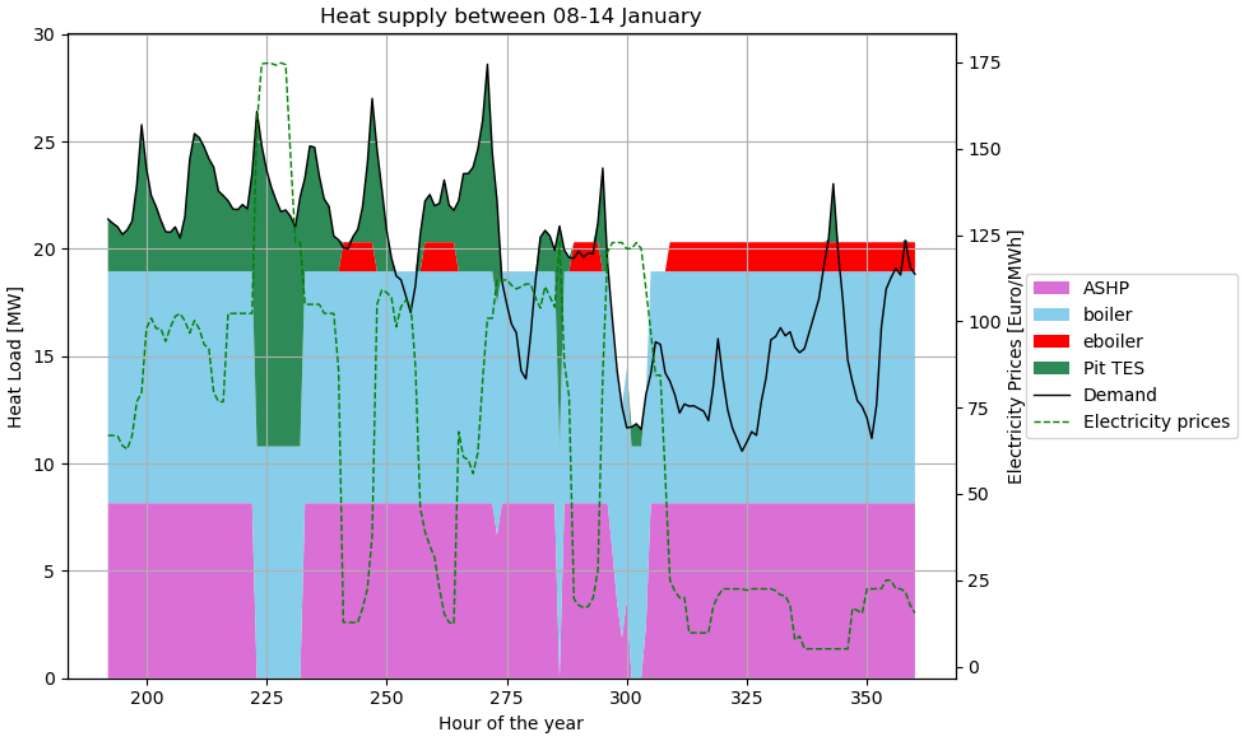

Figure 18: "All technologies" scenario heat supply in the week of peak demand

Again there is no significant correlation between the output of the power to heat units and the PV panels. Still, in both scenarios shown in Table 7 the total input energy for the ASHP is roughly matched by the total output of the PV panels. The numbers behind this behaviour are presented in Appendix D: Additional figures (Table 17).

5.2. Other supply temperatures

Figure 19 shows the LCOH of the RE and RE-ST scenarios per supply temperature. Overall, it is clear that the effects of the increased temperature are minor. The RE scenario performs better than RE-ST in every temperature case. Both scenarios become slightly more expensive when the peak supply temperature increases. Still the change is negligible, singaling that a reduction in the peak supply temperature from 100°C to 70°C enables a relatively small scope for cost reductions, if only the generation side is considered. Conversely, in the fictional case of 60°C supply temperature, the LCOH of both scenarios is marginally reduced, but the change amounts to less than an euro per MWh. This suggests that the conservative set-up of 70°C is an adequate representation of the system's behaviour.

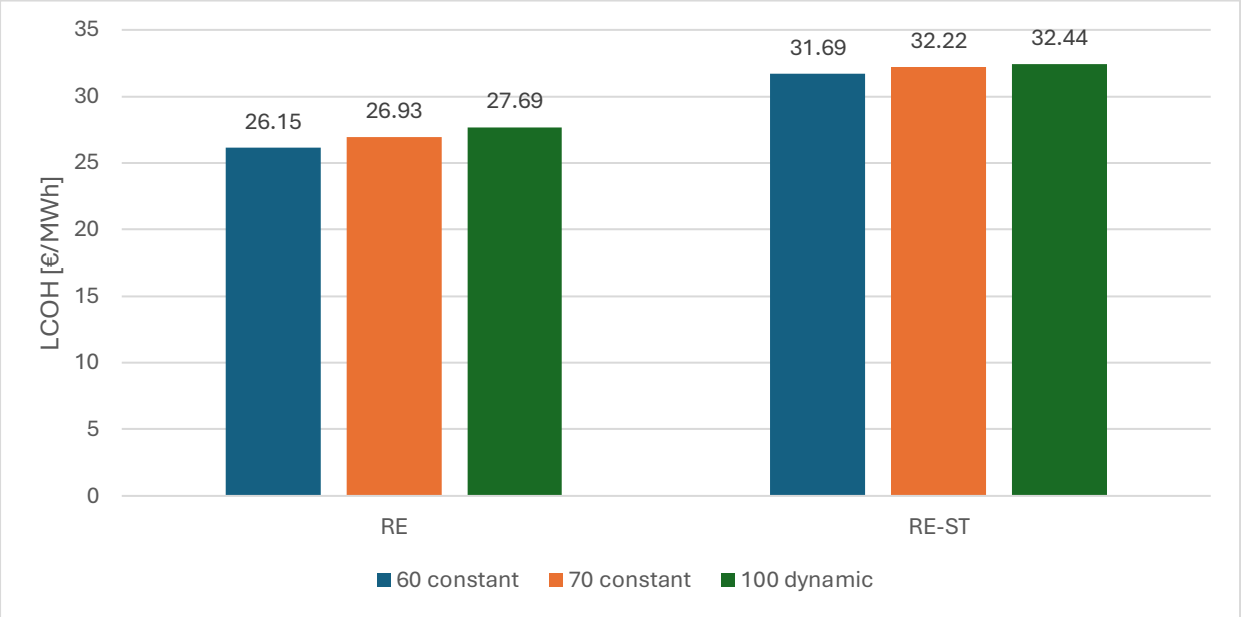

Figure 19: LCOH of RE and RE-ST scenario per supply temperature

More detailed information on the change in portfolio of generators per supply temperature is available in Appendix D4: Other temperatures. It suffices to say that as the supply temperatures increase, especially during the winter months of peak demand, the COP of the ASHP decreases. This prompts the model to rely more heavily on an e-boiler instead. This behaviour is observed in both scenarios.

5.3. Dispatch models

The results of the dispatch modelling are presented in Figure 20, together with the fixed yearly prices charged by the DHN in Sofia during the respective years[6] (KEVR, 2024). The first observation is that all scenarios are performing as well as or even better than the prices charged by the DHN across all dispatches outside of 2022. In that particular instance, the two BAU scenarios performed significantly worse than the DHN.

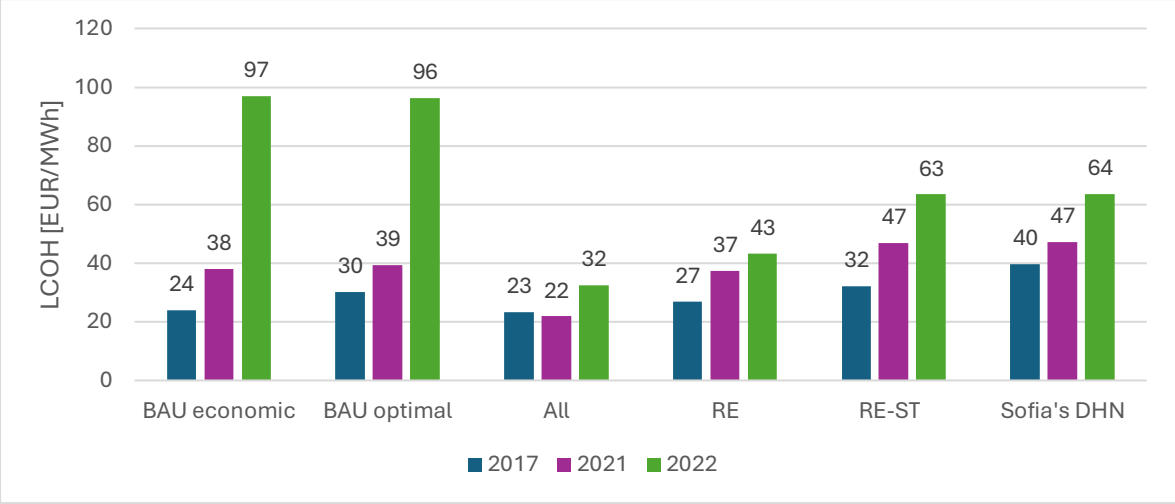

Figure 20: Levelized costs of heat of the main technology scenarios across the different dispatch scenarios

Overall, the "All technologies" scenario has both the lowest prices in each dispatch run, and also the lowest price spread. This suggests that having access to substantial energy storage and a diverse set of energy conversion technologies that require different input fuels can ensure price stability even under adverse circumstances. This is illustrated below with in-depth descriptions of the behaviours of the other scenarios.

The particular matter emissions across the relevant dispatch models is shown below (Figure 21). It is immediately apparent that "All technologies" is performing significantly better than the two BAU scenarios. Even though its boiler is used more than in the 2017 optimisation (CF_{2017}:16%, CF_{2021}:32%, CF_{2022}:22%), it never delivers more than half of the total energy. This signals that even at elevetad electricity prices, renewable energy technologies can be a tool for bringing prices down. Another strong lead in that direction are the lower LCOHs of the RE scenario in 2021 and 2022 than the LCOHs of the two BAU scenarios (Figure 20).

[6] The years 2018, 2019 and 2020 are omitted due to their similarity in the energy prices compared to 2017, yielding essentially identical results. The full figures are available in Appendix D: Additional figures, section D2: Dispatch models

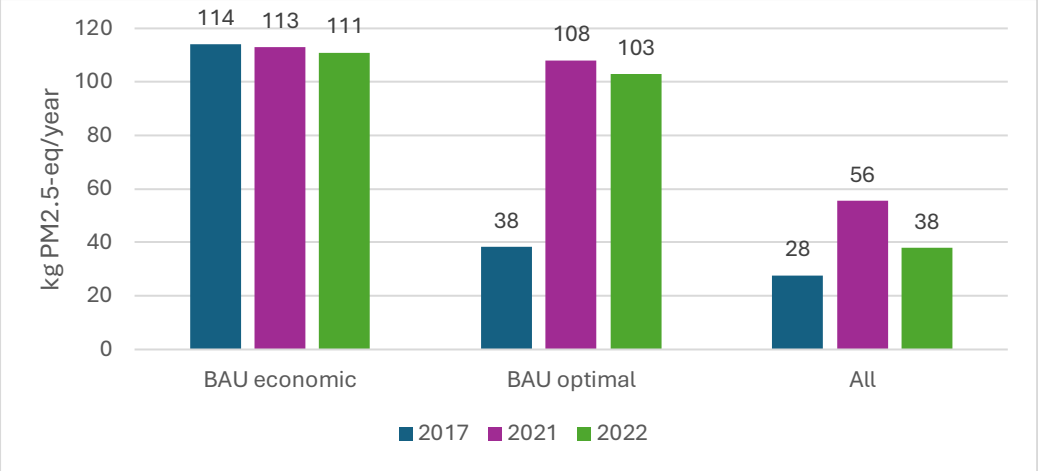

Figure 21: Particulate matter emissions across the dispatch runs

Business as usual scenarios

Table 8: BAU scenarios; produced energy across the dispatch models (Q)

		2017	2021	2022
BAU econ	Q 20 MW boiler	63 378	62 745	61 672
	Q 5 MW e-boiler	1 149	1 782	2 856
BAU opt	Q 17 MW boiler	21 100	56 955	56 955
	Q 16 MW e-boiler	43 456	7 577	7 577

The two BAU scenarios present a reasonably similar performance across the dispatch runs in terms of both emissions and costs (Figure 20, Figure 21). Part of the reason for this is the way the dispatch runs are set – they keep the installed capacities fixed, but allow the model to choose how to dispatch the available units. As the BAU opt has a large natural gas boiler (Table 5), similar in size to the boiler in the BAU econ, and there are no constraints on the total emissions, the model prioritises the use of natural gas in all dispatch runs. The result is the similar emissions profiles visible in Figure 21.

As Table 8 shows, in the BAU economy, the e-boiler output increases between the years, signalling that there are moments in which the cost of purchasing electricity is lower than that of natural gas. Still, these moments are rare, as the capacity factor of the 5 MW e-boiler is only 7% in 2022. Compared to it, in BAU opt the e-boiler delivers significantly more energy with lower fuel costs in both 2021 and 2022. The reason behind this diverging behaviour is the size of the TES unit (132 vs 17 MWh), which allows for a more flexible dispatch of the e-boiler. Still, the capital costs related to the larger e-boiler and TES, shown in Figure 22 below, end up compensating for this difference and the LCOH is largely the same in each year (Figure 20).

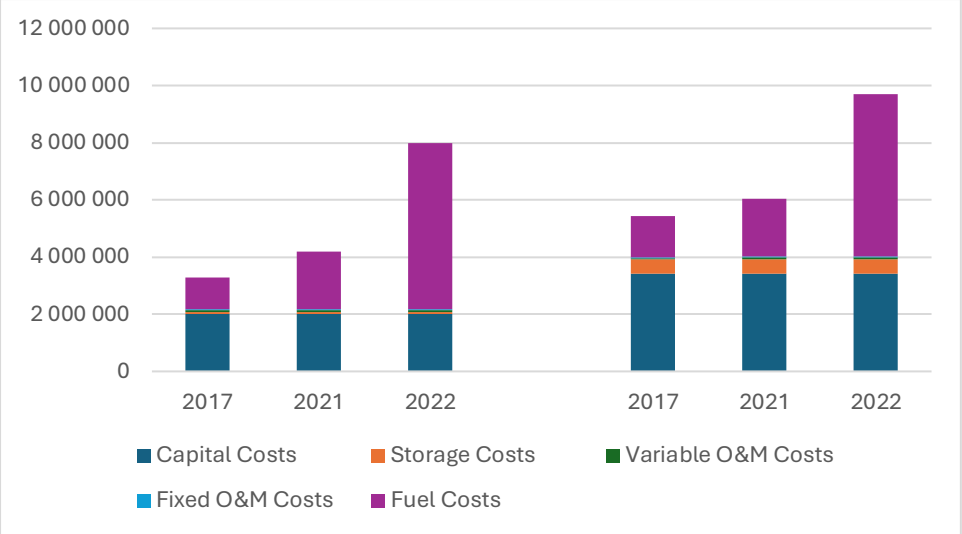

Figure 22: Capital costs + costs for one year of operation; BAU dispatch. BAU economic on the left and BAU optimal on the right

Renewables scenarios

Table 9: Headline figures RE an RE-ST dispatch models. P2H stands for power to heat.

		2017	2021	2022
Renewable Energy	Q 18 MW e-boiler	20 598	16 511	18 306
	Q 8 MW ASHP	44 058	48 215	46 406
	Energy delivered per electricity costs [kWh/€]	71	27	14
Renewable Energy – Solar Thermal	Q 23 MW e-boiler	26 169	24 380	25 800
	Q 4 MW ASHP	18 468	20 298	18 899
	Q 13 MW ETC	20 229	20 228	20 228
	P2H energy delivered per electricity costs [kWh/€]	56	21	11

Figure 20 shows that RE-ST underperforms in LCOH to RE across all dispatch runs. This is somewhat surprising, considering that about a third of RE-ST's energy is generated without any electricity inputs and the dispatch runs are testing both scenarios in the context of elevated electricity supply costs. As already discussed, the main difference between RE and RE-ST is that in RE a larger ASHP produces at high capacity throughout most of the year, whereas in RE-ST a smaller ASHP stays idle during the summer, while the work of the ETC carries the system. This makes RE-ST more reliant on the e-boiler, which is a less efficient devise in converting electrical energy to heat. The resulting difference in the amount of heat that the ASHP and e-boiler produce per euro spent on electricity is shown in Table 9. RE-ST lags behind RE by between 20% and 25% on this metric in every year. This, combined with the missed revenue from PV electricity sales (Figure 23), and the fact that RE-ST CAPEX is about €3 million larger than the one in RE explains why its LCOH is higher across the dispatch runs.

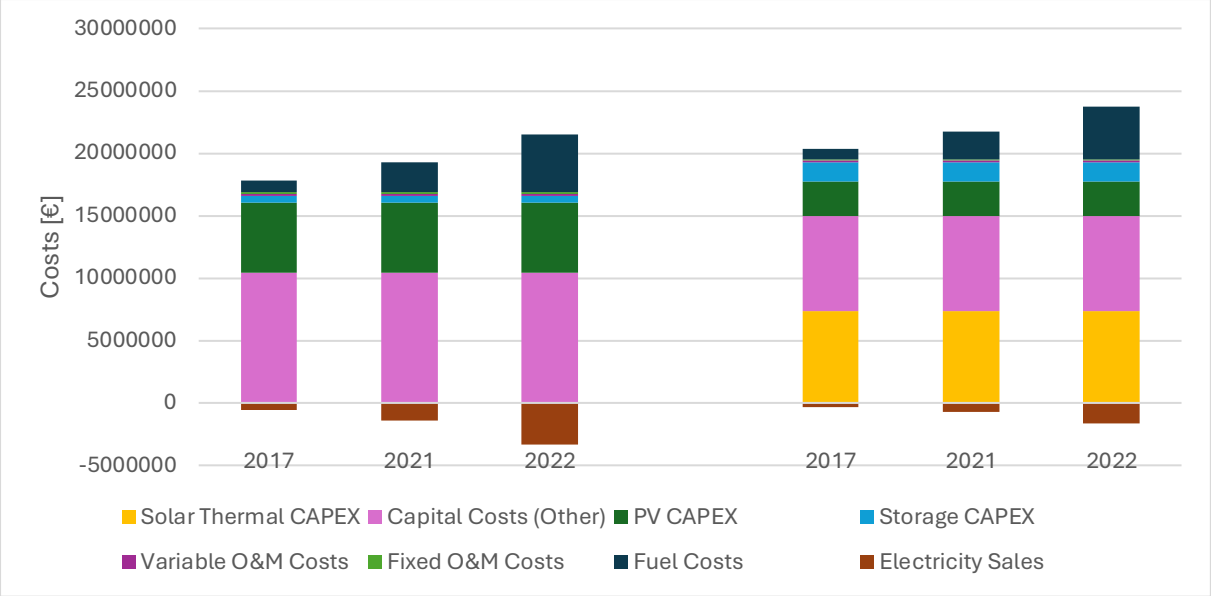

Figure 23: Capital costs + costs for one year of operation; RE on thr left and RE-ST on the right

All technologies

The heat deliveries of scenarios RE and "Al ltechnologies" are shown below (Table 10). The lower LCOH of "All technologies" (Figure 20) can be explained with the dependence the two scenarios have on the e-boiler. In the case of RE, the maximum amount of heat that can be delivered by the 8 MW ASHP seems to be ranging between 44 and 48 GWh, and the remaining heat needs to be delivered by the e-boiler. For "All technologies", on the other hand, the usage of the e-boiler can be replaced by the natural gas boiler when the electricity prices are too high. The natural gas boiler can then be used even further and replace the ASHP as the main energy source of the network, when the ratio between electricity and gas prices is tilted in favour of the fossil fuel. This diversity of energy sources is the main difference between the two scenarios – they are equal in their PV output and their CAPEX is largely identical (M€15 for "All technologies versus M€16.6 for RE).

Table 10: Heat deliveries (Q) of scenarios RE and "All technologies" across the dispatch models in MWh.

		2017	2021	2022
All technologies	Q 11 MW boiler	15 364	30 842	21 033
	Q 1 MW e-boiler	2 232	277	462
	Q 8 MW ASHP	47 001	33 502	43 111
RE	Q 18 MW e-boiler	20 598	16 511	18 306
	Q 8 MW ASHP	44 058	48 215	46 406

5.4. 2022 prices, 70°C

The installed capacities shown in Table 11 reveal drastically different results in this optimisation run, compared to the system optimised for the 2017 energy prices. This puts an important emphasis on making the right assumption about future energy prices, which is crucial for obtaining workable outputs from the model. Further numbers on all solutions along the Pareto fronts are available in Appendix D3: 2022 optimisation.

Table 11: Installed capacities (P), LCOHs and particulate matter pollution in the optimisation run optimised for 2022 energy prices.

	P CHP [MW]	P Boiler [MW]	P E-boiler [MW]	P ASHP [MW]	P tank [MWh]	P pit [MWh]	P PV [MW]	P ETC [MW]	LCOH [€/MWh]	Emissions [kg PM2.5-eq./year]
BAU econ	35	3	14	0	380	0	0	0	-201.14	657.33
BAU opt	35	9	22	0	380	0	0	0	-56.58	219.33
All	35	0	11	12	17	13 467	10	0	-148.81	198
RE	0	0	29	12	30	3 968	10	0	28.55	0
RE-ST	0	0	24	12	26	5 642	5	12.8	42.54	0

First of all, in all scenarios permitting the installation of a CHP unit, deployment has been maximized up to the constraint of 35 MW. Second, the tank storage of the BAU scenarios is as big as it could be (380 MWh). The pit TES sizes have increased considerably in the "All technologies", RE and RE-ST scenarios too. For reference, under the 2017 prices optimisation, these TES were 560, 903 and 2 558 MWh respectively, which signals a 24-fold increase in the case of the "All technologies" scenario.

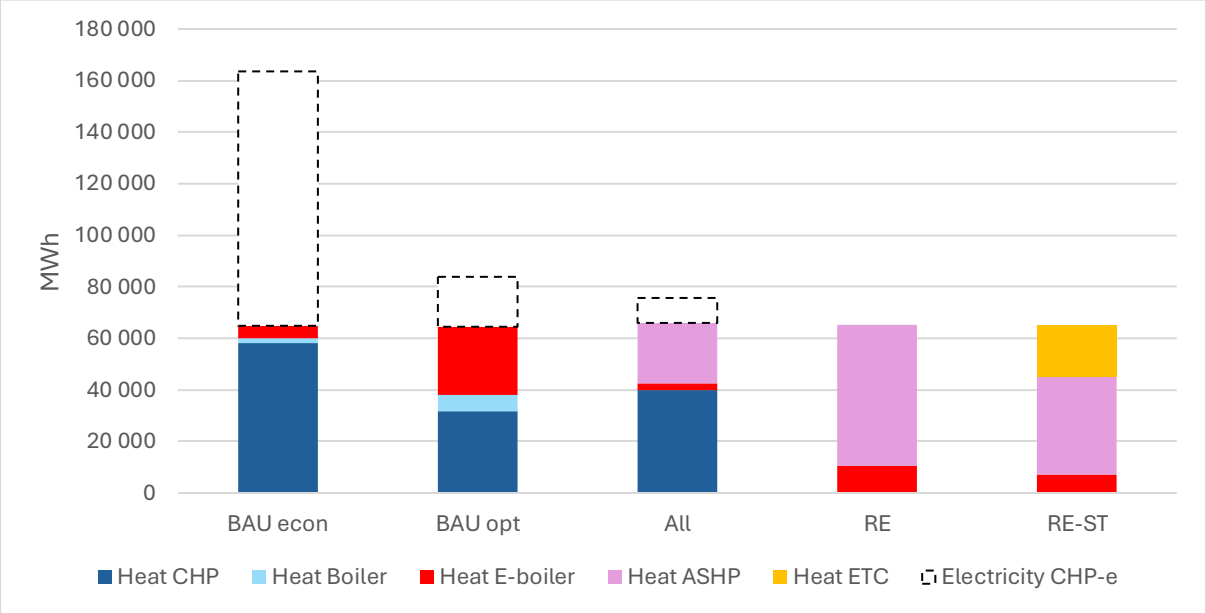

Figure 24: Yearly energy output from the system under the 2022 optimisation. CHP-e denotes the electricity output of the CHP units in electricity-only mode

These changes in CHP and storage installed capacities together explain the extremely low LCOHs of the three scenarios where electricity can be produced on demand. These scenarios leverage their large CHPs with low ramp-up and ramp-down times and turn them on to their maximum possible extent at times of high electricity prices. The TES stores that surplus heat and allows the system to coast through times of low electricity prices when turning the CHP on would yield lower gains (Figure 25 below, left). In BAU econ, where there are no constraints on the total emissions, the CHP is extensively used in electricity only mode (CHP-e), producing more electricity in that mode than heat (Figure 24, above) – 99 GWh of electricity only versus 58 GWh of heat[7]. BAU opt and "All technologies" make use of that ability, but in way more restrictive manner, as this electric output is not free from particulate manner emissions. As this scenario assumes that the energy prices will remain at this level for the entire life of the system, the profits from this behaviour accumulate, leading to the negative LCOHs presented in Table 11.

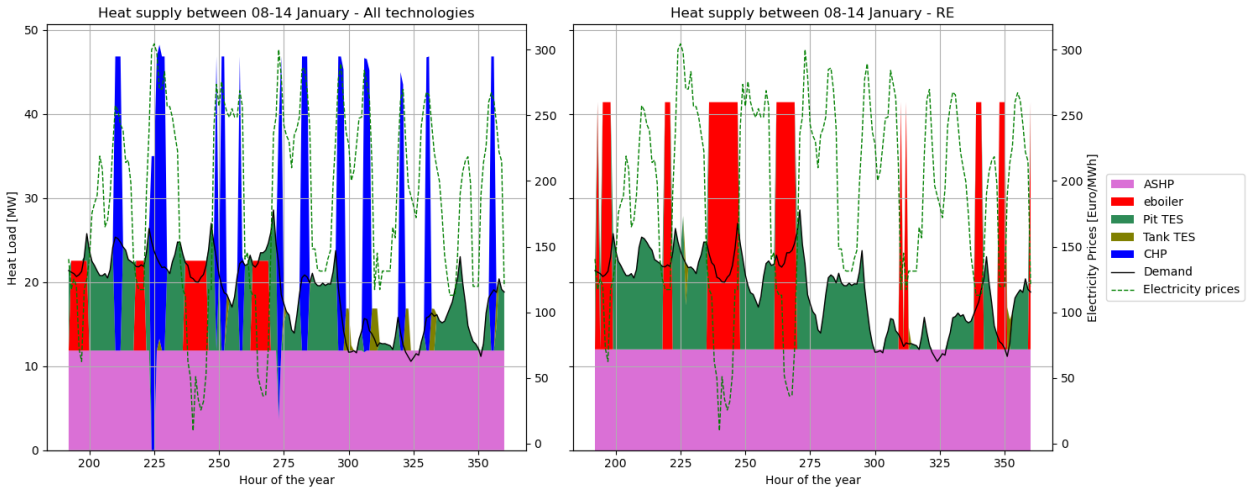

Figure 25: Heat supply during a winter week, scenario "All technologies" on the left and RE on the right[8]

The ASHP is another technology that is built up to its constraining limit in the "All technologies" and the two RE scenarios. All of them cover the baseload demand in the first half of the year, when the pit TES units are not full yet (they start at 0% SOC by default) – see Figure 25. During the summer the ASHP kicks in together with the e-boiler during low electricity prices and keeps the TES full enough to deliver the needed energy (Figure 26).

[7] For clarity, the latter 58 GWh are the output in combined mode – 58 GWh of heat were produced while producing 58 GWh of electricity that is not accounted in the 99 GWh figure above.

[8] There is an odd moment when it seems like the Tank TES is delivering more energy than there is demand. Sometimes the model discharges the Tank TES to charge the Pit TES. It is unclear why.

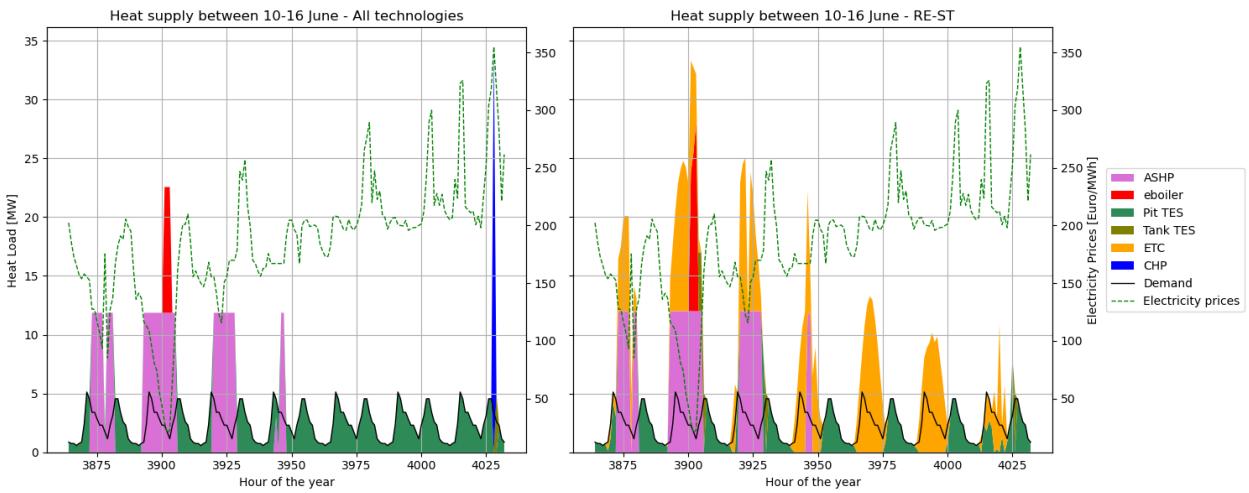

Figure 26: Heat supply during a week in June, scenario "All technologies" on the left and RE-ST on the right

The emission profiles in this optimisation run reflect the different generator portfolios. Particular matter emissions increase considerably from the maximum of 114 kg PM2.5-eq. per year observed under the 2017 optimisation to up to 657 kg in the BAU econ (see the last column of Table 11). It is important to stress that these emissions are well below the roughly 3 t emitted in 2017. The GHG emissions present a different outlook – all non-renewable scenarios exhibit higher GHG emissions compared to 2017's values (Figure 27). In BAU econ the system emits slightly above 70 kt of GHGs per year and in All and BAU opt scenarios it emits between 25 and 35 kt. This is far above the emissions under the 2017 prices optimisation, where all scenarios emitted between 8 and 19 kt. The two renewables scenarios reduce their emissions on the other hand, thanks to the reduced reliance on e-boilers and increased use of ASHPs. The RE scenario goes from roughly 11 kt in the 2017 optimisation to 9 kt in the 2022 optimisation and RE-ST goes from 11 to 6 kt.

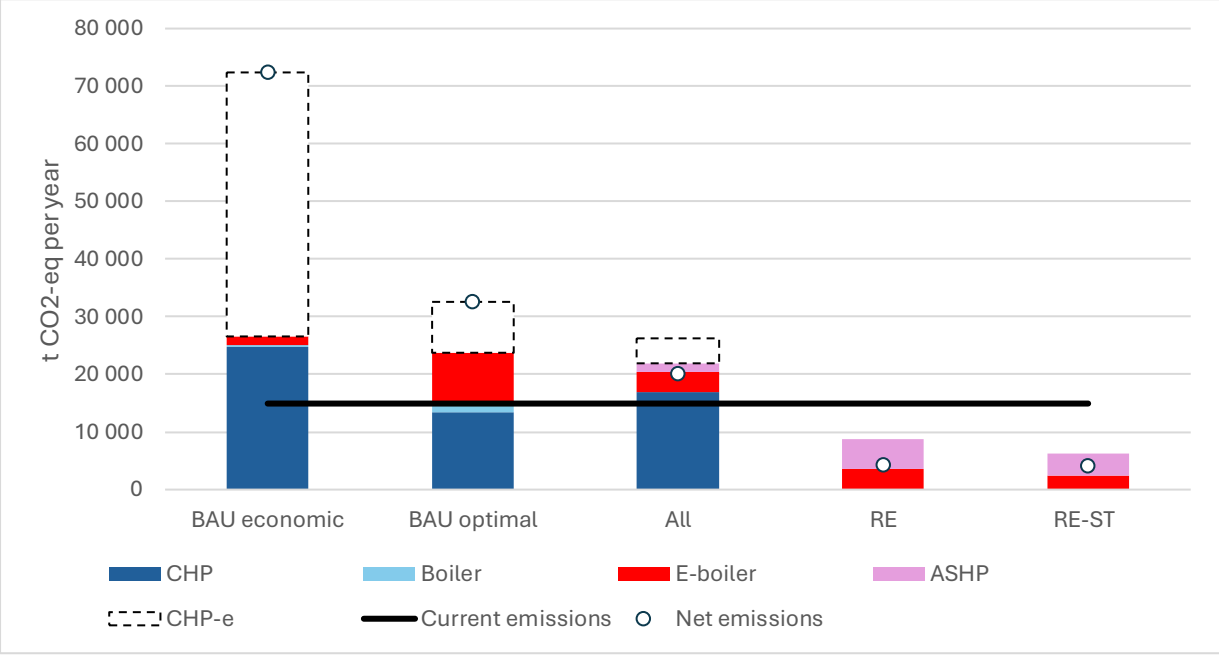

Figure 27: Yearly GHG emissions of all scenarios when optimised for the 2022 prices.

6. Discussion

The section below provides an overview of the results and puts them into a broader context. First, a reflection on the results is given. Then, a list of limitations that were encountered in this work is presented. Suggestions how to structure future work to either address the limitations of this research or how to incorporate its main findings are provided throughout the chapter.

6.1. Reflections on the results

The scenarios

This work demonstrates that different portfolios of generators could meet the heat demand of the neighbourhood of Orlandovtsi in Sofia at a lower cost than the city's DHN and with lower GHG and particulate matter emissions than the currently employed heating technologies in the neighbourhood. Both of these benchmarks are somewhat limited, and yet useful. As the DHN supplies only a fraction of the heat in the neighbourhood, it is difficult to give a direct comparison with the status quo. Still, it provides a yardstick for estimating whether an intervention would be beneficial both to the DHN consumers, and the DHN operators. On the other hand, particulate matter pollution is established based on the concentrations of particles in a given volume of air. It is beyond the scope of this research to convert the yearly emissions into concentrations. Yet, a reduction in terms of yearly emissions is guaranteed to lead to an improvement in the concentration regardless of the correlation between the two.

Overall, the integration of renewable energy technologies leads to tangible improvements in terms of reduced costs, particulate matter and GHG emissions. The scenario in which all technologies could be accessed by the model performed best in terms of levelized cost of heat (LCOH), and had the lowest price spread across the different dispatch models. The latter is especially important in the context of energy poverty, as stable and predictable prices are a key component in ensuring that vulnerable consumers do not slip beneath the poverty line (Koďousková et al., 2023).

A primary factor facilitating this performance was the capability to utilize generators powered by different fuels—in this model these were natural gas and electricity. This diversification allowed for effective cost management by balancing the operation of each generator type during periods of high price fluctuations. The second enabler is the installation of a large thermal energy storage system (TES) that makes it possible to capitalize on the fluctuations in the electricity market. When the TES is coupled with power to heat devices, surplus heat is generated at times of low electricity prices and then stored for later usage to prevent high costs. When the TES is used with combined heat and power plant (CHP), surplus heat is generated at times of maximum electricity prices, thus maximising benefits. The combination of a CHP unit and large TES is especially important in conditions with sustained high electricity prices, as shown by the optimisation runs that used 2022 energy prices.

Emissions and pollution

In terms of emissions, this work highlights the dichotomy between efforts to abate particulate matter emissions and greenhouse gas emissions. Natural gas combustion showed itself as a reliable and cheap way of providing heat while reducing particulate matter emissions by more than 90%, compared to the current status quo. Its use was especially valuable in the model runs where CHP plants were heavily used, as it allows for responsive electricity production and significant financial gains, while still maintaining relatively low particulate matter emissions.

Thus, the findings on setting up a DHN that does not exacerbate air pollution are in line with the literature on individual heating systems. In the literature, natural gas is frequently framed as a transitional fuel which can reduce GHG and/or particulate matter emissions compared to residential coal boilers and biomass stoves (Li et al., 2022; Mahmoud et al., 2021).

Still, the lock-in of new fossil fuel infrastructure ought to be avoided, even if it leads to emissions savings in the short term (IEA, 2024). This begs the question of how to reap the benefits described above without further entrenching fossil fuel use. Leaving the cost aspect aside for a moment, biogas is a direct substitute in terms of physical properties, but its potential is limited. Assuming an equal division of Bulgaria's total technical biogas potential leads to up to 13 GWh available to the residents of Orlandovtsi per year (Ślusarz et al., 2023). Comparing these numbers to the 15 GWh and 105 GWh of natural gas used yearly in the 2017 and 2022-based optimisations of the scenario "All technologies" shows that the biogas availability is insufficient to be a replacement of natural gas.

Biomass combustion more generally is widely used as a means for district heating decarbonisation (FEDENE, 2024; Werner, 2017). Still, its usage is not free of PM2.5 emissions – biomass boilers emit 37 g/GJ, significantly higher than the 0.5 g/GJ of its natural gas-fired counterpart (EEA, 2023a). As explained in the introduction, considering this air pollution impact is generally lacking from the literature. On the other hand, this low-carbon resource is available – if the entire technical potential of the country for biomass energy is considered, Orlandovtsi would have access to 182 GWh/year (IRENA, 2019). A biomass-fired CHP, therefore, could have the resources available to fill the role of a dispatchable and flexible energy source for both heat and electricity, while avoiding the GHG emissions of a natural gas CHP even in a rather extreme scenario of CHP usage. Nonetheless, the costs of these inputs ought to be considered too. This leads to the first recommendation for further research: expanding the current model to include GHG minimisation as a separate objective function and including biomass boilers and CHPs. Such changes will highlight where is the optimal balance between avoided GHG and PM emissions, and the impact this trade-off has on the LCOH of the system.

Supply temperatures

In terms of supply temperatures, the small difference between the LCOHs of 100°C and 70°C provides evidence that the supply temperature is not a prohibitive factor for the integration of low-emission heat technologies, within the studied limits. This represents a positive development for the district heating network operator, as it suggests that emission reductions can be realised through investments solely aimed at decreasing the supply temperature to 100°C, rather than the more substantial reduction to 70°C.

Still, that does not mean that supply temperature reductions are worthless. Firstly, they reduce the heat losses in the heat supply network (Werner, 2022) and improve the longevity of the DHN by reducing material fatigue (Gadd & Werner, 2014). Additionally, in both the RE and RE-ST scenarios, the 100°C optimisation reduced the role of the ASHP and increased the use of a larger e-boiler compared to the 70°C optimisation. Importantly, scenarios with larger heat pumps performed better when the electricity prices were increased. Thus, lower supply temperatures enable more resilient DHNs in their own right. To the knowledge of the author, this is a novel consideration that is not discussed in the literature on supply temperatures and the benefits that they entail (Gadd & Werner, 2014; Lund et al., 2014; Werner, 2022).

Other considerations

Even under the current version of the model that considered only power to heat and solar thermal renewable energy technologies, the two scenarios based on these technologies performed better than the DHN of Sofia in terms of prices under most conditions and had the lowest PM emission footprint of all

scenarios. They did not have the lowest GHG footprint of all scenarios, owing to the reliance of the Bulgarian electricity grid on coal. As that changes, their performance on that metric should improve. In future work, renewable energy technologies could be modelled better by including FPC solar thermal collectors as a standalone technology option (outside of the FPC-PTC series) and the exploration of a scenario where no PV and solar thermal technology is available. The latter would simulate a land-constraint scenario where all energy generation facilities need to have a limited spatial footprint. Lastly, the inclusion of photovoltaic thermal (PVT) technology could be a valuable addition to the model. Based on the current results, the combination of PV panels and ASHP forms the backbone renewables-based DHN. As PVT offers an integrated PV-ASHP technology with improved COP of the heat pump and better PV electricity generation (Kang et al., 2022), adding it to the model appears to be a logical next step.

The prices of the CO_2 emissions permits are another, more silent input condition. As already mentioned in the section on CHPs of the Research context chapter, in this work, the natural gas boiler is capped at 20 MW of fuel input in order to avoid its inclusion in EU's emissions trading scheme (ETS) with the respective costs for CO_2 permits. The CHP on the other hand, is always included in the ETS market. This decision was made based on the propensity of the model to install large CHP units in cases when the cost of the ETS permits is zero[9]; such units are big enough to be covered by the ETS regulation. A more granular approach is recommended for future work. One avenue would be to limit the CHP size to 20 MW of fuel input in a similar vein to the boiler. Another way would be to change the model from a linear programming to a multi-integer programming model. This would permit the inclusion of binary variables that reflect whether the boiler and the CHP are larger than the threshold of the ETS. A MILP would have other benefits to the overall accuracy of the results, for example, by allowing for better modelling of non-linear cost functions like the tank TES units[10].

Lastly, energy poverty as a topic was lightly discussed by this work. A reasonable and effective first step towards grasping Orlandovtsi's context in that regard would be to find reliable estimates of the LCOH of the individual heating systems used by the residents of the neighbourhood in the present, and how sensitive they are to the changes in energy prices. This will give a high-level understanding of whether the discussed scenarios under consideration potentially jeopardize or ameliorate the risk of energy poverty among vulnerable residents.

6.2. Limitations

The limitations section is structured according to a gradient of abstraction. First, the limitations of the input data are elaborated upon. Then, the model, in general, is scrutinised and the key areas in which it could be improved are presented. Lastly, the sections is rounded up by an exploration of the most salient elements that, although not addressed by the current methodology, possess the potential to substantially influence the study outcomes.

Input data

The chief limitation in terms of inputs is that heat consumption data is available only for 2017. The accuracy of the results depends on 2017 being representative, both in terms of total demand and temperature

[9] Key figures of such a run are available in Appendix D: Additional figures

[10] As already explained in the Thermal energy storage section of the Research context chapter, the cost function of the tank TES is not linearly related to its size. Introducing binary variables could allow the function to be divided in multiple linear segments with the right cost picked depending on the size of the TES.

variation. Climate-wise, the mean daily minima and maxima were compared with the long-term averages available in meteoblue, the meteorological service of the University of Basel (*Simulated Historical Climate & Weather Data for Sofia*, n.d.). The comparison (Figure 28) shows that overall, the year was rather average, with the exception of the colder month of January.

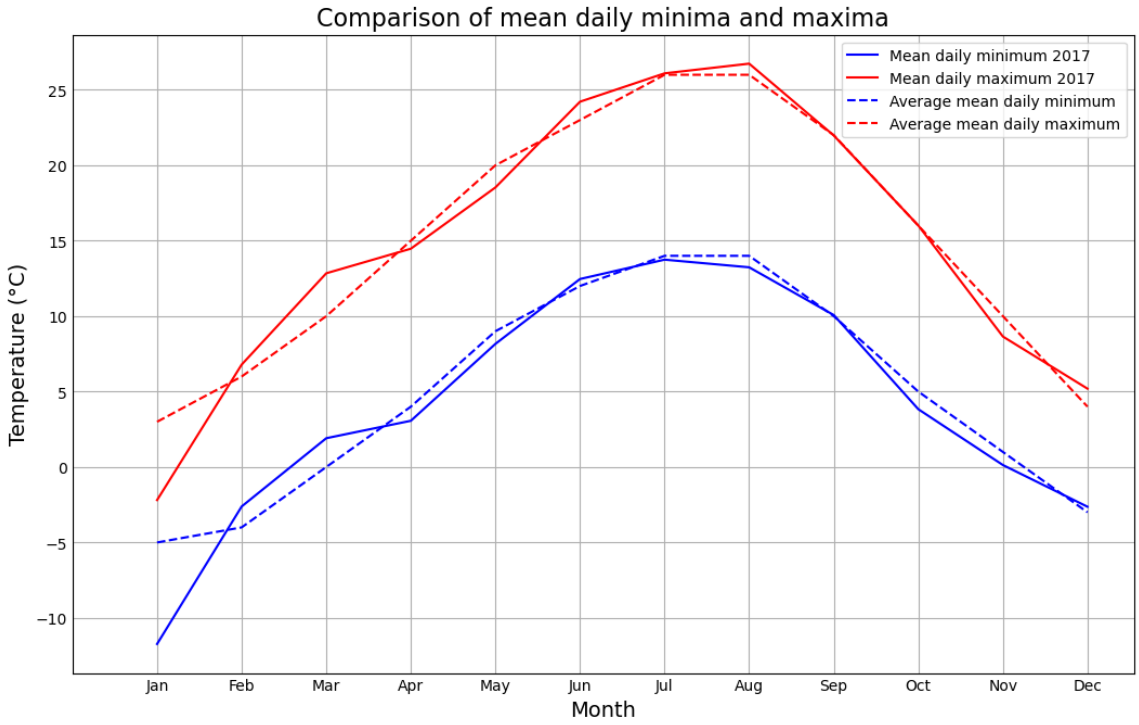

Figure 28: Comparison of mean daily minimum and maximum temperatures. Source: own work and (Simulated Historical Climate & Weather Data for Sofia (n.d.)

A second data limitation was the lack of irradiation values on the PV GIS website past 2020 (*PVGIS*, 2024). For consistency pursues, only 2017 values were used across the optimisations and dispatch models. This is especially important in the case of the dispatch runs with 2021-2022 data, as the sales of PV-generated electricity are crucial for their final LCOHs. PV-generated electricity is prone to flooding the electricity market, thus reducing the prices and cannibalising the profit of other PV generators (IEA et al., 2020). As there is a mismatch between the hourly electricity prices used in the dispatch models and the irradiation values, it is highly likely that this effect is not fully reflected in this model. It is recommended that in the future irradiation data is sourced from the ERA5 database (C3S, 2018). This would require change in the model, such that the PV output is calculated based on the irradiance values, rather than relying on the hourly capacity factor that is currently sourced from PV GIS.

Lastly, in the model, it is assumed that the same quantity of domestic hot water (DHW) is consumed every day, regardless of the time of the year, based on the work of (Dorotić et al., 2019b). No better quantification of the DHW consumption was found, although it is clear that there will be seasonal differences.

On the model itself

The proper scaling of the coefficients in a model ensures that small changes in the input of one variable do not lead to an outsized impact on the objective function (Nocedal & Wright, 2006). All dispatch models and the BAU optimisations were considered well scaled by the algorithm. In the other scenarios, the

algorithm performed automatic scaling, reducing the ratio of the largest to smallest coefficient (the constraint matrix) to be in the order of 10^1. This is significantly better than the initial ratios of 10^{12}, and yet it shows that there is scope for further improvements in future work.

Another field of improvement is the modelling of the PTC-FPC array. The methodology devised for modelling the arrays combining Parabolic Trough Collectors (PTC) and Flat Plate Collectors (FPC) proved ineffective. After the array code was included in the model, the ratio within the constraints matrix escalated to approximately 10^7 post-scaling, accompanied by discrepancies between energy supply and demand on the order of tens of kilowatt-hours per year. As the model did not select the PTC-FPC array in any scenario, the PTC-FPC array was excluded from the model framework during the last model run. Thus, the final results presented in this work are not skewed by the above-mentioned issues. Future work should identify how to model the array better.

Last but not least, the model does not consider any hydraulic constraints, nor the layout of the proposed DHN. This means that no consideration is given to the pumping costs and the O&M of the DHN network, nor are there thermal losses that occur during the transportation of heat. As the geography of the neighbourhood is not taken into account, it is unknown if all households could be economically connected to the DHN.

Matters of scope and simplifications

The most important simplification of this work is the way that the net present value of the costs is calculated – for the sake of simplicity and computational ease it was assumed that each year of the system's lifetime will be the same in terms of demand, energy prices, etc. This is broadly implausible, and even though it was partially ameliorated with the inclusion of the dispatch models, it remains as the main handicap of this work. Despite its limitations, this is the predominant way in which similar calculations are performed in the literature on DHN optimisations (Delangle et al., 2017; Dominković et al., 2020; Tian et al., 2018).

Related to this are the assumptions that all DHN equipment has a lifetime of 25 years and that all capital investments will be completed within the first year of operations. This is especially crucial for the DHN network itself, a building which would be the largest infrastructural undertaking discussed in this work. In reality, the rollout of the DHN would be executed in phases to minimise nuisance to the residents and to be done at minimum costs; see (Lambert et al., 2016) for an optimisation framework of this step alone. Again, even though this is an overly-simplified model, its computational ease makes it appealing among scholars (Dominković et al., 2020; Tian et al., 2018).

Another simplification made in the course of the research was to focus solely on particulate matter pollution, excluding terrestrial acidification and photochemical oxidant formation. That does not mean that they are not causing damage to human life and the natural environment. Still, given the severity of PM pollution in the country (Dimitrova & Velizarova, 2021) and the breadth of this research, it was decided that considering PM impacts alone is sufficient. In future work, the impact in these other categories can be tracked in a similar way to the way GHG emissions were considered.

As already explained in the research method chapter, a simplified sketch of the electricity market is embedded in the model. The assumption regarding the energy prices the system is optimised for is crucial for obtaining reasonable modelling results. This study assumed that the CHP units are price takers on the hourly electricity market. In fact, the electricity market in Bulgaria is split into two parts, with different producers either subject to fixed electricity prices determined by the state, or selling their produce on a free market (Ivanov, 2019). The abolition of this structure and the transition to a fully liberalized market is part of a package of reforms that the Bulgarian government has committed long ago (Ivanov, 2019), yet

completion is postponed consistently. Therefore, reflecting on this structure better (most importantly the fact that CHP units receive certain levies (KEVR, 2019)) could be included in future work. Moreover, similar to the work of Mandel et al. (2023) the model can be optimised using forecasts of the future prices, rather than relying on data from the past. In this way, the bias that the future should resemble the past could be circumvented. Other considerations that were not accounted for include the fact that the electricity prices would react to the behaviour of the DHN, or that the grid might not be able to take all the electricity produced by the DHN's CHP and PV at all times due to grid congestion. Lastly, it is reasonable to assume that DHN electricity generators will be bound to long-term contracts for generation, which would diminish their capacity to ramp up and down at full capacity on a whim. Again, despite its limitations, the method employed in this work is in line with the state of the art on the matter (Dominković et al., 2020; Dorotić et al., 2019a).

A deeper consideration of the inhabitants of Orlandovtsi was not encompassed in this study either. No research efforts could be dedicated to (i) better understanding the socio-economic background of the neighbourhood, (ii) how vulnerable to energy poverty its residents are and (iii) what is the status of the buildings in terms of insulation. All these aspects matter as it is entirely possible that other interventions could have a large impact on reducing PM pollution, GHG emissions and energy expenditure of the people there than constructing a new DHN. For example, a recent paper found that in the case of an abstracted Bulgarian neighbourhood, a combination of advanced building retrofits and the installations of ground-water heat pumps and wood-chip boilers is the most cost-effective mix of measures for a reduction of energy expenditure (Mandel et al., 2023). Still, that research takes a high-level perspective on designing the hypothetical DHN, excluding CHP and TES units, while assuming average yearly electricity prices between €65 and 105/MWh. At these price levels, it is highly likely that a combination of CHP and TES will have a decisive impact on the cost performance of the DHN, given that the lower price bound is already 33% higher than the yearly average electricity price in 2017 (see Appendix C: Energy prices).

7. Conclusion

The goal of this work was to establish to what extent renewable energy technologies in a district heating network could reduce air pollution and greenhouse gas emissions while maintaining minimal system costs. Considering the severity of particulate matter pollution in Bulgaria, the emissions of this pollutant were taken as a proxy for air pollution more generally. To approach this question, a linear programming optimisation was developed, in which the installed capacities and hourly output of pre-defined bundles of energy technologies are optimised. Five separate scenarios were crafted, based on three different technology bundles – using only traditional DHN technologies (BAU), using only renewable energy technologies and a bundle that employs both. Two scenarios were developed out of the BAU bundle, one in which the system is optimised for best economic performance and an optimal scenario in which air pollution and costs are balanced. The renewable energy bundle served as a basis for two other scenarios – RE and RE-ST. In the first one (RE), the system is optimised for the lowest costs without additional conditions. In RE-ST a minimum installed capacity of solar thermal technology is defined, while keeping the lowest cost. In these two scenarios, the air pollution emissions of the system are equal to zero by default, as no polluting technologies are included. Lastly, the scenario developed from all technologies is another scenario in which air pollution and costs are balanced.

These scenarios were optimised for the energy prices in 2017 and 2022 to explore how the changing energy markets call for different solutions, both in terms of installed capacities and their dispatch. Moreover, the optimal capacities of each scenario obtained under the 2017 prices, were dispatched assuming the energy prices observed in each year between 2018 and 2022. In this way, the ability of each

scenario to deliver heat at a consistent price was tested. Lastly, the RE and RE-ST scenarios were optimised for different supply temperatures, again while using 2017 prices. This was done both to overcome the handicap of the available data with regards to the dynamic behaviour of supply temperatures in DHNs, and to map the effects of supply temperature reductions on levelized costs of heat.

The integration of renewable energy technologies in the proposed DHN was found to significantly facilitate improvements across all metrics of the study. The best-performing scenario – "All technologies" – under the 2017 price optimisation reduced PM2.5-equivalent emissions by more than 90% and GHG emissions by 45% compared to the current status quo in the neighbourhood while consistently maintaining significantly lower and prices than the current DHN.

Each energy technology that was used in this work has its own characteristics that contribute to the outcome of the model. The inclusion of natural gas technologies enabled further decarbonisation, as the dependence on the Bulgarian electricity grid with its reliance on coal was reduced, and it ensured price stability by insulating the DHN from the fluctuations of the electricity market. Both of these benefits come at the cost of some PM emissions and the lock-in of fossil fuels. Further discussion on how to balance these in future work is presented in the Discussion chapter. Thermal energy storage, especially large pit storage units, was found to have a decisive impact in allowing flexible power to heat renewable sources to make use of the fluctuations of the electricity market. Electric boilers were used across all scenarios in that role thanks to their low investment costs, which justifies their more sporadic use. Air source heat pumps, on the other hand, were found to play a baseload role with considerably higher full-load hours. Solar thermal technology was found to fall short of being an asset for the DHN – its inclusion requires the installation of larger and more expensive storage units to accommodate for the summer peak in heat production. On the other hand, this seasonal peak dents the opportunity of the ASHP to work with a high capacity factor, which results in an overall smaller ASHP. All these developments increased the reliance on electric boilers, which are less efficient than an ASHP, thus decreasing the resilience of the network against high electricity prices. Lastly, when coupled with TES, the CHP units were found to be of great benefit when the system is confronted with high electricity prices, as they can produce surplus heat and electricity in moments of peak electricity demand. When the system was optimised for lower electricity prices, however, they were excluded in favour of cheaper natural gas boilers.

Overall, the optimal portfolio of generators consists of an ASHP unit for baseload work, an electric boiler for making use of low electricity prices, a moderately big TES unit to provide the ASHP and e-boiler with the needed flexibility and a natural gas technology to tap into an alternative energy source at times of high electricity prices.

The precise installed capacities of these technologies vary depending on the expected techno-economic conditions. Higher electricity prices make e-boilers less competitive vis-à-vis more efficient ASHPs and favour the use of CHP units over natural gas boilers as the CHP can make extra revenue from selling electricity. A large ASHP is helpful in absorbing high natural gas prices too, as the role of a natural gas boiler can be covered by the usage of the ASHP. On the other hand, increased supply temperatures reduce the role of ASHPs as they diminish their efficiency. This, in turn, leads to reduced resilience in the face of escalatin electricity prices for the scenarios based on renewables. Overall, a portfolio that mixes these technologies proved to be rather resilient and capable of meeting the heat demand in the network while still offering modest prices to the consumers even when the natural gas and electricity prices are touching extreme values.

Based on all written above the following recommendations can be reiterated. First, the potential of biomass CHP in taking over the role outlined for the natural gas CHP should be investigated further. The benefits associated with a low-carbon, responsive energy technology that does not depend on the

electricity market are too significant to be left without consideration. Second, the results of this study show unequivocally that the transition away from fossil fuels is needed beyond addressing climate change. The integration of renewable energies holds promise to both reduce the cost of energy for the final consumer while also addressing air pollution issues.

These results contribute to the literature on optimisations of district heating networks, as this is the first study to incorporate air pollution as part of its objective function. Although the work of Dorotić and colleagues (Dorotić et al., 2019a, 2019b) significantly inspired the conceptual framework of this study, the model presented herein was independently developed from the ground up. From a societal perspective, it provides the most comprehensive analysis of the impact of renewable energy technologies on district heating in Sofia to date. It is hoped that the findings will be taken to hearth and used to address the contributions of the city's heating systems to air pollution, climate change and rising energy costs.

References

Alias, M., Hamzah, Z., & Kenn, L. S. (2007). *PM10 and total suspended particulates (TSP) measurement in various power stations*. *11*(1).

Bare, J. (2011). TRACI 2.0: The tool for the reduction and assessment of chemical and other environmental impacts 2.0. *Clean Technologies and Environmental Policy*, *13*(5), 687–696. https://doi.org/10.1007/s10098-010-0338-9

Bynum, M. L., Hackebeil, G. A., Hart, W. E., Laird, C. D., Nicholson, B. L., Siirola, J. D., Watson, J.-P., & Woodruff, D. L. (2021). *Pyomo—Optimization Modeling in Python* (Vol. 67). Springer International Publishing. https://doi.org/10.1007/978-3-030-68928-5

C3S. (2018). *ERA5 hourly data on single levels from 1940 to present* [Dataset]. Copernicus Climate Change Service (C3S) Climate Data Store (CDS). https://doi.org/10.24381/CDS.ADBB2D47

Conolly, D., Drysdale, D., Hansen, K., & Novosel, T. (2015). *Creating Hourly Profiles to Model both Demand and Supply*. https://heatroadmap.eu/wp-content/uploads/2018/09/STRATEGO-WP2-Background-Report-2-Hourly-Distributions-1.pdf

Dal Cin, E., Carraro, G., Lazzaretto, A., Tsatsaronis, G., Volpato, G., & Danieli, P. (2023). Integrated Design and Operation Optimization of Multi-Energy Systems Including Energy Networks. *36th International Conference on Efficiency, Cost, Optimization, Simulation and Environmental Impact of Energy Systems (ECOS 2023)*, 3362–3373. https://doi.org/10.52202/069564-0302

Danish Energy Agency. (2018). *Energy storage; Technology descriptions and projections for long-term energy system planning*. https://ens.dk/en/our-services/technology-catalogues/technology-data-energy-storage

Danish Energy Agency. (2024). *Generation of Electricity and District heating*. Danish Energy Agency. https://ens.dk/sites/ens.dk/files/Analyser/technology_data_catalogue_for_el_and_dh.pdf

Delangle, A., Lambert, R. S. C., Shah, N., Acha, S., & Markides, C. N. (2017). Modelling and optimising the marginal expansion of an existing district heating network. *Energy*, *140*, 209–223. https://doi.org/10.1016/j.energy.2017.08.066

Dimitrova, R., & Velizarova, M. (2021). Assessment of the Contribution of Different Particulate Matter Sources on Pollution in Sofia City. *Atmosphere*, *12*(4), Article 4. https://doi.org/10.3390/atmos12040423

Dominković, D. F., Stunjek, G., Blanco, I., Madsen, H., & Krajačić, G. (2020). Technical, economic and environmental optimization of district heating expansion in an urban agglomeration. *Energy*, *197*, 117243. https://doi.org/10.1016/j.energy.2020.117243

Dorotić, H. (2022). *Multi criteria method for evaluation of district heating and cooling with regard to individual systems*. https://repozitorij.fsb.unizg.hr/

Dorotić, H., Pukšec, T., & Duić, N. (2019a). Economical, environmental and exergetic multi-objective optimization of district heating systems on hourly level for a whole year. *Applied Energy*, *251*, 113394. https://doi.org/10.1016/j.apenergy.2019.113394

Dorotić, H., Pukšec, T., & Duić, N. (2019b). Multi-objective optimization of district heating and cooling systems for a one-year time horizon. *Energy*, *169*, 319–328. https://doi.org/10.1016/j.energy.2018.11.149

EEA. (n.d.-a). *Air quality statistics* [Dashboard (Tableau)]. Retrieved 13 June 2024, from https://www.eea.europa.eu/data-and-maps/dashboards/air-quality-statistics

EEA. (n.d.-b). *European Air Quality Index*. Retrieved 12 June 2024, from https://airindex.eea.europa.eu/AQI/index.html#

EEA. (n.d.-c). *Nitrogen oxides, NOx* [Term]. European Environment Agency. Retrieved 17 June 2024, from https://www.eea.europa.eu/help/glossary/eper-chemicals-glossary/nitrogen-oxides-nox

EEA. (2023a). *EMEP/EEA air pollutant emission inventory guidebook 2023: Technical guidance to prepare national emission inventories.* Publications Office. https://data.europa.eu/doi/10.2800/795737

EEA. (2023b, October 24). *Greenhouse gas emissions from energy use in buildings in Europe*. https://www.eea.europa.eu/en/analysis/indicators/greenhouse-gas-emissions-from-energy

EMBER. (2024, July 3). *European wholesale electricity price data*. Ember. https://ember-climate.org/data-catalogue/european-wholesale-electricity-price-data/

EU Carbon Permits. (n.d.). Retrieved 24 October 2024, from https://tradingeconomics.com/commodity/carbon

Euroheat & Power. (2024, June). *DHC Market Outlook 2024; Executive Summary*. https://www.euroheat.org/news/dhc-market-outlook-2024-the-most-comprehensive-publication-on-district-heating-and-cooling-to-date-1

European Commission. (n.d.). *EU air quality standards*. Retrieved 31 May 2024, from https://environment.ec.europa.eu/topics/air/air-quality/eu-air-quality-standards_en

European Commission. (2023, October 31). *Report on the functioning of the European carbon market in 2022*.

Eurostat. (2022). *Gas statistics* [Dataset]. Eurostat. https://doi.org/10.2908/NRG_PC_203

Eurostat. (2023, June). *Energy consumption in households*. https://ec.europa.eu/eurostat/statistics-explained/index.php?title=Energy_consumption_in_households

Fadzlin, W. A., Hasanuzzaman, Md., Rahim, N. A., Amin, N., & Said, Z. (2022). Global Challenges of Current Building-Integrated Solar Water Heating Technologies and Its Prospects: A Comprehensive Review. *Energies*, *15*(14), 5125. https://doi.org/10.3390/en15145125

FEDENE. (2024, March 7). *Heating and cooling network data library 2023*. Fedene. https://fedene.fr/ressource/bibliotheque-de-donnees-des-reseaux-de-chaleur-et-de-froid-2023/

Gadd, H., & Werner, S. (2014). Achieving low return temperatures from district heating substations. *Applied Energy*, *136*, 59–67. https://doi.org/10.1016/j.apenergy.2014.09.022

Garbev, V. (2023). Power-to-Heat in district heating systems—A case study for Sofia's DHC. *2023 18th Conference on Electrical Machines, Drives and Power Systems (ELMA)*, 1–4. https://doi.org/10.1109/ELMA58392.2023.10202327

Geels, F. W. (2012). A socio-technical analysis of low-carbon transitions: Introducing the multi-level perspective into transport studies. *Journal of Transport Geography*, *24*, 471–482. https://doi.org/10.1016/j.jtrangeo.2012.01.021

Georgiev, Z., Shindarski, P., & Rafailova, Z. (2020). *Analysis of energy supply and demand in the municipality of Sofia. Spatial model and scenarios for sustainable energy development in the residential sector for the period 2020-2050*. https://sofiaplan.bg/wp-content/uploads/2021/03/I.5.3_%D0%95%D0%BD%D0%B5%D1%80%D0%B3%D0%B8%D1%8F_%D0%9F%D1%80%D0%B8%D0%BB%D0%BE%D0%B6%D0%B5%D0%BD%D0%B8%D0%B5.pdf

GIS Sofiaplan. (n.d.). *Енергийни паспорти*. Retrieved 23 May 2024, from https://gis.sofiaplan.bg/arcgis/apps/dashboards/7e6d26b48f644b578d87b15398f78440

GreenDelta. (2017, February 20). *ILCD 2011 v1.0.10 method update in openLCA*.

Huijbregts, M. A. J., Steinmann, Z. J. N., Elshout, P. M. F., Stam, G., Verones, F., Vieira, M., Zijp, M., Hollander, A., & van Zelm, R. (2017). ReCiPe2016: A harmonised life cycle impact assessment method at midpoint and endpoint level. *The International Journal of Life Cycle Assessment*, *22*(2), 138–147. https://doi.org/10.1007/s11367-016-1246-y

IEA. (n.d.). *Bulgaria—Countries & Regions*. IEA. Retrieved 24 October 2024, from https://www.iea.org/countries/bulgaria

IEA. (2024). *World Energy Outlook 2024 – Analysis*. IEA. https://www.iea.org/reports/world-energy-outlook-2024

IEA, NEA, & OECD. (2020). *Projected Costs of Generating Electricity*. https://iea.blob.core.windows.net/assets/ae17da3d-e8a5-4163-a3ec-2e6fb0b5677d/Projected-Costs-of-Generating-Electricity-2020.pdf

IRENA. (2019). *Renewable energy market analysis Southeast Europe*. https://www.irena.org/-/media/Files/IRENA/Agency/Publication/2019/Dec/IRENA_Market_Analysis_SEE_2019.pdf

Ivanov, M. J. (2019). Governed by tensions: The introduction of renewable energies and their integration in the Bulgarian energy system (2006–2016). *Environmental Innovation and Societal Transitions*, *32*, 90–106. https://doi.org/10.1016/j.eist.2018.10.002

Jodeiri, A. M., Goldsworthy, M. J., Buffa, S., & Cozzini, M. (2022). Role of sustainable heat sources in transition towards fourth generation district heating – A review. *Renewable and Sustainable Energy Reviews*, *158*, 112156. https://doi.org/10.1016/j.rser.2022.112156

Kaczmarczyk, M., Sowiżdżał, A., & Tomaszewska, B. (2020). Energetic and Environmental Aspects of Individual Heat Generation for Sustainable Development at a Local Scale—A Case Study from Poland. *Energies*, *13*(2), Article 2. https://doi.org/10.3390/en13020454

Kalogirou, S. A. (2004). Solar thermal collectors and applications. *Progress in Energy and Combustion Science*, *30*(3), 231–295. https://doi.org/10.1016/J.PECS.2004.02.001

Kalogirou, S. A. (2014a). Environmental Characteristics. In *Solar Energy Engineering* (pp. 51–123). Elsevier. https://doi.org/10.1016/B978-0-12-397270-5.00002-9

Kalogirou, S. A. (2014b). Performance of Solar Collectors. In *Solar Energy Engineering* (pp. 221–256). Elsevier. https://doi.org/10.1016/B978-0-12-397270-5.00004-2

Kang, A., Korolija, I., & Rovas, D. (2022). Photovoltaic Thermal District Heating: A review of the current status, opportunities and prospects. *Applied Thermal Engineering*, *217*, 119051. https://doi.org/10.1016/j.applthermaleng.2022.119051

KEVR. (2019). *Как се образуват цените на тока?*

KEVR. (2020, September 25). *Решение № И8-Л-032*. https://www.dker.bg/uploads/reshenia/2020/res_i8_l_032_20.pdf

KEVR. (2024). *Заявления за цени*. Комисия за енергийно и водно регулиране. https://www.dker.bg/bg/toploenergetika/tseni-3.html

KNG. (n.d.). *Rostock power plant*. Retrieved 30 October 2024, from https://kraftwerk-rostock.de/

Koďousková, H., Ilavská, A., Stašáková, T., David, D., & Osička, J. (2023). Energy transition for the rich and energy poverty for the rest? Mapping and explaining district heating transition, energy poverty, and vulnerability in Czechia. *Energy Research & Social Science*, *100*, 103128. https://doi.org/10.1016/j.erss.2023.103128

Kristmannsdóttir, H., & Ármannsson, H. (2003). Environmental aspects of geothermal energy utilization. *Geothermics*, *32*(4), 451–461. https://doi.org/10.1016/S0375-6505(03)00052-X

Lambert, R. S. C., Maier, S., Shah, N., & Polak, J. W. (2016). Optimal phasing of district heating network investments using multi-stage stochastic programming. *International Journal of Sustainable Energy Planning and Management*, *9*, 57–74. https://doi.org/10.5278/ijsepm.2016.9.5

Li, Y., Liu, M., Tang, Y., Jia, Y., Wang, Q., Ma, Q., Hong, J., Zuo, J., & Yuan, X. (2022). Life cycle impact of winter heating in rural China from the perspective of environment, economy, and user experience. *Energy Conversion and Management*, *269*, 116156. https://doi.org/10.1016/j.enconman.2022.116156

Lotrecchiano, N., & Sofia, D. (2022). Analysis of the Air Quality of a District Heating System with a Biomass Plant. *Atmosphere*, *13*(10), Article 10. https://doi.org/10.3390/atmos13101636

Lund, H., Werner, S., Wiltshire, R., Svendsen, S., Thorsen, J. E., Hvelplund, F., & Mathiesen, B. V. (2014). 4th Generation District Heating (4GDH): Integrating smart thermal grids into future sustainable energy systems. *Energy*, *68*, 1–11. https://doi.org/10.1016/J.ENERGY.2014.02.089

Mahmoud, M., Ramadan, M., Naher, S., Pullen, K., & Olabi, A.-G. (2021). The impacts of different heating systems on the environment: A review. *Science of The Total Environment*, *766*, 142625. https://doi.org/10.1016/j.scitotenv.2020.142625

Mandel, T., Worrell, E., & Alibaş, Ş. (2023). Balancing heat saving and supply in local energy planning: Insights from 1970-1989 buildings in three European countries. *Smart Energy*, *12*, 100121. https://doi.org/10.1016/j.segy.2023.100121

Meindl, B., & Templ, M. (2012). *Analysis of commercial and free and open source solvers for linear optimization problems*. https://www.researchgate.net/publication/265117825_Analysis_of_commercial_and_free_and_open_source_solvers_for_linear_optimization_problems

Möller, B. (2021). *Pan-European Thermal Atlas*. sEEnergies. https://www.seenergies.eu/peta5/

Moradpoor, I., Syri, S., & Hirvonen, J. (2022). Sustainable heating alternatives for 1960's and 1970's renovated apartment buildings. *Cleaner Environmental Systems*, *6*, 100087. https://doi.org/10.1016/j.cesys.2022.100087

Nocedal, J., & Wright, S. J. (2006). *Numerical Optimization*. Springer New York. https://doi.org/10.1007/978-0-387-40065-5

Paardekooper, S., Lund, H., Chang, M., Nielsen, S., Moreno, D., & Thellufsen, J. Z. (2020). Heat Roadmap Chile: A national district heating plan for air pollution decontamination and decarbonisation. *Journal of Cleaner Production*, *272*, 122744. https://doi.org/10.1016/j.jclepro.2020.122744

Peneva, T. (2022). *Енергийната бедност в България: Измерения и фактори* (1st ed.). Bulgarian Academy of Sciences 'Marin Drinov'. https://www.iki.bas.bg/files/Energiina_bednost-19.09.pdf

PVGIS. (2024). https://pvgis.com

Ravina, M., Panepinto, D., & Zanetti, M. (2021). District heating networks: An inter-comparison of environmental indicators. *Environmental Science and Pollution Research*, *28*(26), 33809–33827. https://doi.org/10.1007/s11356-020-08734-z

RIVM. (2017). *A harmonized life cycle impact assessment method at midpoint and endpoint level Report I: Characterization*. https://www.rivm.nl/documenten/recipe2016v11

Salva, J., Poništ, J., Rasulov, O., Schwarz, M., Vanek, M., & Sečkár, M. (2023). The impact of heating systems scenarios on air pollution at selected residential zone: A case study using AERMOD dispersion model. *Environmental Sciences Europe*, *35*(1), 91. https://doi.org/10.1186/s12302-023-00798-1

Shesho, I., Filkoski, R., & Tashevski, D. (2018). Techno-economic and environmental optimization of heat supply systems in urban areas. *Thermal Science*, *22*(Suppl. 5), 1635–1647. https://doi.org/10.2298/TSCI18S5635S

Sifnaios, I., Gauthier, G., Trier, D., Fan, J., & Jensen, A. R. (2023). Dronninglund water pit thermal energy storage dataset. *Solar Energy*, *251*, 68–76. https://doi.org/10.1016/j.solener.2022.12.046

Simulated historical climate & weather data for Sofia. (n.d.). Meteoblue. Retrieved 23 October 2024, from https://www.meteoblue.com/en/weather/historyclimate/climatemodelled/sofia_bulgaria_727011

Ślusarz, G., Twaróg, D., Gołębiewska, B., Cierpiał-Wolan, M., Gołębiewski, J., & Plutecki, P. (2023). The Role of Biogas Potential in Building the Energy Independence of the Three Seas Initiative Countries. *Energies 2023, Vol. 16, Page 1366*, *16*(3), 1366. https://doi.org/10.3390/EN16031366

Solar Keymark. (n.d.). Retrieved 25 October 2024, from https://solarkeymark.eu/database/

Sporleder, M., Rath, M., & Ragwitz, M. (2022). Design optimization of district heating systems: A review. *Frontiers in Energy Research*, *10*. https://doi.org/10.3389/fenrg.2022.971912

Stanimirov, N. (2008, March 7). *Основни технически изисквания към абонатни станции с топлоносител гореща вода*. https://toplo.bg/media/%D0%90%D0%BA%D1%82%D1%83%D0%B0%D0%BB%D0%BD%D0%BE/%D0%97%D0%B0%D0%BA%D0%BE%D0%BD%D0%BE%D0%B4%D0%B0%D1%82%D0%B5%D0%BB%D0%BD%D0%B0%20%D1%80%D0%B0%D0%BC%D0%BA%D0%B0/%D0%92%D1%8A%D1%82%D1%80%D0%B5%D1%88%D0%BD%D0%B8%20%D0%B4%D0%BE%D0%BA%D1%83%D0%BC%D0%B5%D0%BD%D1%82%D0%B8/instrukzia_ab_st_tpm.pdf

Statista. (2024). *Bulgaria: Power sector carbon intensity 2023*. Statista. https://www.statista.com/statistics/1290143/carbon-intensity-power-sector-bulgaria/

SW Rostock. (n.d.). *Power-to-Heat plant | Stadtwerke Rostock*. Retrieved 30 October 2024, from https://www.swrag.de/wir-fuer-hier/fuer-die-region/power-to-heat

Tchounwou, P. B., Yedjou, C. G., Patlolla, A. K., & Sutton, D. J. (2012). Heavy Metals Toxicity and the Environment. *EXS*, *101*, 133–164. https://doi.org/10.1007/978-3-7643-8340-4_6

Tian, Z., Perers, B., Furbo, S., & Fan, J. (2018). Thermo-economic optimization of a hybrid solar district heating plant with flat plate collectors and parabolic trough collectors in series. *Energy Conversion and Management*, *165*, 92–101. https://doi.org/10.1016/j.enconman.2018.03.034

Toplofikatsiya Sofia. (n.d.). *Отоплителен сезон*. Топлофикация София ЕАД. Retrieved 31 May 2024, from http://toplo.bg/heating-season

Toplofikatsiya Sofia. (2022a, January 21). *Announcement of an investment proposal Sofia Iztok*. https://toplo.bg/media/%D0%97%D0%B0%D0%BA%D0%BE%D0%BD%D0%BE%D0%B4%D0%B0%D1%82%D0%B5%D0%BB%D0%BD%D0%B0%20%D1%80%D0%B0%D0%BC%D0%BA%D0%B0/ip_si_2022.pdf

Toplofikatsiya Sofia. (2022b, May 5). *Announcement of an investment proposal Orlandovtsi*. https://toplo.bg/media/%D0%97%D0%B0%D0%BA%D0%BE%D0%BD%D0%BE%D0%B4%D0%B0%D1%82%D0%B5%D0%BB%D0%BD%D0%B0%20%D1%80%D0%B0%D0%BC%D0%BA%D0%B0/%D0%B8%D0%BD%D0%B2%D0%B5%D1%81%D1%82%D0%B8%D1%86%D0%B8%D0%BE%D0%BD%D0%BD%D0%BE-%D0%BF%D1%80%D0%B5%D0%B4%D0%BB%D0%BE%D0%B6%D0%B5%D0%BD%D0%B8%D0%B5-%D0%B7%D0%B0-%D0%B2%D0%BE%D1%86-%D0%BE%D1%80%D0%BB%D0%B0%D0%BD%D0%B4%D0%BE%D0%B2%D1%86%D0%B8-%D1%83%D0%B2%D0%B5%D0%B4%D0%BE%D0%BC%D0%BB%D0%B5%D0%BD%D0%B8%D0%B5-%D0%BF%D1%80%D0%B8%D0%BB%D0%BE%D0%B6%D0%B5%D0%BD%D0%B8%D1%8F.pdf

United Nations. (n.d.). *What Is Climate Change?* United Nations; United Nations. Retrieved 6 June 2024, from https://www.un.org/en/climatechange/what-is-climate-change

US EPA, O. (2021, January 22). *How are Oxides of Nitrogen (NOx) defined in the NEI?* [Overviews and Factsheets]. https://www.epa.gov/air-emissions-inventories/how-are-oxides-nitrogen-nox-defined-nei

Vašek Novotný (Director). (2020, November 18). *CHP units—Czech Technical University in Prague* [Video recording]. https://www.youtube.com/watch?v=KEJ7kAZzlL4

Weinand, J. M., Kleinebrahm, M., McKenna, R., Mainzer, K., & Fichtner, W. (2019). Developing a combinatorial optimisation approach to design district heating networks based on deep geothermal energy. *Applied Energy*, *251*, 113367. https://doi.org/10.1016/j.apenergy.2019.113367

Weng, Z., Wang, Y., Yang, X., Cheng, C., Tan, X., & Shi, L. (2022). Effect of cleaner residential heating policy on air pollution: A case study in Shandong Province, China. *Journal of Environmental Management*, *311*, 114847. https://doi.org/10.1016/j.jenvman.2022.114847

Werner, S. (2017). International review of district heating and cooling. *Energy*, *137*, 617–631. https://doi.org/10.1016/j.energy.2017.04.045

Werner, S. (2022). Network configurations for implemented low-temperature district heating. *Energy*, *254*. Scopus. https://doi.org/10.1016/j.energy.2022.124091

WHO. (n.d.). *Types of pollutants*. Air Quality, Energy and Health. Retrieved 13 May 2024, from https://www.who.int/teams/environment-climate-change-and-health/air-quality-and-health/health-impacts/types-of-pollutants

Wojdyga, K., Chorzelski, M., & Rozycka-Wronska, E. (2014). Emission of pollutants in flue gases from Polish district heating sources. *Journal of Cleaner Production*, *75*, 157–165. https://doi.org/10.1016/j.jclepro.2014.03.069

Yoon, T., Ma, Y., & Rhodes, C. (2015). Individual Heating systems vs. District Heating systems: What will consumers pay for convenience? *Energy Policy*, *86*, 73–81. https://doi.org/10.1016/j.enpol.2015.06.024

ECO. (2024). *Статистическа книжка 2023*. ECO. https://www.eso.bg/fileObj.php?oid=4990

Общ устройствен план на СО. (n.d.). *Софияплан*. Retrieved 23 October 2024, from https://sofiaplan.bg/portfolio/oup-sofia/

Appendix A: Air pollution details

Which pollutants to focus on?

As Table 12 shows, even a limited literature review points at a wide variety of pollutants related to residential heating that can affect air quality. Moreover, different researchers consider different sets of them without necessarily providing arguments on their selection criteria. Several points are important to note. First, total suspended particles (TSP), PM_{10} and $PM_{2.5}$ are related categories. TSP refers to all particles in the atmosphere, PM_{10} considers only particles with aerodynamic diameter smaller than 10 µm, and $PM_{2.5}$ only the ones with aerodynamic diameter smaller than 2.5 µm (Alias et al., 2007). The smaller particles are considered to pose greater threat to human health (Alias et al., 2007), and thus have stricter limits in terms of concentration (WHO, n.d.). Second, NO_x is compiled from emissions of NO and NO_2 (EEA, n.d.-c) expressed as the molecular weight of nitrogen dioxide (NO_2) (US EPA, 2021).

Therefore, most studies consider air pollution caused by (i) some particulate matter pollutant and (ii) some nitrous oxides The pollution caused by sulphur dioxide (SO_2) and carbon monoxide (CO) is frequently researched, though to a lesser extent.

Table 12: Summary of the measured air pollutants in the context of residential heating. TSP stands for Total suspended particles. Source: own work.

Study/pollutant	$PM_{2.5}$	PM_{10}	TSP	SO_2	NO_2	NO_x	CO	Hydrogen fluoride	Hydrochloric acid
WHO (n.d.)[11]	x	x		x	x		x		

[11] Note that the World Health Organisation (WHO) website lists heavy metal pollutants too, but they are not emitted by heating-related sources (Tchounwou et al., 2012).

Weng et al. (2022)	x	x		x	x				
Salva et al. (2023)					x		x		
Ravina et al. (2021)			x			x	x		
Kaczmarczyk et al. (2020)	x	x		x	x		x		
Li et al. (2022)	x			x		x			
Wojdyga et al. (2014)				x		x		x	x
Paardekooper et al. (2020)	x	x							

The European Environment Agency (EEA) of the European Union keeps track of many different air pollutants. Out of the pollutants in Table 12, the EEA database lists measurements for $PM_{2.5}$, PM_{10}, SO_2, NO_2 and CO. The compliance of all available Bulgarian air monitoring stations in 2022 with World health Organisation (WHO) and EU air pollution regulations is presented in

Table 13 below (EEA, n.d.-a).

Table 13: Compliance of Bulgarian air monitoring stations with air pollution regulations. Source: (EEA, n.d.-a)

Pollutant	**Number of stations**	**% of stations that meet WHO's hourly limit**	**% of stations that meet WHO's annual limit**	**% of stations that meet EU's annual limit**
NO_2	25	25%	25%	96%
$PM_{2.5}$	9	0%	0%	100%
PM_{10}	40	8%	10%	100%
CO	18	100%	n.a.	n.a.
SO_2	28	86%	n.a.	n.a.

Based on this data, there are several observations that can be made:

- The EU standards are considerably more relaxed than the WHO standards in all categories where both bodies have provided a threshold.
- There are few stations across Bulgaria, which gives a limited picture of air pollution

- NO_2 and PM emissions are a considerable issue in Bulgaria, if the WHO standards are considered
- CO and SO_2 emissions are largely within the prescribed limits

In conclusion, this study should focus on the air pollution caused by particulate matter and nitrous oxides. These are both considered more in the literature and appear to be more problematic in Bulgaria's case.

How to measure air pollution?

Air pollution is measured as the concentration of a type of pollutant per cubic metre of air (EEA, n.d.-b, n.d.-a; WHO, n.d.; Wojdyga et al., 2014). This data can be combined in an index, where the concentrations of multiple pollutants are considered to obtain an ordinal description of air quality, for example in the European air quality index (EEA, n.d.-b). Techno-economic studies, on the other hand, consider the emissions of the systems they consider either in absolute terms over a period of time or per unit of delivered energy (Kaczmarczyk et al., 2020; Moradpoor et al., 2022). This is a considerably simpler approach that signals the expected impact of a technology, without necessitating field observations or modelling of the surrounding air. A significant drawback of this approach, however, is that it does not merge the emissions of different pollutants in any over-arching index that captures all of them.

The field of life cycle impact assessment (LCIA) bridges the gap between these two approaches. By combining the emissions of different pollutants into a limited number of environmental impact scores, LCIA simplifies the interpretation of a dashboard of emissions (RIVM, 2017). This is done using characterisation factors that indicate the environmental impact per unit of pollutant or stressor (e.g. per mass of emission). Characterisation can be done at midpoint or endpoint level. Endpoint level characterisation corresponds to three areas of protection, i.e. human health, ecosystem quality and resource scarcity (RIVM, 2017) and provides an aggregate view of the system. Midpoint characterisation considers more impact categories (ionising radiation, toxicity, etc.) and assigns characterisation factors to all flows assigned to an impact category (RIVM, 2017). Moreover, the characterisation factors can take three different perspectives on uncertainty (RIVM, 2017), namely:

- Individualistic perspective – based on short-term interest, undisputed impact types, and technological optimism with regard to human adaptation.
- Hierarchist perspective – based on scientific consensus with regard to the time frame and plausibility of impact mechanisms.
- Egalitarian perspective – the most precautionary perspective, which takes into account the longest time frame and all impact pathways for which data is available

The ReCiPe 2016, a LCIA framework developed by the Dutch National Institute for Public Health and the Environment (RIVM), has three midpoint impact categories related to air pollution – fine particulate matter formation, terrestrial acidification and photochemical oxidant formation (with separate impacts on humans and ecosystems). As the case study of this research takes place in urban environment, the ecosystems' impact of photochemical oxidant formation will be disregarded. The hierarchist characterisation factors of these categories are presented in Table 14.

Table 14: Midpoint characterisation factors of the air pollution impact categories of the ReCiPe 2016. Source: RIVM (2017)

Impact category	**Pollutant**	**Characterisation factor**
Fine particulate matter	$PM_{2.5}$	1
	NH_3	0.24

Characterisation factor unit: $PM_{2.5}$-eq./kg	SO	0.39
	SO_2	0.29
	SO_3	0.23
	NO	0.17
	NO_2	0.11
	NO_3	0.8
Photochemical ozone formation Characterisation factor unit: NO2-eq./kg	NO	1.53
	NO_2	1
	NO_3	0.74
	NMVOC	0.29
Terrestrial acidification Characterisation factor unit: SO_2-eq./kg	NH_3	1.96
	SO	1.33
	SO_2	1
	SO_3	0.65
	H_2SO_4	0.65
	NO	0.55
	NO_2	0.36
	NO_3	0.27

As explained in the previous section, this study focuses on the pollution caused by particulate matter and nitrous oxides. The fine particulate matter impact category includes both of these pollutant groups and will therefore be used in the optimisation framework as a proxy for air pollution.

Appendix B: Energy technologies input data

The table below discusses the main technologies, the reasons for their inclusion or exclusion, their technical potential in Orlandovtsi and associated costs. This section relies heavily on the technological descriptions of energy storage and conversion technologies of the Danish Energy Agency (Danish Energy Agency, 2018, 2024). In the few cases when the data does not originate from these documents, this is

indicated in the table. The key assumptions made regarding the different technologies are described below.

Table 15: Reasons for the inclusion and exclusion of certain technologies for heat and electricity production. Certain costs are not included in the sources and are thus omitted. For more information see Danish Energy Agency (2018, 2024).

Technology	Reasoning for inclusion or exclusion	Potential	Capital costs M€/MW	Fixed operational costs €/MW/ year	Variable operational costs €/MWh	Efficiency
Natural gas CHP	**Included**. Backbone of numerous DHNs across the world, including the rest of Sofia's network.	Practically unlimited potential, depends on the natural gas supply.	1	10 000	5.4[12]	0.96 or 0.44[13]
Natural gas boiler	**Included**. Frequently used to cover peak loads in larger networks or to fully supply smaller networks.	Practically unlimited potential, depends on the natural gas supply.	0.06	2 000	1.1	1.05
Air source heat pump (ASHP)	**Included**. Highly efficient technology that supports the electrification of the energy system. No in-situ emissions.	Practically unlimited potential, depends on the electricity supply.	1.01	2127	2.33	Dynamic. Lorentz efficiency: 0.53
Electric boiler (e-boiler)	**Included**. Efficient technology that supports the electrification of the energy system. No in-situ emissions. When combined with storage it allows the DHN operator to take advantage of periods of low electricity prices	Practically unlimited potential, depends on the electricity supply.	0.16	1100	0.5	0.98

[12] The variable O&M costs are calculated based on only on the heat output of the CHP, rather than the heat and electricity combined.

[13] Depending whether the plant produces both heat and electricity or only electricity

Solar thermal energy (ST)	**Included**. Mature technology for providing heat with no emissions related to the heat production, expected to play a large role in the future decarbonisation of residential heating. Three ST technologies considered	Limited by solar irradiation and land availability. In 2017 Sofia boasted an average global horizontal irradiation of 70 W/m^2 with a peak of 1011 W/m^2 (*PVGIS*, 2024).	ETC: 400 €/m^2 of apertura area PTC: 450 €/m^2 of apertura area (Tian et al., 2018) FPC: 240 €/m^2 of apertura area	-	ETC: 5 PTC: 8% of CAPEX FPC: 0.2	Dynamic
PV panels	**Included**. Mature technology for electricity production that has revolutionised the energy system. Its output could be used in conjunction with ASHPs and e-boilers.	See above.	0.56	11 300	-	Dynamic
Steel tank thermal energy storage (TES)	**Included**. Established technology for thermal energy storage. Predominantly used for intra-day storage.	Largest storage units are up to 10 000 m^3.	3 700 €/MWh capacity	8.8 €/MWh capacity	-	Daily heat loss of 0.2%
Pit TES	**Included**. Established technology for thermal energy storage. Predominantly used for seasonal storage.	Largest storage units are up to 210 000 m^3.	590 €/MWh capacity	3 €/MWh capacity	-	Daily heat loss of 0.1%.

Appendix C: Energy prices

A breakdown of the electricity prices is provided below (Table 16), taken from (EMBER, 2024). The data shows a clear spike in the post-2020 period, with both higher mean prices and higher variation. 2022 forms a peak in the data, with 2023 resembling the price levels of 2021. As the model and all input data are configured to work with an hourly timestep, the full integration of the data from 2020 (a leap year) was a challenge. Considering the similarity between the average and standard deviation of the 2018 and 2020 electricity prices, 2018 data was combined with the natural gas prices for 2020 to form a meaningful proxy.

Table 16: Summary statistics of the hourly electricity prices in Bulgaria 2017-2023 in €/MWh. Source: (EMBER, 2024)

	2017	2018	2019	2020	2021	2022	2023
count	8760	8760	8760	8784	8760	8760	8760
mean	39.32	39.89	47.47	39.29	108.70	252.82	103.4
std	20.22	19.46	20.82	17.60	75.01	131.56	50.32

The half-yearly gas prices exhibit similar fluctuation throughout the covered years with the second semester of 2021 marking the beginning of a new normal for gas prices far exceeding €20/MWh (Figure 29). The data is obtained from (Eurostat, 2022) and it reflects the prices for consumers in Bulgaria who purchase between 100 PJ and 999 PJ. The half-yearly values were averaged for each year.

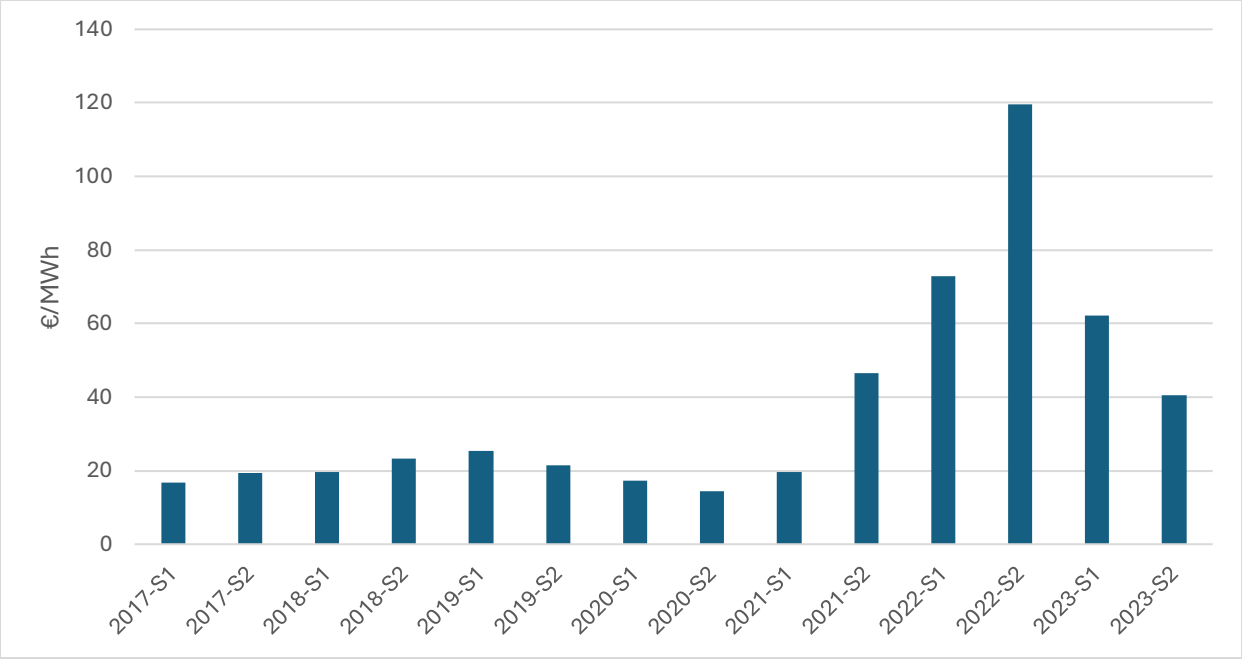

Figure 29: Gas prices in Bulgaria 2017-2023. Source: (Eurostat, 2022)

Appendix D: Additional figures

D1: 2017 prices, 70°C

Pareto fronts

BAU

The table below shows some of the important variables across the BAU Pareto front. The optimal solution (BAU opt) and the cheapest solution (BAU econ) are highlighted in green and its values are rounded, as per the way they were reported in the report so far. The installed capacities are measured in MW, and the capacity factors (CF) in percentages.

PM emissions [kg PM2.5-eq./year]	Costs [€]	Installed capacity boiler	Installed capacity e-boiler	Installed capacity tank	CF boiler	CF e-boiler	LCOH [€/MWh]
0	47857142	0	24.89476	220.506		30%	42.61974
12.77778	39917508	12.75832	20.50791	212.5693	6%	32%	35.549
25.55556	36149111	16.0594	17.71481	168.6266	10%	32%	32.19301
38.33333	33897261	17	16	132	14%	31%	30.1876
51.11111	32052380	17.8002	14.02309	99.41178	18%	29%	28.54462
63.88889	30604423	18.20913	11.52829	54.40175	22%	29%	27.25513
76.66667	29390445	18.75794	8.389547	37.22065	26%	30%	26.174
89.44444	28284629	20	5.47878	28.31304	28%	31%	25.18921
102.2222	27495845	20	4.894758	16.74681	32%	18%	24.48675
114.1405	26965495	20	5	17	36%	3%	24.01444

All technologies

The table below shows some of the important variables across the All technologies Pareto front. The optimal solution is highlighted in green and its values are rounded, as per the way they were reported in the report so far. The installed capacities are measured in MW, and the capacity factors (CF) in percentages.

PM emissions [kg PM2.5-eq./year]	Costs [€]	Installed capacity boiler	Installed capacity e-boiler	Installed capacity ASHP	Installed capacity pit	Installed capacity PV	CF boiler	CF e-boiler	CF ASHP	CF PV	LCOH [€/MWh]
0	30235615	0	18.36517	7.642625	905.751	10		12%	67%	15%	26.92668
9.222222	28304801	6.832504	9.472658	8.104486	741.2475	10	9%	15%	66%	15%	25.20717
18.44444	27121634	9.156287	4.669009	8.159891	619.5378	10	13%	18%	66%	15%	24.15349
27.66667	26171237	11	1	8	563	10	16%	19%	66%	15%	23.3071
36.88889	25366371	12.17085	0	7.604931	498.9459	10	19%		66%	15%	22.59032
46.11111	24767474	13.25179	0	6.450846	497.4836	10	22%		69%	15%	22.05696
55.33333	24224360	14.12937	0	5.323767	516.8102	10	25%		73%	15%	21.57329
64.55556	23727836	15.08786	0	4.230396	519.8951	10	27%		78%	15%	21.1311
73.77778	23279062	16.18289	0	3.137613	510.8092	10	29%		86%	15%	20.73144
82.2426	23074403	17.80079	0	2.418595	381	10	29%		89%	15%	20.54918

BAU economic

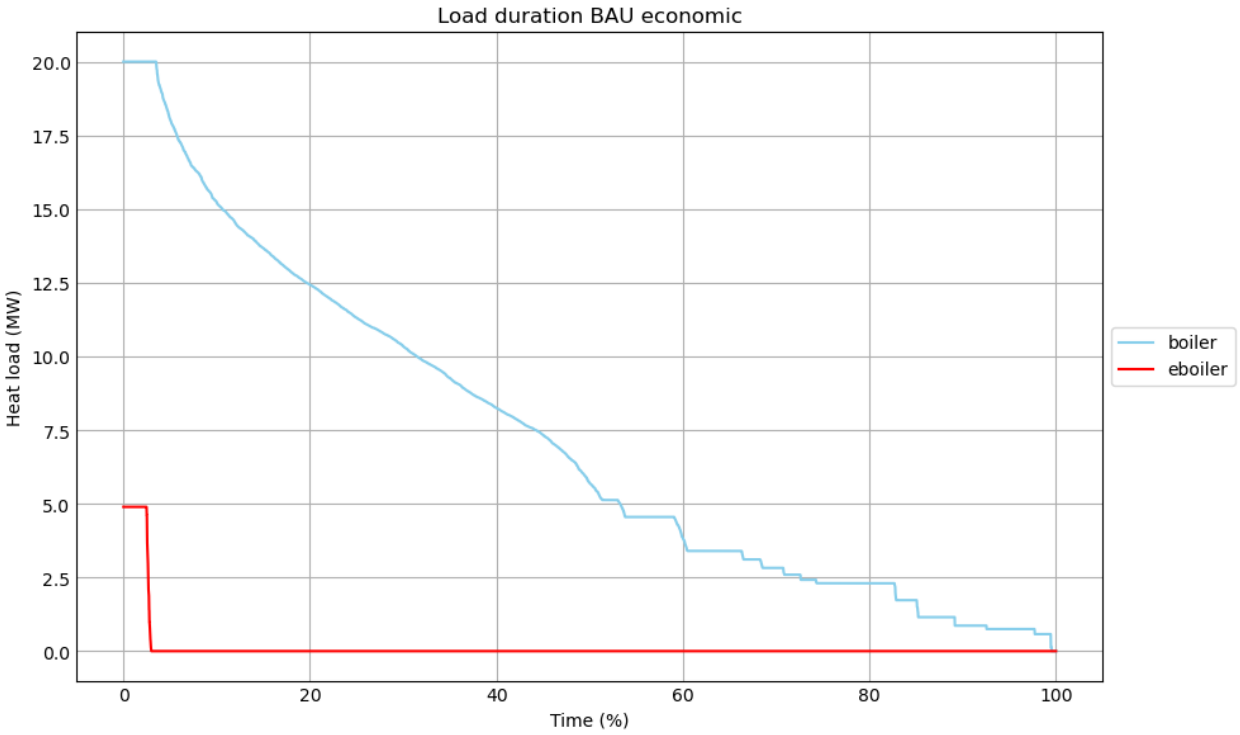

The figure above shows how the e-boiler acts in an on-off mode depending on the electricity prices, while the natural gas boiler balances the demand.

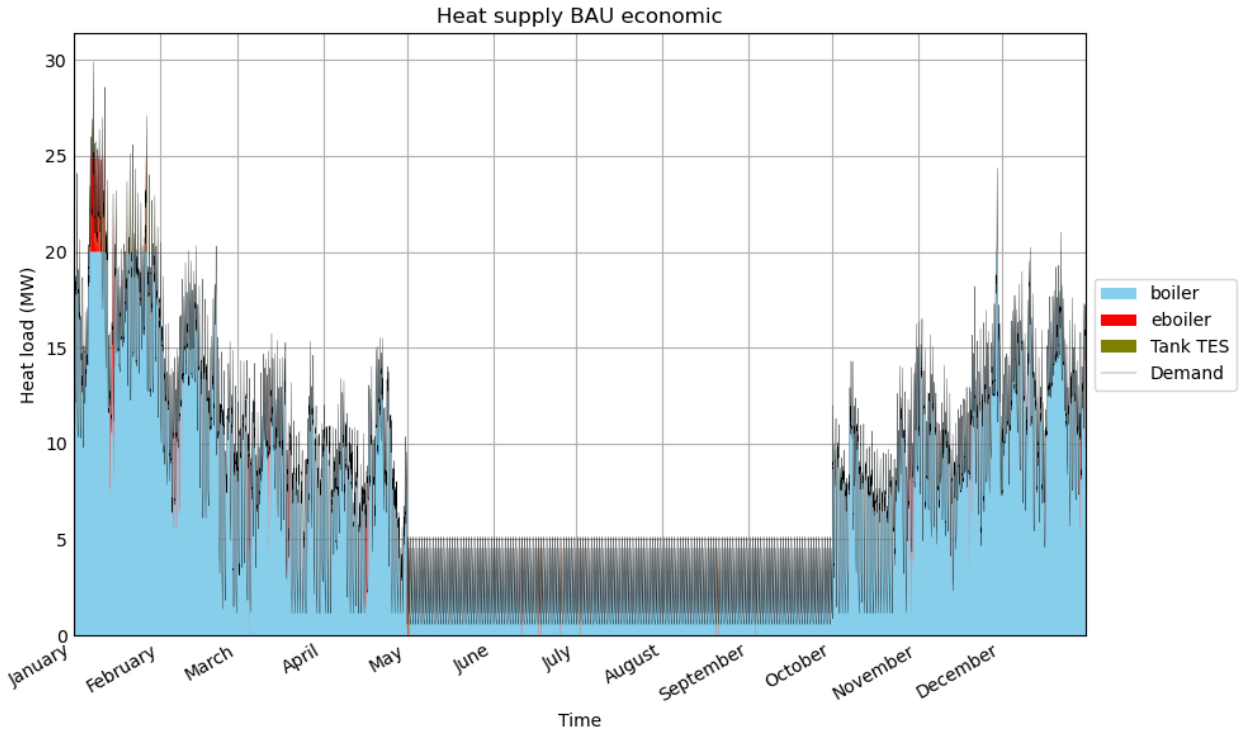

The figure above shows very clearly how the demand is almost entirely met by the natural gas boiler. As its size is limited to 20 MW, an e-boiler of at least 5 MW capacity is necessary to cover the largest peak in demand.

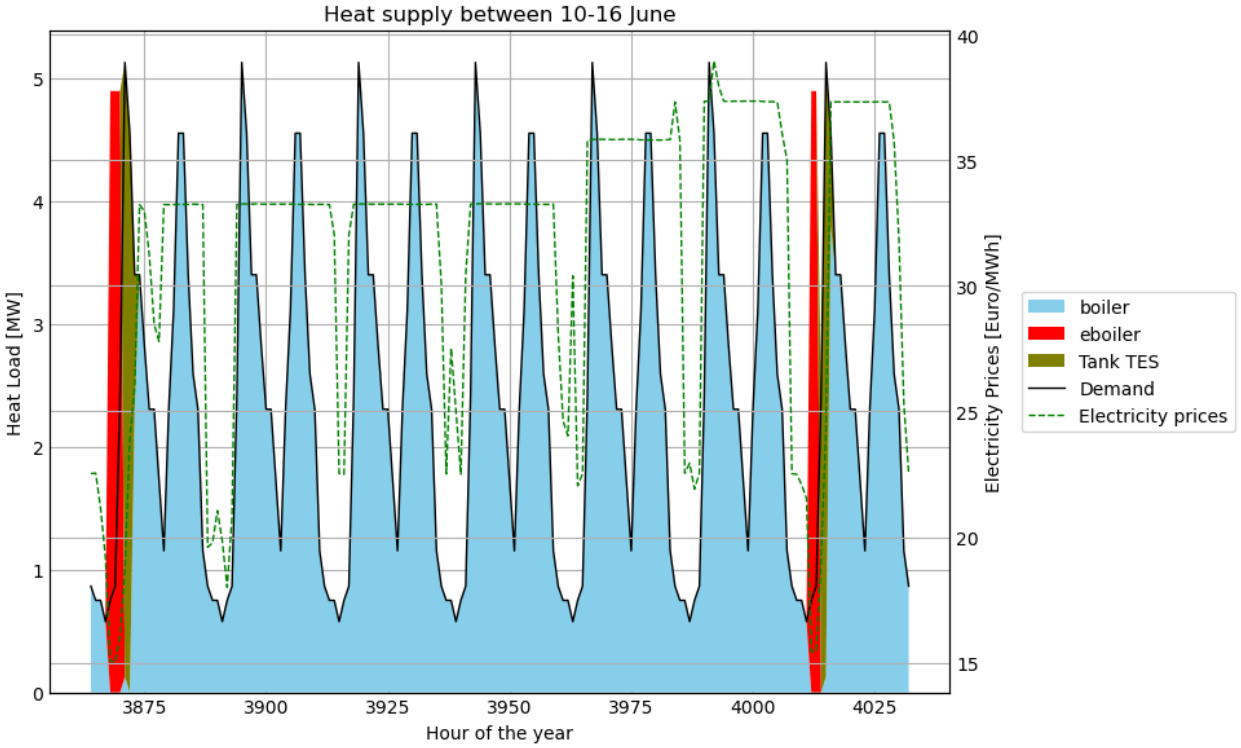

See how the e-boiler ramps up when the electricity price falls roughly below €20/MWh (above and below). Surplus heat production is stored in the TES and the gas at a later point is avoided.

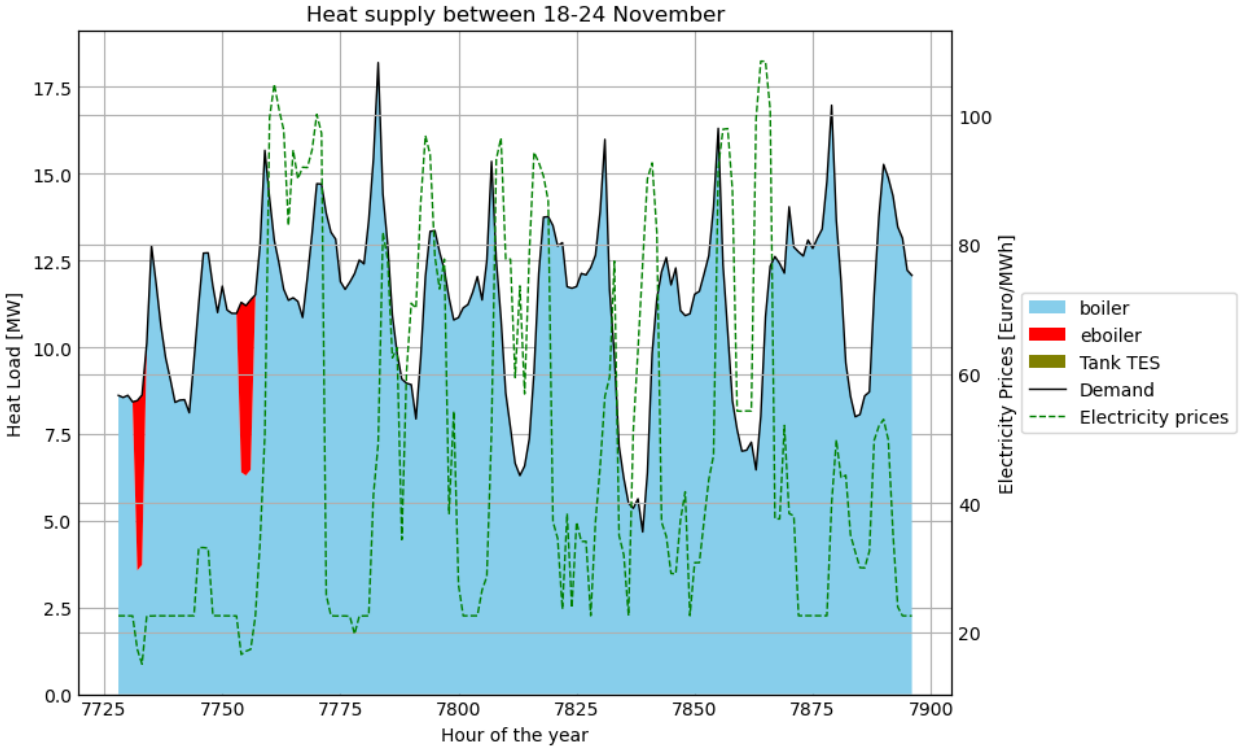

BAU Economic, no ETS

	P CHP [MW]	P boiler [MW]	P e-boiler [MW]	P tank [MWh]	Q CHP [GWh/yr]	Q Boiler [GWh/yr]	Q E-boiler [GWh/yr]	LCOH [€/MWh]	Emissions [kg PM2.5/yr]
BAU econ	0	20	5	17	0	63.38	1.15	24.01	114
No ETS	16	9	0	127	50.25	14.38	0	15.51	281

Comparison between the headline figures of BAU econ when optimised with and without emission costs of €50/tonne CO_2. Notice the much larger tank capacity which allows the CHP to ramp up only when the prices are above a certain threshold, the significantly lower LCOH and the higher emissions.

BAU optimal

A radically different way of meeting the demand, compared to BAU economic. The e-boiler is used in a highly responsive way, and meets the majority of the energy demand. The sector coupling between heat and electricity production is way more pronounced with the respective reliance on the TES.

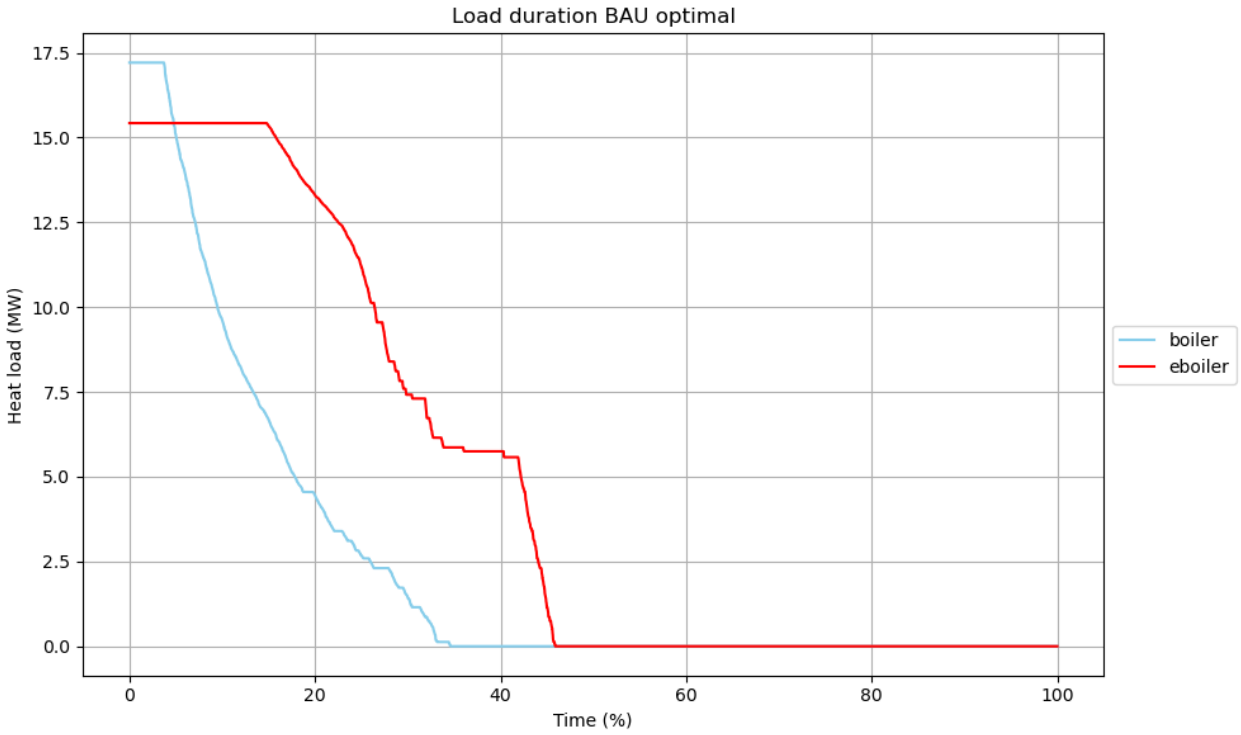
Load duration BAU optimal
Heat load (MW)
17.5
15.0
12.5
10.0
7.5
5.0
2.5
0.0
0
20
40
60
80
100
Time (%)
boiler
eboiler

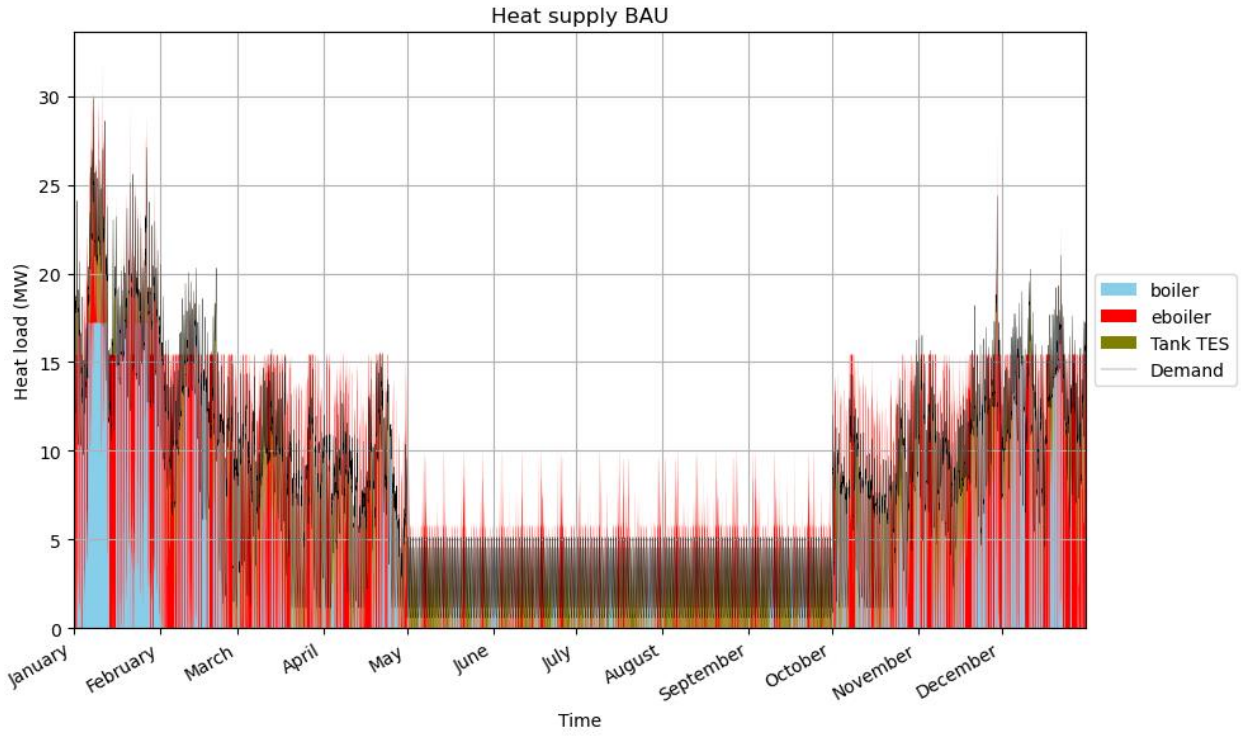
Heat supply BAU
Heat load (MW)
30
25
20
15
10
5
0
January
February
March
April
May
June
July
August
September
October
November
December
Time
boiler
eboiler
Tank TES
Demand

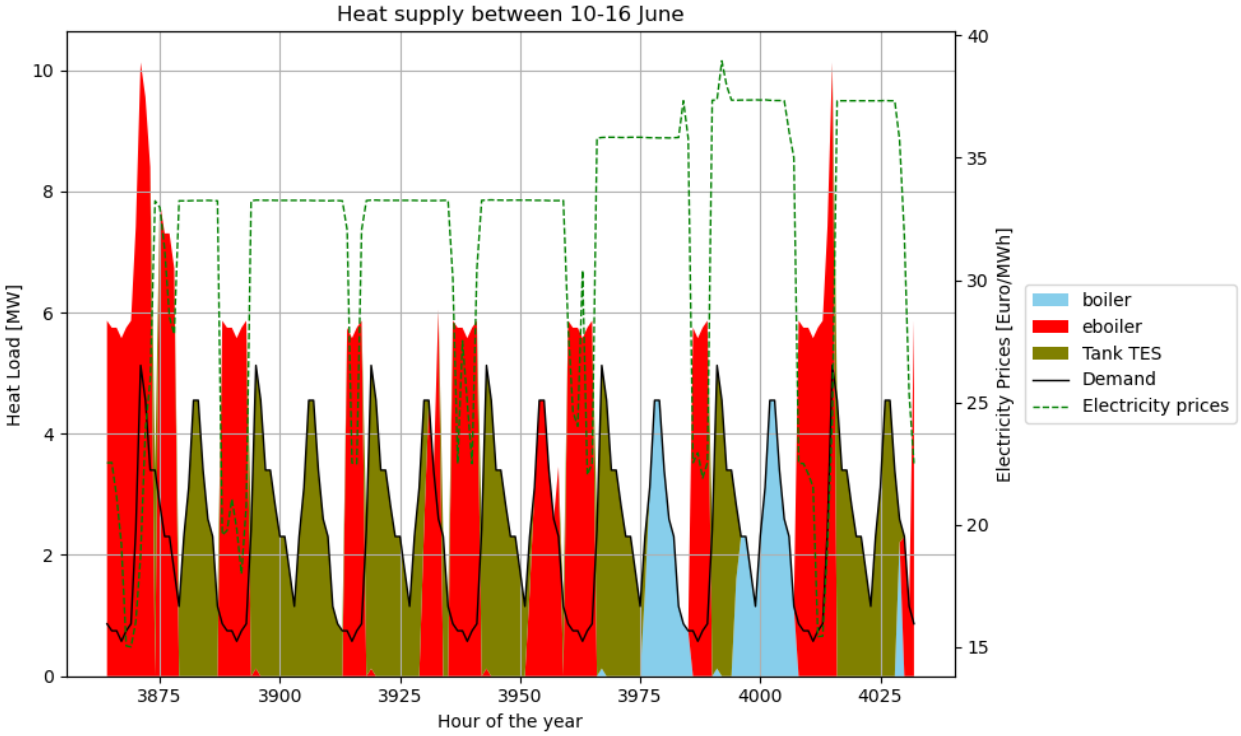
Heat supply between 10-16 June
Heat Load [MW]
Electricity Prices [Euro/MWh]
Hour of the year
boiler
eboiler
Tank TES
Demand
Electricity prices

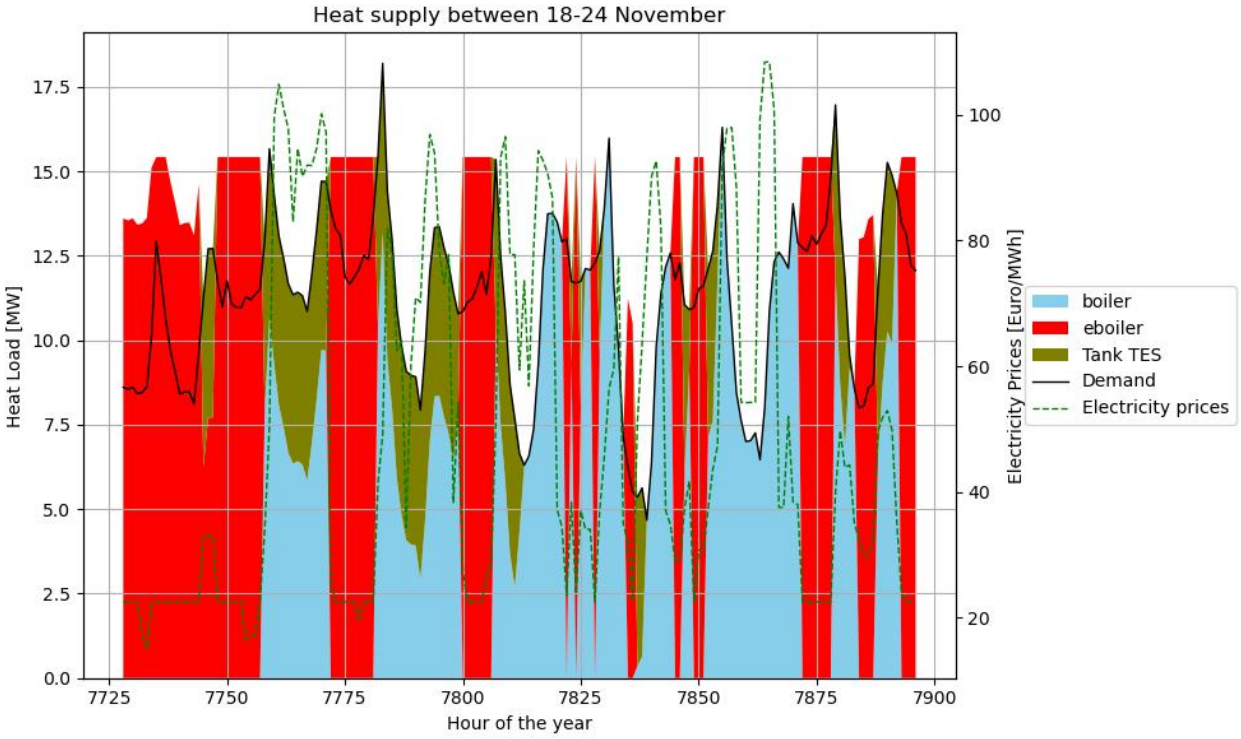
Heat supply between 18-24 November
Heat Load [MW]
Electricity Prices [Euro/MWh]
Hour of the year
boiler
eboiler
Tank TES
Demand
Electricity prices

RE

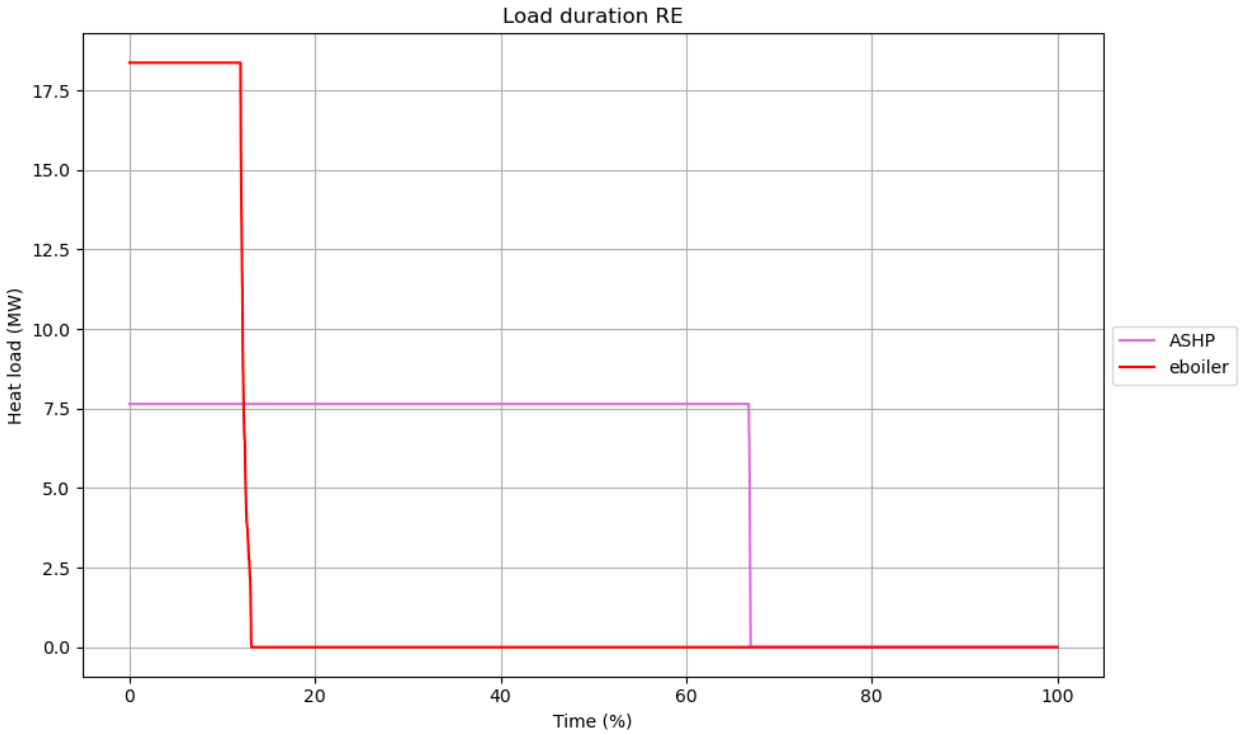
Load duration RE
Heat load (MW)
Time (%)
ASHP
eboiler

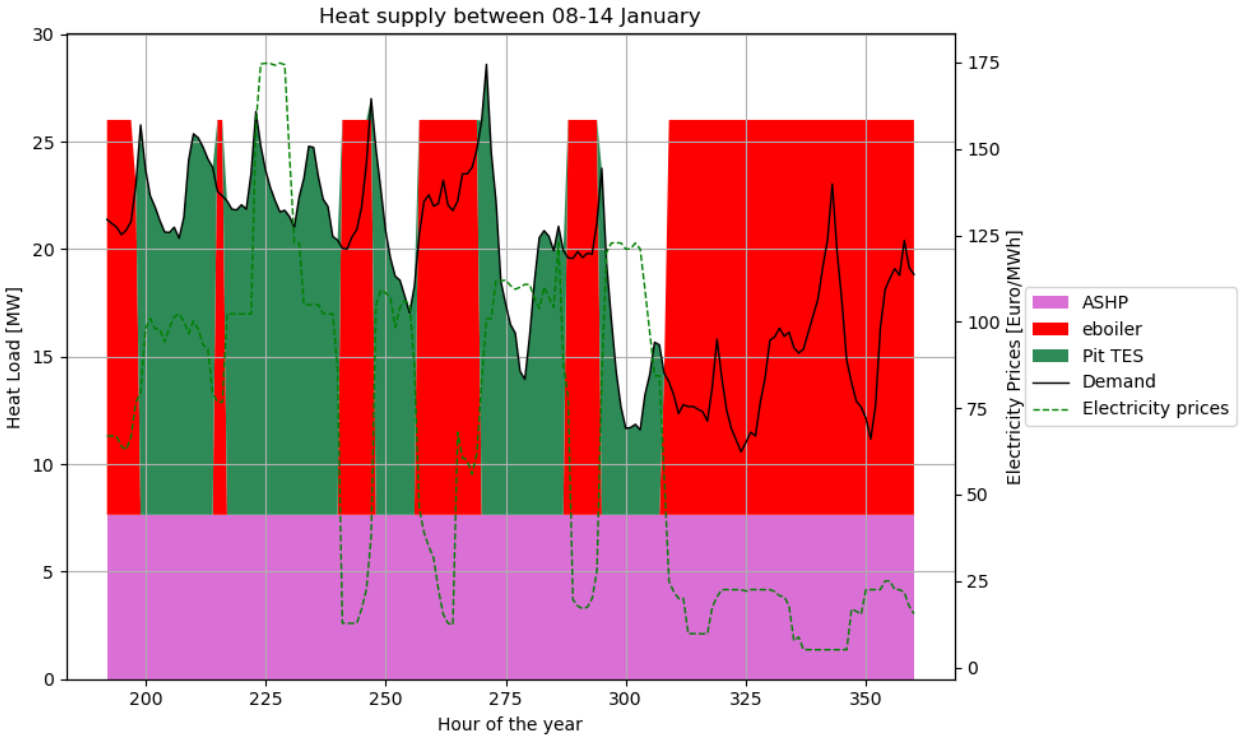
Heat supply between 08-14 January
Heat Load [MW]
Electricity Prices [Euro/MWh]
Hour of the year
ASHP
eboiler
Pit TES
Demand
Electricity prices

RE-ST

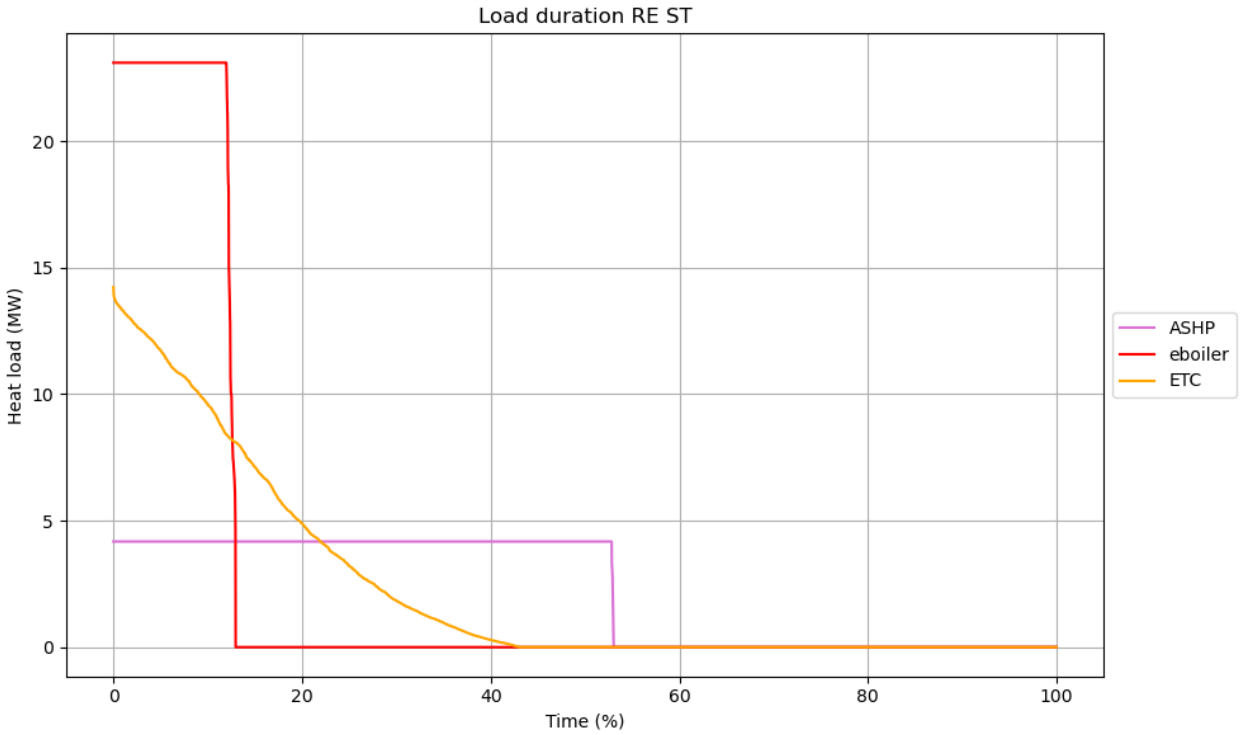
Load duration RE ST
Heat load (MW)
Time (%)
ASHP
eboiler
ETC

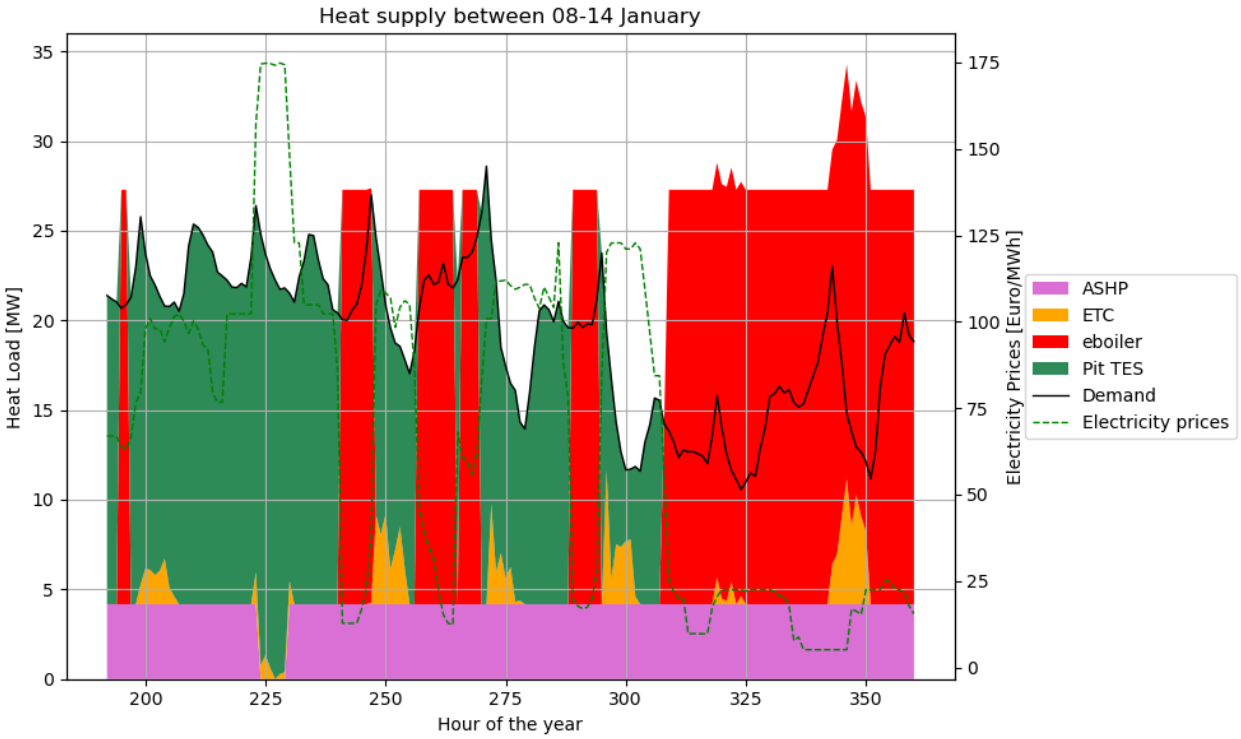
Heat supply between 08-14 January
Heat Load [MW]
Electricity Prices [Euro/MWh]
Hour of the year
ASHP
ETC
eboiler
Pit TES
Demand
Electricity prices

All technologies

Table 17: Input energy ASHP and PV output

	PV output [GWh]	ASHP input energy [GWh]
All	13.28	13.22
RE	13.28	12.52

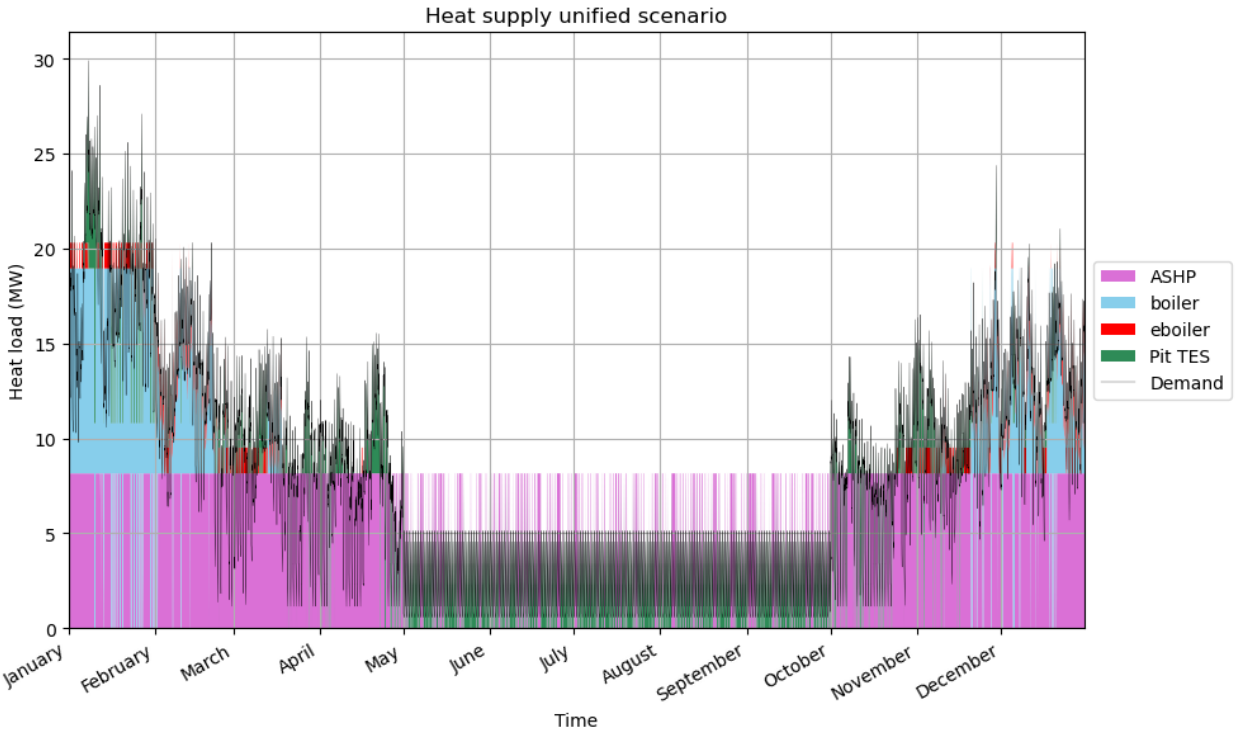

Full heat supply profile in the “All technologies” scenario.

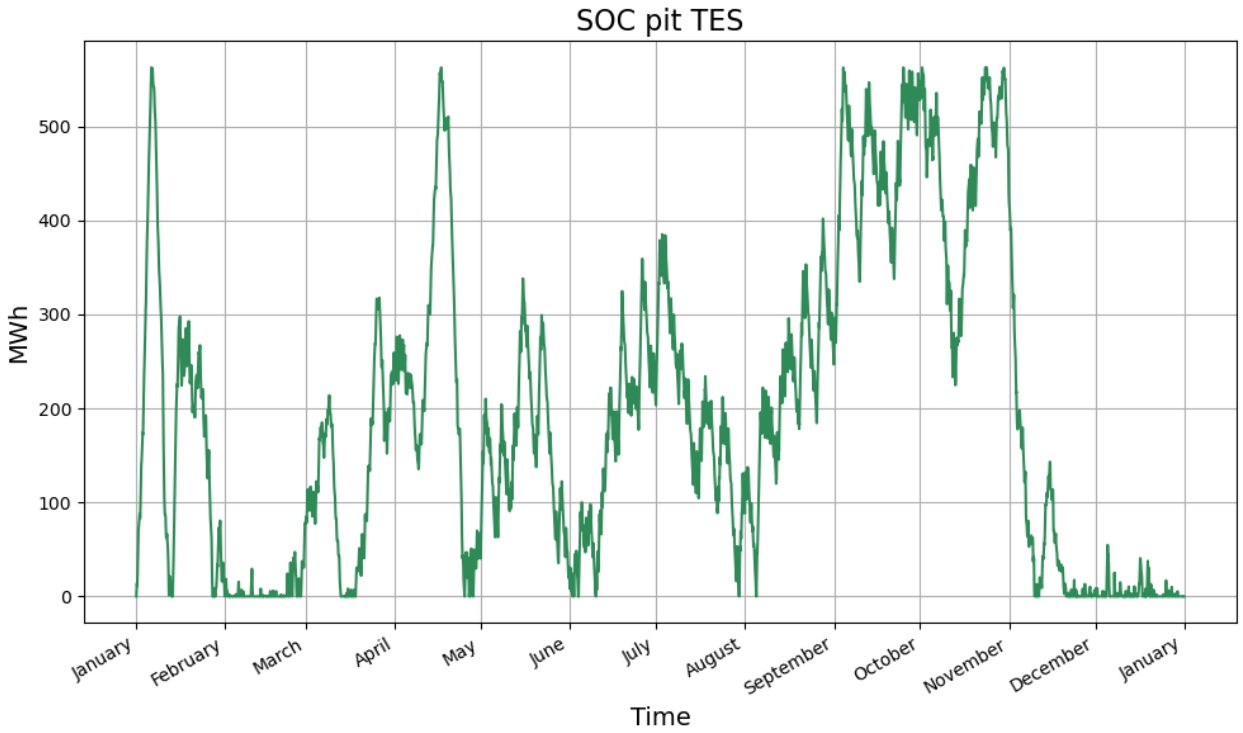

State of charge of the pit TES in the “All technologies” scenario.

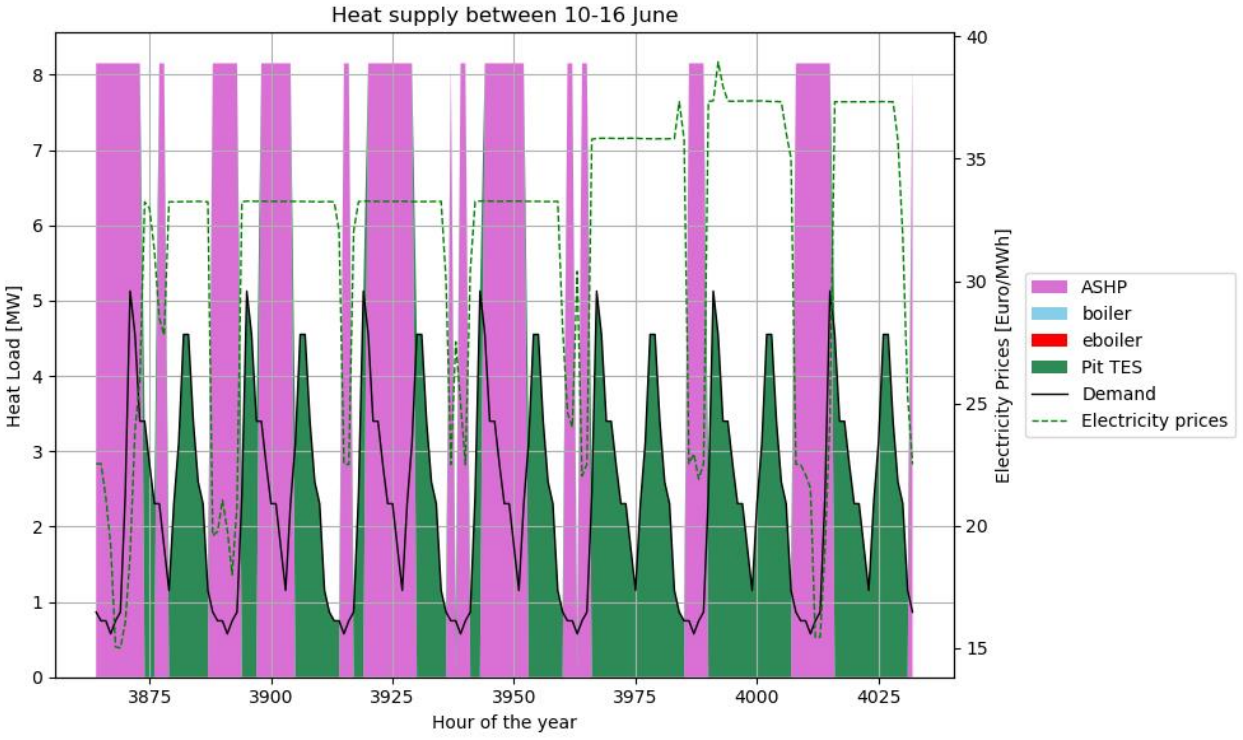

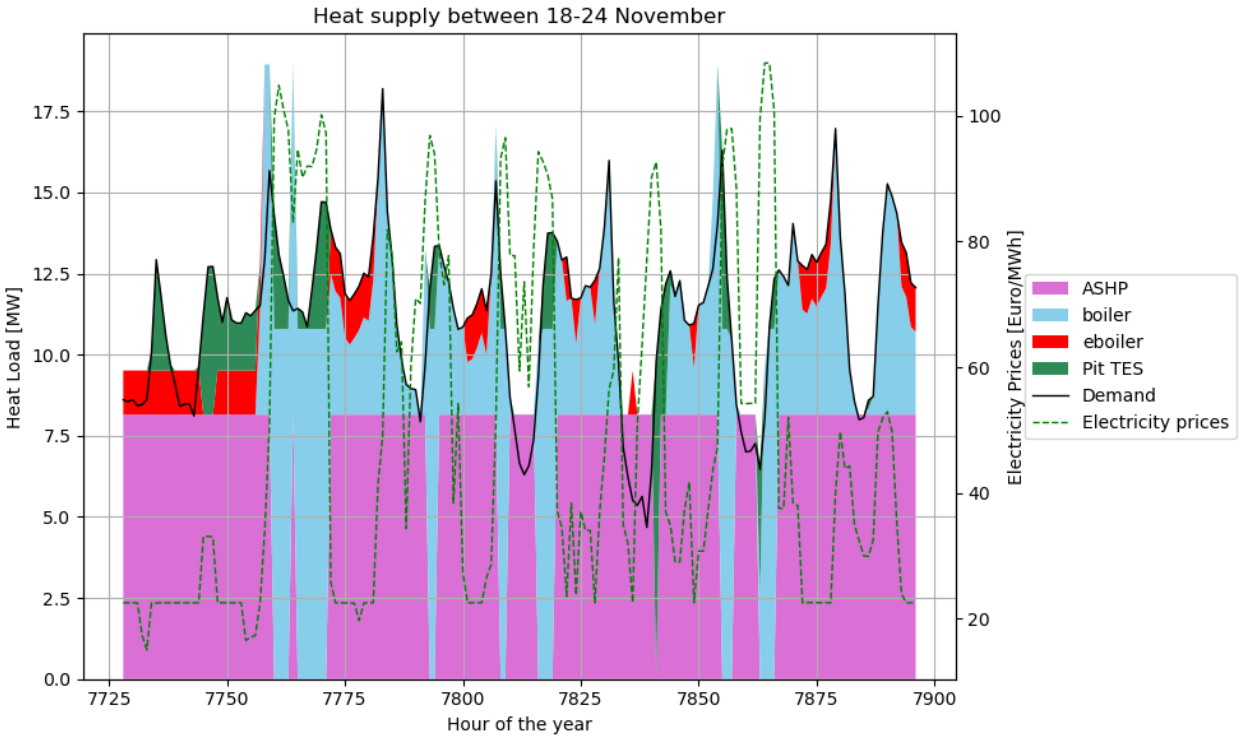

D2: Dispatch models

The rest of this section is dedicated to the results of the dispatch model runs. Please do not confuse with the previous section, in which the results of the 2017 prices optimisation are shown.

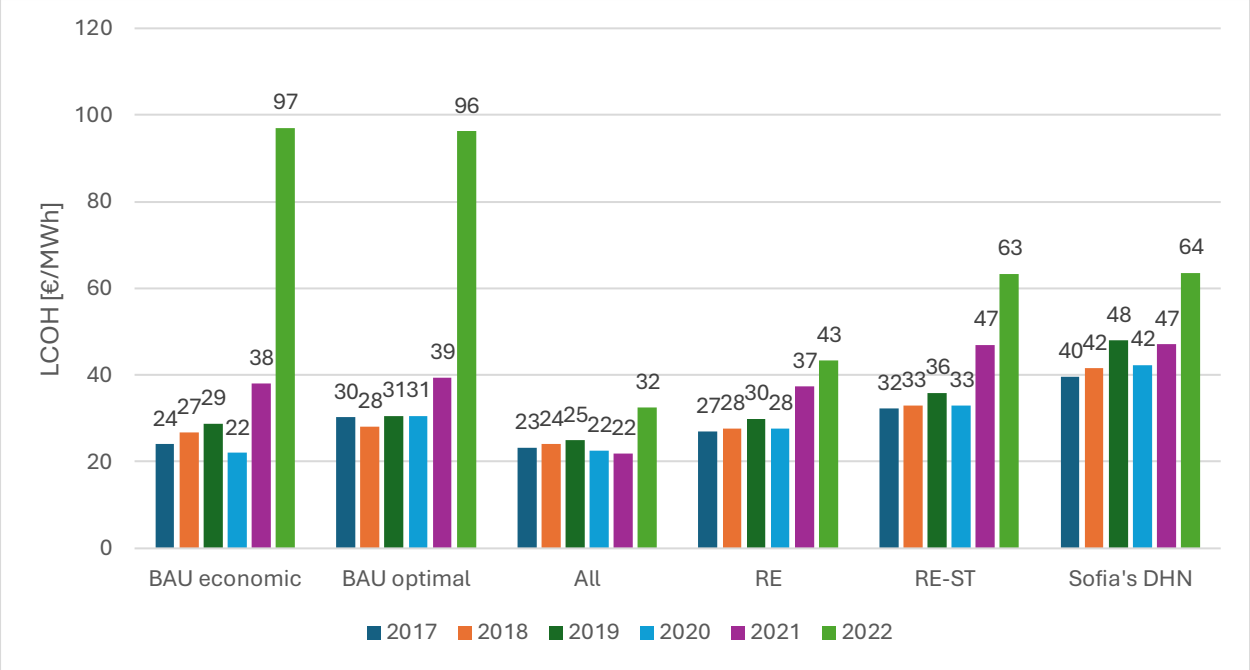

Figure 30: Levelized costs of heat of the main technology scenarios across the different dispatch scenarios

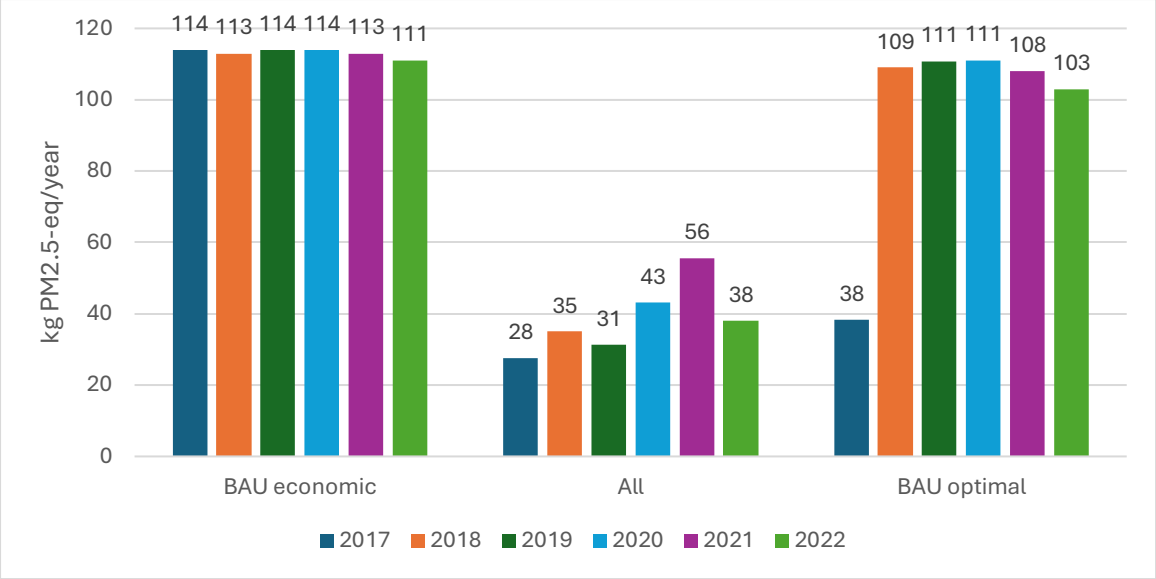

Figure 31: Particulate matter emissions across the dispatch runs

All technologies

Table 18: Headline figures All technologies, RE and BAU econ scenarios across the dispatch models

		2017	2021	2022
All technologies	11 MW boiler	15 364	30 842	21 033
	1 MW e-boiler	2 232	277	462
	8 MW ASHP	47 001	33 502	43 111
BAU econ	20 MW boiler	63 378	62 745	61 672
	5 MW e-boiler	1 149	1 782	2 856
RE	18 MW e-boiler	20 598	16 511	18 306
	8 MW ASHP	44 058	48 215	46 406

The All technologies scenario features the best performance across the dispatch runs (Figure 20).

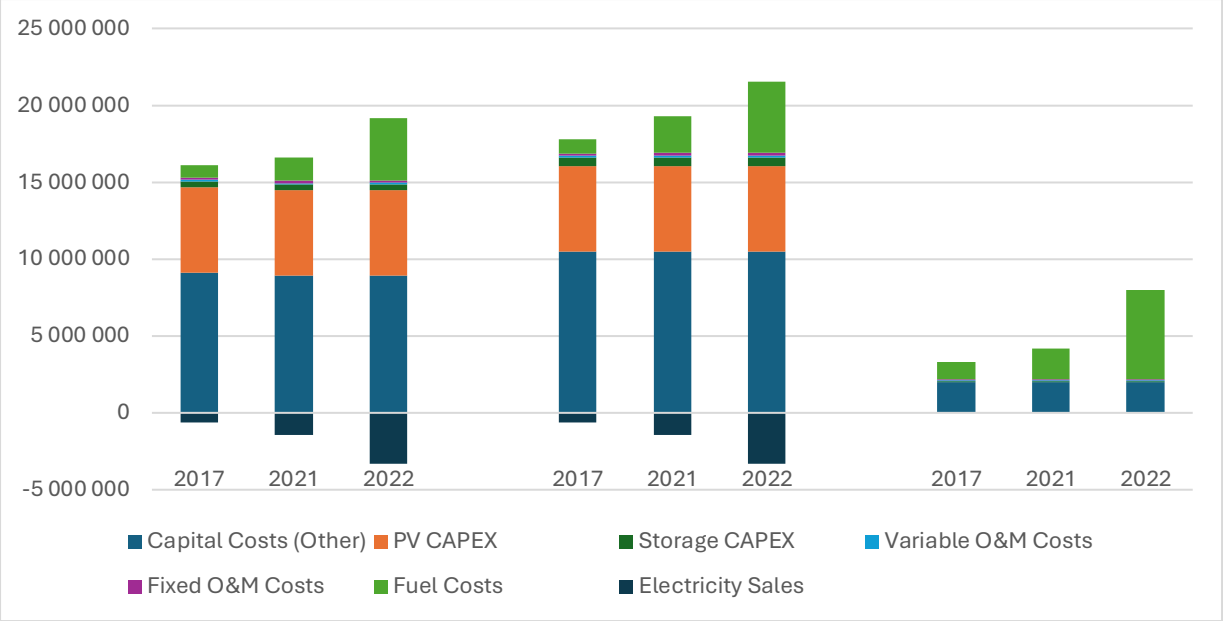
25 000 000
20 000 000
15 000 000
10 000 000
5 000 000
0
-5 000 000
2017
2021
2022
2017
2021
2022
2017
2021
2022
Capital Costs (Other)
PV CAPEX
Storage CAPEX
Variable O&M Costs
Fixed O&M Costs
Fuel Costs
Electricity Sales

D3: 2022 optimisation

Pareto fronts

BAU technologies

PM emissions [kg PM2.5-eq./year]	Costs [€]	Installed capacity CHP	Installed capacity boiler	Installed capacity e-boiler	Installed capacity tank	CF CHP	CF CHPe	CF boiler	CF e-boiler	LCOH [€/MWh]
0	2.23E+08			24.89476	380				30%	198.3706
73.11111	81571384	12.26645	9.938141	24.6541	380	13%	1%	8%	20%	72.64435
146.2222	274141.7	19.80574	9.101289	22.97567	380	16%	4%	9%	15%	0.24414
219.3333	-6.4E+07	35	9	22	380	10%	6%	9%	14%	-56.5829
292.4444	-1.2E+08	35	7.89055	20.18346	380	13%	10%	8%	11%	-104.062
365.5556	-1.6E+08	35	7.405736	18.65888	380	15%	14%	8%	9%	-141.075
438.6667	-1.9E+08	35	6.956446	17.4622	380	16%	18%	8%	7%	-169.302
511.7778	-2.1E+08	35	5.930247	15.75634	380	17%	22%	8%	6%	-188.005
584.8889	-2.2E+08	35	3.815877	15.10072	380	18%	27%	7%	5%	-198.189
657.3277	-2.3E+08	35	3	14	380	19%	32%	6%	4%	-201.137

The table above shows some of the important variables across the BAU Pareto front under 2022 prices optimisation. The optimal solution (BAU opt) and the cheapest solution (BAU econ) are highlighted in green and its values are rounded, as per the way they were reported in the report so far. The installed capacities are measured in MW, and the capacity factors (CF) in percentages.

All technologies

PM emissions [kg PM2.5-eq./year]	Costs [€]	P CHP	P boiler	P e-boiler	P ASHP	P tank	P pit	P PV	CF CHP	CF CHPe	CF boiler	CF e-boiler	CF ASHP	CF PV	LCOH [€/MWh]
0	32054103	0	0	29	12	30	3968	10				4%	52%	15%	28.54616
66	-49751699	23	0	27	12	24	6463	10	8%	0%		4%	38%	15%	-44.307
132	-118245884	35	0	21	12	54	13404	10	11%	0%		3%	26%	15%	-105.305
198	-167312041	35	0	11	12	17	13467	10	13%	3%		3%	23%	15%	-149.002
264	-206980824	35	0	14	8	17	11241	10	15%	6%		3%	23%	15%	-184.329
331	-240095768	35	0	18	4	19	8819	10	17%	9%		3%	23%	15%	-213.82
397	-267906450	35	0	16	1	21	6781	10	20%	12%		3%	22%	15%	-238.587
463	-288528444	35	0	9	0	23	4445	10	21%	16%		2%		15%	-256.952
529	-298834815	35	1	0	0	9	3346	10	21%	21%	3%			15%	-266.131
594	-301658642	35	0	0	0	3	2371	10	21%	26%				15%	-268.646

The table below shows some of the important variables across the All technologies Pareto front under 2022 price conditions. The optimal solution is highlighted in green and its values are rounded, as per the way they were reported in the report so far. The installed capacities are measured in MW, and the capacity factors (CF) in percentages.

Other figures

GHG emissions in tons per year for the results of the optimisation run with 2022 prices. Net emissions take into account the 0 emissions from the PV array and that its electricity is consumed behind the meter, thus avoiding consuming Bulgarian electricity from the grid.

	CHP	CHP-e	Boiler	E-boiler	ASHP	Total emissions	Net emissions
BAU economic	24 702 203	45 673 846	321 864	1 624 162	0	72 322 074	72 322 074
BAU optimal	13 424 900	8 901 964	1 263 211	9 041 536	0	32 631 611	32 631 611
All	16 885	4 411	0	3 576	1 446	26 318	20 101
RE	0	0	0	3 576	5 120	8 697	4 248
RE-ST	0	0	0	2 493	3 754	6 248	4 023

D4: Other temperatures

Table 19 shows the installed capacities and the LCOHs across the three scenarios where the supply temperatures are changed. The ETC and PV capacities are not displayed, as they remain constant across all scenarios.

Table 19: Installed capacities that differ between the three temperature scenarios and their respective LCOHs. RE values on the left and RE-ST values on the right

	RE scenario				RE-ST scenario			
	E-boiler [MW]	ASHP [MW]	Pit TES [MWh]	LCOH [€/MWh]	E-boiler [MW]	ASHP [MW]	Pit TES [MWh]	LCOH [€/MWh]
60°C constant	18	8	887	26.15	23	4	2664	31.69
70°C constant	18	8	906	26.93	23	4	2558	32.22
100°C dynamic	24	6	1092	27.69	30	1	2498	32.44

In the 100°C setup: The main effect in both technology scenarios is the increased reliance on e-boilers and the reduced role of ASHPs. This stems from the fact that ASHPs run in baseload mode during the winter in both scenarios; when the supply temperature is dynamic and higher overall, it stands to reason that ASHPs COP will be reduced. This gives an incentive for the installation of an e-boiler, which is unaffected by this change, versus an investment in a larger ASHP. As was shown in previous sections, larger e-boilers can make better use of larger TES unit, hence the change in the RE scenario. Curiously, the opposite trend unfolds in the case of RE-ST. A possible explanation is that as the efficiency of the ETC has decreased, the output of the "summer energy harvest" decreases, and thus needs a smaller TES.

In the in the fictional setup of 60°C supply temperature: Cost reduction is expected as the output of the ETC and the ASHP increases. For the RE scenario that means reducing the dependency on the e-boiler and, therefore smaller TES. For the RE-ST, it means a larger "summer energy harvest", which justifies larger TES.

Appendix E: Sofia's DHN

The future plans of the DHN operator include a significant investment in interconnecting the system. The main districts will be brought together, and most of the standalone networks will be integrated as well; a breakdown of this plan is shown in the table below (Table 20). This new network will be augmented with the installation of 480 MW_{th} and 480 MW_e of combined cycle natural gas CHP in the power plants Sofia East and Liulin. Another important plan is the expansion of the Orlandovtsi network (Toplofikatsiya Sofia, 2022b). It will be expanded to include all municipal buildings in the neighbourhood (schools, nurseries, etc.) and all other buildings along the proposed trench (Toplofikatsiya Sofia, 2022b). Its heavy fuel oil boiler will be replaced with two natural gas internal combustion engines with a combined maximum output of 7 MW_{th} and 7 MW_e.

Table 20: Breakdown of the different networks and their capacities. The four main districts are marked with (m). Source: Toplofikatsiya Sofia, 2022a

Network	Planned integration in the main loop	Thermal power and heat plants	Electrical capacity (MW)	Thermal capacity (MW)	Fuel
Sofia (m)	Yes	Sofia	72	1323	Natural gas
East (m)	Yes	Sofia East	167	1464	Natural gas
Zemlyane (m)	Yes	Zemlyane	0	581	Natural gas
Liulin (m)	Yes	Liulin	0	581	Natural gas
Northeast	Yes	Hadzhi Dimitar	0	47	Natural gas
		Suha reka	0	35	Natural gas
Levski	Yes	Levski	0	44	Natural gas
Orlandovtsi	No	Orlandovtsi	0	5	Heavy fuel oil
Ovcha kupel	No	Ovcha kupel 1	0	44	Natural gas
		Ovcha kupel 2	0	44	Natural gas
Zaharna Fabrika	Yes	Inzhstroi	0	20	Natural gas